LITHOGEOCHEMICAL STUDIES IN THE VICINITY OF THE BUCHANS MASSIVE SULPHIDE DEPOSITS, CENTRAL NEWFOUNDLAND

J. GEOFFREY THURLOW

LITHOGEOCHEMICAL STUDIES IN THE VICINITY OF THE BUCHANS MASSIVE SULPHIDE DEPOSITS, CENTRAL NEWFOUNDLAND

by

© J. Geoffrey Thurlow

A Thesis
Submitted in partial fulfilment of the requirements
for the degree of
MASTER OF SCIENCE

Memorial University of Newfoundland
October, 1973

ABSTRACT

The Buchans orebodies are stratiform massive volcanogenic sulphide deposits associated with calc-alkaline volcanism of probable Silurian age. Since 1928, approximately 16 million tons of ore have been mined with an average grade of 14.97% Zn, 7.73% Pb, 1.37% Cu, 3.73 oz. Ag and .046 oz. Au. The ore is intimately associated with volcaniclastic siltstones and laharic breccias within rhyolitic ash flows. It was deposited in chemically favourable depressions by precipitation of base metals from (sea?)water which was enriched in these components by submarine fumarolic activity during quiescent phases in volcanism. Most of the massive sulphide deposits are underlain by less important stringer and stockwork mineralization which is distinct in both time and space from the major orebodies.

Two hundred and ninety three chemical analyses of diamond drill core samples for eleven major and fourteen trace elements were performed in order to obtain reconnaissance lithogeochemical data on the volcanic rocks and in an attempt to develop a new exploration technique based on rock geochemistry. The area of study was restricted to a single cross section two miles long by one mile deep containing a representative portion of most lithologic units and three major orebodies. Studies of elemental distributions in the vicinity of the orebodies indicate that dispersion of ore metals is generally restricted to within one hundred feet of the orebodies. Study of lateral elemental variations within lithologic units indicates a broad increase of base metals in most units from northwest to southeast over a distance of about two miles.

The abundances of Ba, Pb and Zn are distinctly higher in volcanic rocks and sediments related to ore compared to those unrelated to ore. These differences are consistent throughout the entire cross section and are statistically significant at a high level of confidence. Cu, Ag and Hg in some instances are likewise higher in units associated with mineralization. The enrichment of these elements is attributed to a metal-rich volatile phase which accompanied volcanism which produced lithologic units related to mineralization. An expanded geological-lithogeochemical exploration program appears justified on the basis of these results.

TABLE OF CONTENTS

Page

CHAPTER 3

FIELD, LABORATORY AND STATISTICAL METHODS

CHAPTER 4

GENERAL PETROCHEMICAL SETTING

CHAPTER 5

THE RELATIONSHIP BETWEEN GEOCHEMISTRY AND MINERALIZATION

LIST OF FIGURES

Page

LIST OF TABLES

LIST OF PLATES

CHAPTER 1

GENERAL INFORMATION

1.1. Introduction

The Buchans mines are situated in central Newfoundland about four miles north of Red Indian Lake, at latitude 48° 50' N, longitude 56° 46' W and elevation 900 feet (Fig. 1). It is connected to the Trans-Canada Highway by 47 miles of paved highway originating at Badger.

The Buchans area is characterized by gently rolling boggy lowlands, low rounded peaks and ridges, and numerous shallow ponds. Vegetation varies from near tundra conditions at higher altitudes to heavy spruce forest in protected areas. Outcrop is generally sparse and is restricted to local topographic highs and to river channels.

The Buchans Unit of the American Smelting and Refining Co. (ASARCO) currently employs over 600 people. The mineral rights are leased from Terra Nova Properties Ltd. (a subsidiary of the Price Newfoundland Development Co. Ltd.) with whom profits are shared on a 50:50 basis.

1.2. History of Mining

Matty Mitchell, an Indian prospector/woodsman, is credited with the discovery of the first orebody in 1905 - an outcrop of one of the Buchans River orebodies in the banks of the Buchans River. It has been rumored that he sold the site of his discovery to a local geologist for a sack of flour.

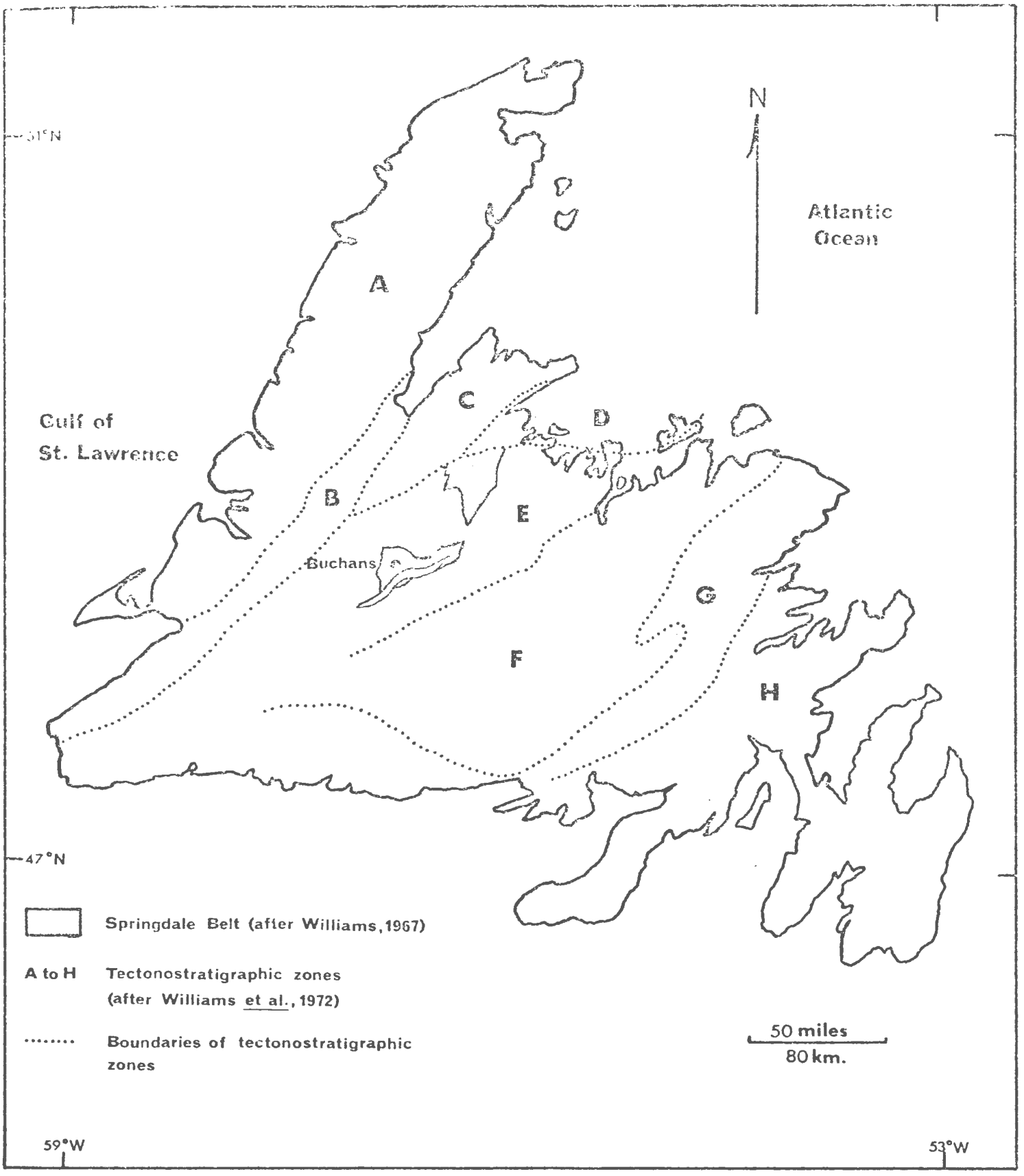

Fig. 1. Location of Buchans with respect to tectonostratigraphic zones of Newfoundland and Springdale Belt.

Development work on the property was carried out between 1906 and 1911, but efforts were suspended due to metallurgical difficulties with the fine grained sulphide aggregate. Development began in earnest in 1926 by ASARCO as a result of their discovery of selective flotation, and production began in 1928 at a rate of 500 tons per day (tpd). In 1930 the milling capacity was increased to its present rate of 1250 tpd.

The near-surface Oriental No. 1 and Lucky Strike Orebodies were discovered by resistivity surveys carried out in 1926 under the direction of Hans Lundberg. (These discoveries represent the first successful application of geophysics in North America). The Rothermere and MacLean (formerly Rothermere #4) orebodies were discovered between 1947 and 1950 as a result of intensive drilling under the direction of H.J. MacLean. E.A. Swanson became chief geologist in 1951 and was responsible for the discovery of the Oriental #2 orebody in 1953. Since that time the sub-economic Clementine and Sandfill prospects have been discovered but available tonnages are not sufficient to warrant production to date.

During the past twenty years virtually every conceivable method of surface geochemistry and ground and airborne geophysics has been used in an attempt to outline new ore but with only limited success. Diamond drilling has always played a major role in the detailed local exploration, and over one million feet of drill core is stored in the core sheds at Buchans. The careful logging and re-logging of this core has made the Buchans area the most thoroughly studied local volcanic environment in the province.

Production to date (June 1973) has amounted to about sixteen million tons at an average grade of 14.97% Zn, 7.73% Pb, 1.37% Cu, 3.73 oz. Ag and .046 oz. Au. Reserves are estimated at about two million tons.

1.3. Previous Work

1.3.1. Previous Work in the Buchans Area

In view of the economic importance of the Buchans deposits to central Newfoundland and their general geological significance, it is unfortunate that more published material dealing with the area is not available. Newhouse (1931) and George (1937) provided early interpretations of the regional and local geology, but it was not until Relly's work (1960) that a unified summary of all the available information was compiled. Swanson and Brown (1962) published a summary of Relly's work and also included most of the ideas of the mine staff at the time.

William's map (1970) represents the only published account of the regional geology which includes the Buchans area.

Apart from Relly (1960), there also exist several unpublished B.Sc. and M.Sc. theses concerning various aspects of individual orebodies. These include Catherall (1960), Alcock (1961) and Woakes (1954).

1.3.2. Previous Lithogeochemical Studies in General

The geological literature abounds with isolated references to economically oriented lithogeochemical studies. General references such as Bradshaw et al. (1970), Boyle and Garrett (1970), Hawkes and Webb (1962)

and Sakrison (1971) discuss the techniques and problems encountered in economic lithogeochemical surveys and refer to the various successes and failures of numerous individual studies. Regional lithogeochemical surveys have met with varying degrees of success. Davenport and Nichol (1972), Descarreaux(1972) and Govett and Pantazis (1971) report definite anomalies in regions surrounding ore deposits,whereas Boyle (1961, 1965) in similar surveys was unable to detect any indication of nearby mineralization. Local lithogeochemical studies (eg. Sakrison, 1967; Boyle et al., 1969; Gale, 1969; Bradshaw and Koksoy, 1968; Graf and Kerr, 1950; and Konstantynowicz, 1972) have determined the existence of wallrock anomalies on the scale of tens, and sometimes hundreds of feet from ore zones. Only rarely (e.g. Morris and Lovering, 1952) have aureoles been detected in the order of one thousand feet from orebodies.

The limited success of rock geochemistry in exploration applications has made these surveys an often contemplated but seldom executed exploration tool. There is a need for integrated local and regional lithogeochemical programs in all geological environments in order to fully assess the potential of the method.

1.4. Present Study

The present study was undertaken in order to obtain new geochemical data which might provide insight into the petrogenesis of the volcanic rocks and possibly provide information of significance to exploration. It was decided to concentrate on a detailed study of one cross section, and the North 60° West (N60W) section was chosen for the following reasons:

(1) The section includes a portion of three major orebodies and one minor orebody, i.e., MacLean, Rothermere, Lucky Strike and Two Level, as well as an area of footwall ore below Lucky Strike, while a large area of unmineralized rocks at a distance from ore is also represented.

(2) The section contains a portion of all major lithologic units in the mine area (except the Footwall Arkose).

(3) The section probably best represents the local stratigraphy and lithologic relationships within the volcanic pile.

(4) The stratigraphy of the section is known with a high level of confidence as a result of intensive diamond drilling.

(5) Drill holes on the section are spaced at more or less equal intervals, a favourable aspect with regard to geochemical correlation.

General questions which might be answered by such a study include:

(1) Are there any geochemical aureoles or dispersion patterns surrounding the orebodies? If the existence of such can be demonstrated, are they of sufficient magnitude and extent to be of use to either regional or local exploration?

(2) Can the geochemistry be used to answer specific questions concerning ore genesis?

(3) What is the petrogenesis of these rocks in terms of modern global tectonic thought?

With these broad questions in mind, drill core samples were taken from the N60W section and 293 analyses were performed for 11 major and 14 trace elements. The interpretation of these data, in terms of the known geology of the area, forms the bulk of this study.

1.5. Acknowledgements

The writer is indebted to many people without whose help this study would not be possible.

The writer is especially grateful to D.F. Strong who suggested the project and provided supervision and guidance throughout. Dr. Strong was also responsible for providing assistants during various portions of the study and for providing the necessary computer time. Thanks must also be extended to Mrs. G. Andrews for her patient help in the analytical lab, and to D. Press who performed phosphorus and loss on ignition determinations.

Special thanks are due to the American Smelting and Refining Company who provided employment and accommodation to the author while in Buchans. E.A. Swanson was of invaluable aid to the author at the mine site in answering many questions on the geology and providing many ideas to be checked geochemically.

Dr. L.D. James, through his keen interest in the project, was responsible for the analysis of most of the trace elements and for numerous checks and re-checks for precision.

The writer would also like to thank K.B. Larsen for numerous underground tours and discussions, and E. Perkins for assistance in a variety of matters. Additional help received in the office from P. Brockie

and M. Verbiski, and in the field from M. Harris, D. Pardee, and K. Elliott is also gratefully acknowledged.

The author also gratefully acknowledges financial support received in the form of a Memorial University Fellowship and a National Research Council Bursary.

CHAPTER 2

GEOLOGY AND ORE DEPOSITS OF THE BUCHANS AREA

2.1. Regional Geology

The Buchans deposits occur in central Newfoundland at the northern extension of the North American Appalachian structural province (Fig. 1). The geology of the island of Newfoundland has been interpreted as a two-sided symmetrical system (Williams 1964) consisting of a central mobile belt between eastern and western platforms of late Precambrian and lower Paleozoic ages respectively. The central mobile belt is symmetrical within itself consisting of polyphase deformed margins of pre Middle-Ordovician age enclosing a generally younger (mainly Ordovician and Silurian) sedimentary and volcanic sequence. The symmetry of the system breaks down within this inner portion of the central mobile belt as the region can be divided into three contrasting structural-stratigraphic zones (zones D, E, and F of Williams, Kennedy and Neale, 1972). Zone D, north of the Lukes Arm Fault in Notre Dame Bay, is dominated by complex Ordovician ophiolite and island arc stratigraphy (Kean, 1972; Strong, 1973a) whereas zone F on the eastern side of the mobile belt is mainly a Silurian clastic terrane. Zone E, which hosts the Buchans deposits, is in fault contact between zones D and F.

Zone E is a volcano-sedimentary terrane consisting of lithologically contrasting facies of Ordovician and Silurian age and is cut by a variety of plutons and composite batholiths of probable Devonian age. Small Carboniferous basins unconformably overlie all rocks in the zone.

Basement to the zone is not exposed. All lithologies (except the Carboniferous) have been subjected to sub-greenschist to low greenschist facies metamorphism and contain a single Acadian fabric. Folds are generally upright and vary locally from open to near isoclinal.

The Ordovician of Zone E is an assemblage of mafic pyroclastics with less abundant pillow lava and associated marine greywacke, siltstone, argillite and chert. Lower to Middle Ordovician graptolites occur in black shales throughout the zone (Williams, et al., 1972). Minor felsic volcanic rocks occur locally.

In contrast to the Ordovician, Silurian lithologies assume a generally shallow water to terrestrial character and display a fairly consistent stratigraphic sequence throughout Newfoundland (Williams, 1967). This sequence consists of thick basal greywackes and plutonic boulder conglomerates overlain by mafic agglomerates, felsic pyroclastics and ignimbrites, which are in turn overlain by red micaceous sandstones, commonly of fluviatile origin.

The Buchans area lies near the western margin of zone E and is underlain by a volcano-sedimentary sequence which forms the southern margin of the Springdale Belt (Fig. 1) of probable Silurian age (Williams, 1967). Assignment to the Silurian is based on the similarity of the various lithologies to the typical Silurian types in the Springdale and Botwood Groups to the northeast, and the general dissimilarity to Ordovician types. Silurian type red sandstones are found on the south side of Red Indian Lake in a group of lithologies thought to predate those at Buchans.

2.2. Local Geology

2.2.1. General

A unit known locally as the Footwall Andesite crops out along the northern shore of Red Indian Lake (Fig. 2) and forms the base of a group of lithologies informally known as the Buchans Group (Relly, 1960). The region to the north and west of Buchans is intruded by composite batholiths of presumed Devonian age. The Footwall Andesites are devoid of significant sulphide mineralization, but the area enclosed by the Footwall Andesites and the Devonian intrusives contains the host rocks of the Buchans deposits. This represents the area of most intensive exploration during the past 40 years.

Within this favourable zone four cycles of generally mafic to felsic volcanism have been recognized (Fig. 2, after E.A. Swanson). Cycle one includes the Footwall Andesite as the basal mafic unit which is overlain by felsic pyroclastics and local siltstone. This cycle forms the host rocks for the MacLean, Rothermere and Lucky Strike orebodies as well as the footwall orebodies. Cycle two conformably overlies cycle one and hosts the Oriental and Buchans River orebodies. Cycles three and four are considerably more widespread than the initial cycles and comprise a large portion of the favourable zone, but no ore is known to be associated with these cycles.

Four major structural depressions within the Footwall Andesites have been outlined by diamond drilling (Fig. 2). The largest of these and the one of most immediate relation to ore lies north of the Buchans orebodies and is largely occupied by Sandy Lake. This depression is roughly circular

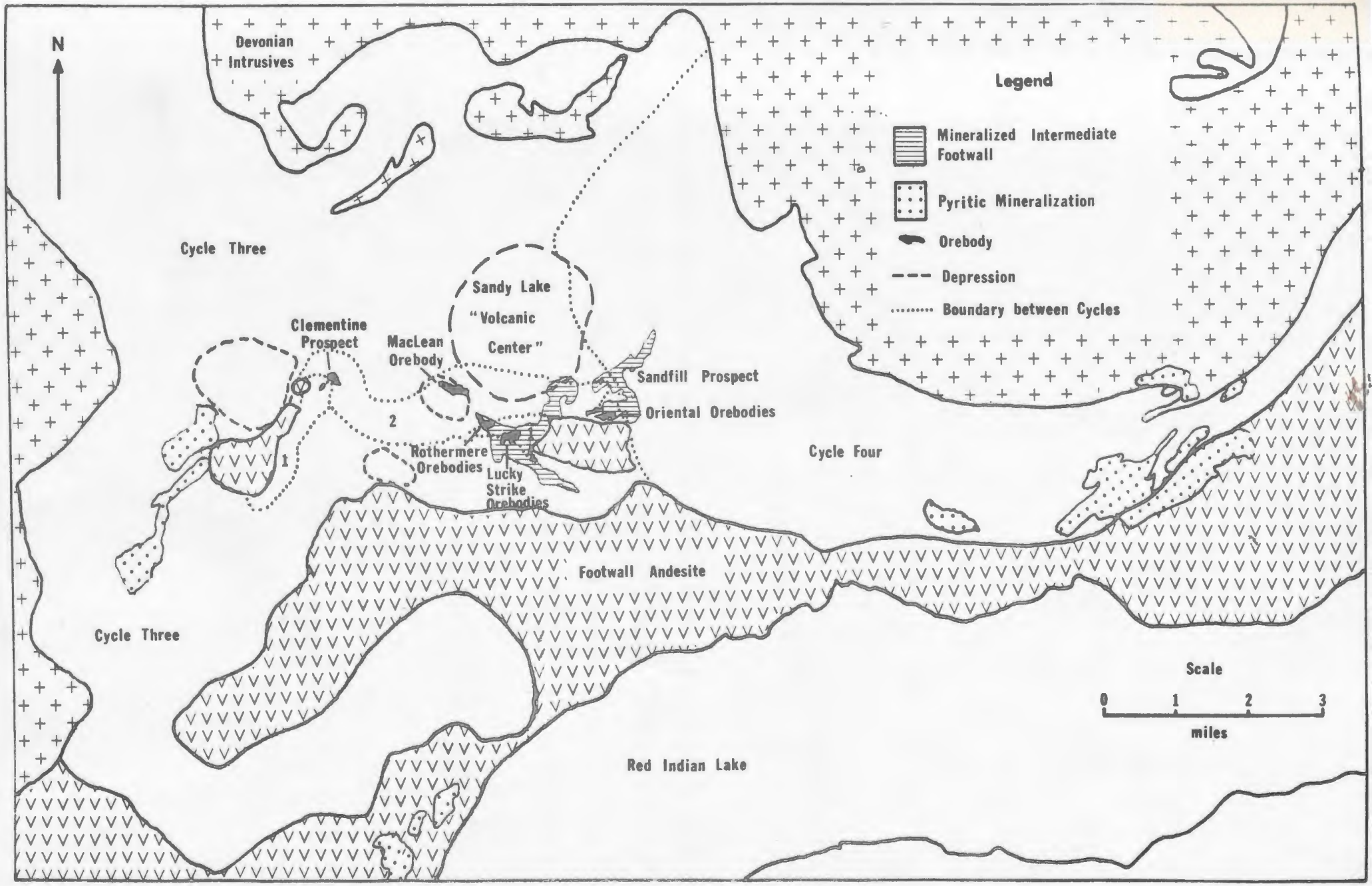

Fig. 2. Generalized geological map of the Buchans area (after E.A. Swanson).

with a diameter of two miles, and is characterized by the apparent subsidence of the rocks of cycles one and two into a deep depression and subsequent infilling by large volumes of cycle three volcanics. The mine staff have mapped the surface and subsurface distribution of the felsic stages of cycle one and cycle two and have found that they form an elongate area around the depression. This appears to suggest that the depression represents a volcanic center and has led E.A. Swanson to interpret the depression as a small collapse caldera.

Little is known of the depression west of the Clementine prospect although this may represent a similar, but smaller, "volcanic center" or pit crater.

The two smaller depressions extending radially from the Sandy Lake "volcanic center" are of somewhat different character. They have steep fault-bounded sides and are filled mainly with cycle one and cycle two volcanics. No effusive activity is known to be associated with these depressions. The more northerly of the two, the MacLean depression, is about 3000 feet in diameter and has a minimum relief of 3000 feet at its center. The MacLean orebody is situated near the edge of this depression. The size, shape, distribution and lack of effusive activity suggest that these depressions are pit craters developed on the volcanic surface during a quiescent phase in volcanism. The other major orebodies are associated with smaller more gentle downwarps in the footwall.

2.2.2. Stratigraphy

2.2.2.1. Footwall Andesite: The thickness of this unit is not known with confidence but it does exceed 8000 feet several miles east of Buchans. The unit consists mainly of andesitic basalts, agglomerates, tuffs and flow breccias, with less abundant flows and only local occurrences of pillowed flows and pillow breccias. Moderate chloritization and development of calcite amygdules in blocks and bombs are characteristic of the unit. Local alteration by vein and matrix calcite is common and other areas are strongly hematized.

The Footwall Andesites consist dominantly of plagioclase (andesine) and less abundant clinopyroxene phenocrysts set in a fine grained matrix of plagioclase laths with abundant interstitial chlorite. Alteration of plagioclase varies from slight to intense and consists of clay minerals, epidote, sericite and calcite. Pyroxene phenocrysts are colourless to light brown augite which is mildly altered to calcite, epidote, chlorite and actinolite. Opaque oxides form less than one percent of most samples.

2.2.2.2. Footwall Arkose: The Footwall Arkose is interbedded with the Footwall Andesite and forms several persistent horizons up to 3500 feet thick. The unit is composed predominantly of massive leucocratic arkose with locally interbedded conglomerate, greywacke, sandstone, siltstone and chert.

The Arkose is medium to coarse grained, well sorted but poorly bedded and immature. It consists of varying proportions of quartz, fresh

plagioclase (oligoclase-andesine) with rhyolite and less abundant chert fragments (Plate 1). Mafic lava fragments are rare despite the fact that the Arkose is interbedded with the Footwall Andesite. The matrix forms only a small portion of the rock and consists of fine grained detritus of similar composition to the larger fragments. Alteration of the matrix is minor and consists of sericite and clay minerals with less abundant calcite and chlorite. Matrix sericite often assumes shapes which may represent pseudomorphs of original glass shards.

The thick, massive, immature nature of the unit, the felsic volcanic composition, and the lack of an erosional source rock suggests that the Footwall Arkose represents a rapidly deposited, slightly reworked rhyolite crystal-lithic tuff.

2.2.2.3. Intermediate Footwall: The Intermediate Footwall is chemically intermediate in composition between the Footwall Andesite and the overlying Dacite. The unit in most places lies conformably upon or interbedded with the Footwall Andesite although locally it overlies the Footwall Arkose. It is extensive, especially to the east of Buchans, but its thickness is largely unknown due to its lithologic similarity and its interbedded relationship with the Footwall Andesite, and also due to erosion of the upper contact. The Intermediate Footwall is dominantly pyroclastic, consisting of grey to grey-green tuff and agglomerate with less abundant flows and breccias.

Strong alteration is characteristic of the unit (especially in the immediate Buchans area) and has resulted in complete obliteration of

PLATE 1: Photomicrograph of Footwall Arkose consisting of anhedral to sub-rounded plagioclase with less abundant rhyolite fragments. Plane polarized light. x35.

primary plagioclase and mafic minerals by sericite, clay minerals and chlorite with additional widespread silicification. Quartz amygdules and phenocrysts, as well as ubiquitous fine grained disseminated pyrite, are also characteristic of the unit.

In the vicinity of the massive sulphide orebodies the fine grained disseminated pyrite grades upwards into coarser grained, disseminated, stringer, stockwork and massive Zn, Pb, Cu mineralization (Fig. 2, 3). This mineralization is described and interpreted in sections 2.3.2. and 2.4.

2.2.2.4. Cycle I Siltstone: There was a break in volcanism following deposition of the Intermediate Footwall, with the development of the MacLean pit-crater in which there was deposited fine siltstone and fine sandstone (Fig. 3). The siltstone is medium grey, siliceous, well sorted and thinly bedded or laminated, with common cross beds and slump structures. The unit is composed of angular to sub-rounded quartz and feldspar crystals and lithic fragments similar to the overlying Dacite, and it also contains volcanic fragments similar to the Intermediate Footwall. Conglomerate is not developed at the base of the unit.

Very fine grained disseminated matrix pyrite is a characteristic feature of all siltstones below the orebodies. The pyrite is sub-rounded and is consistently finer grained than the siltstone. Pyrite forms distinct beds in cross bedded siltstone and pyrite grains are graded in size in graded silt beds. These features suggest that the pyrite is allogenic. Polished sections of the siltstone (Plate 2) reveal the distinctly detrital nature of the pyrite and also show a small proportion of detrital

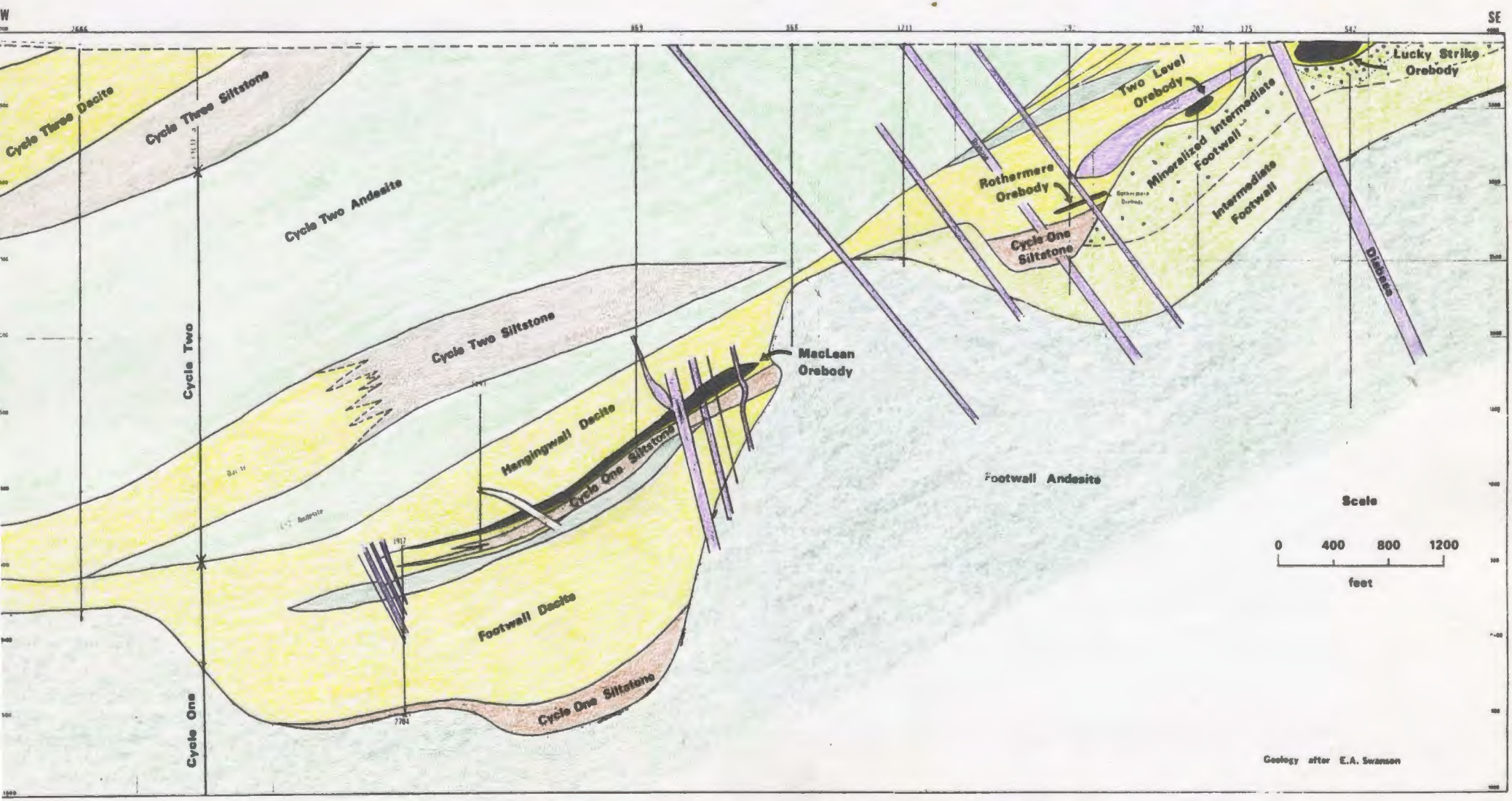

Fig. 3. Geology of the North 60^{o} West cross section.

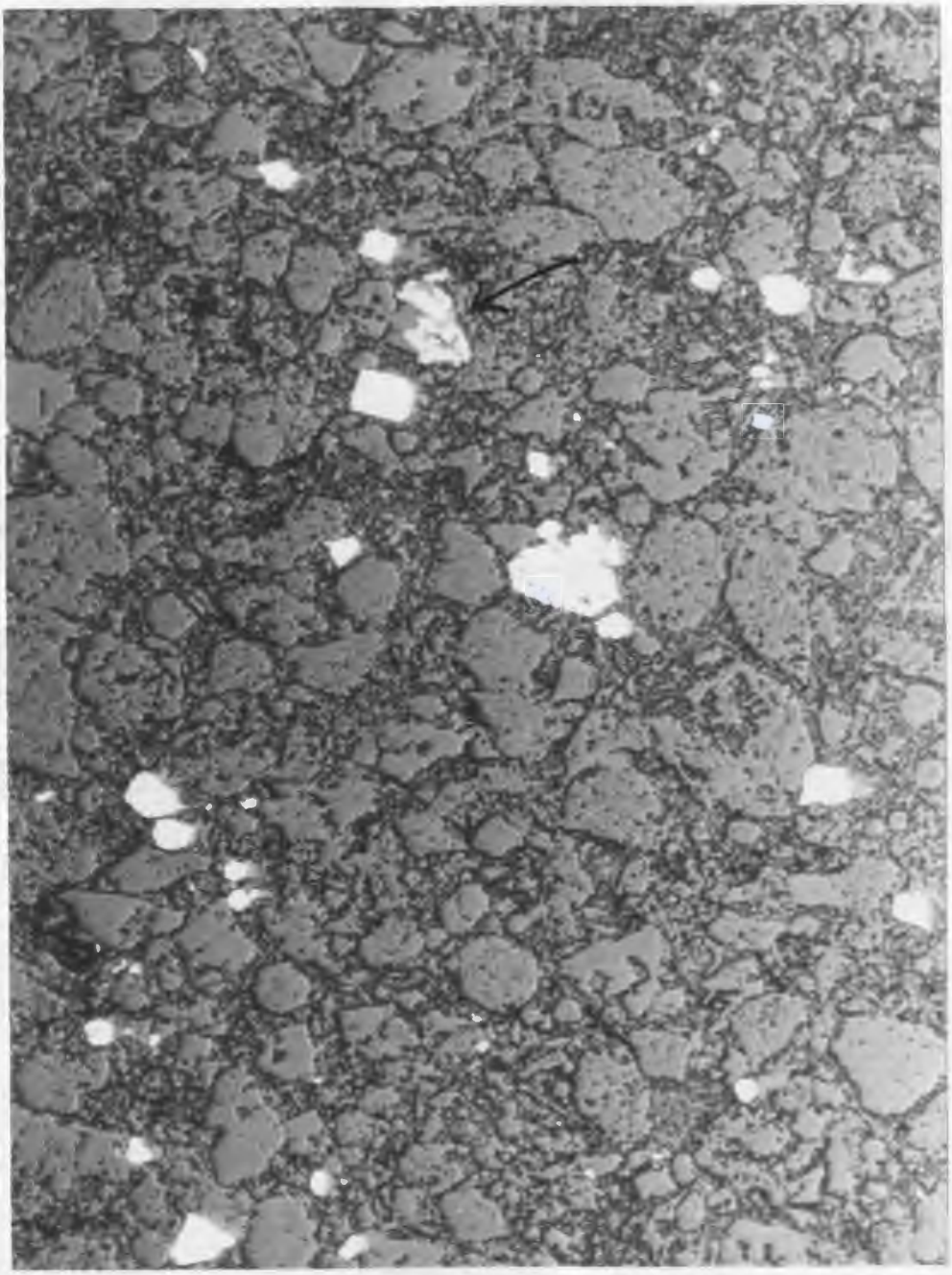

PLATE 2: Photomicrograph of Cycle One Siltstone showing rounded and broken detrital pyrite. Arrow indicates a sphalerite-bearing fragment of Intermediate Footwall. Plane polarized reflected light. x35.

sphalerite both in separate grains and in mineralized volcanic fragments. A trace of (detrital?) chalcopyrite was present in one polished section.

Provenance of the Siltstone is a problem analagous to that of the Footwall Arkose. It may be derived from erosion of dacite near the volcanic center, but it more probably represents reworked dacite ash fall which preceded the main dacite eruption. The presence of detrital pyrite, sphalerite and local intermediate volcanic fragments suggests that the mineralized Intermediate Footwall has also contributed a considerable portion of the detritus. As such, at least a part of the mineralization of the Intermediate Footwall predates the overlying massive sulphide ore deposition.

2.2.2.5. Cycle One Dacite: After it partially filled the MacLean depression, deposition of siltstone was interrupted by a rapid influx of massive and flow banded Cycle One Dacite ash flows. The Dacite lies conformably on the Siltstone but is unconformable on the Intermediate Footwall and the Footwall Andesite (Fig. 3). The thickness of the Dacite varies widely from near zero on paleotopographic highs to over 1000 feet in depressions (Fig. 4).

The unit consists of grey-green to yellow-green ignimbrite (commonly welded) with less abundant crystal-vitric, lithic and lapilli tuff and agglomerate. Typical dacite ash flows consist of quartz and plagioclase crystals (often broken) and minor lithic fragments set in a holocrystalline very fine grained quartzo-feldspathic matrix. Quartz crystals (2-4 mm) generally comprise about 10% of the dacite and are commonly

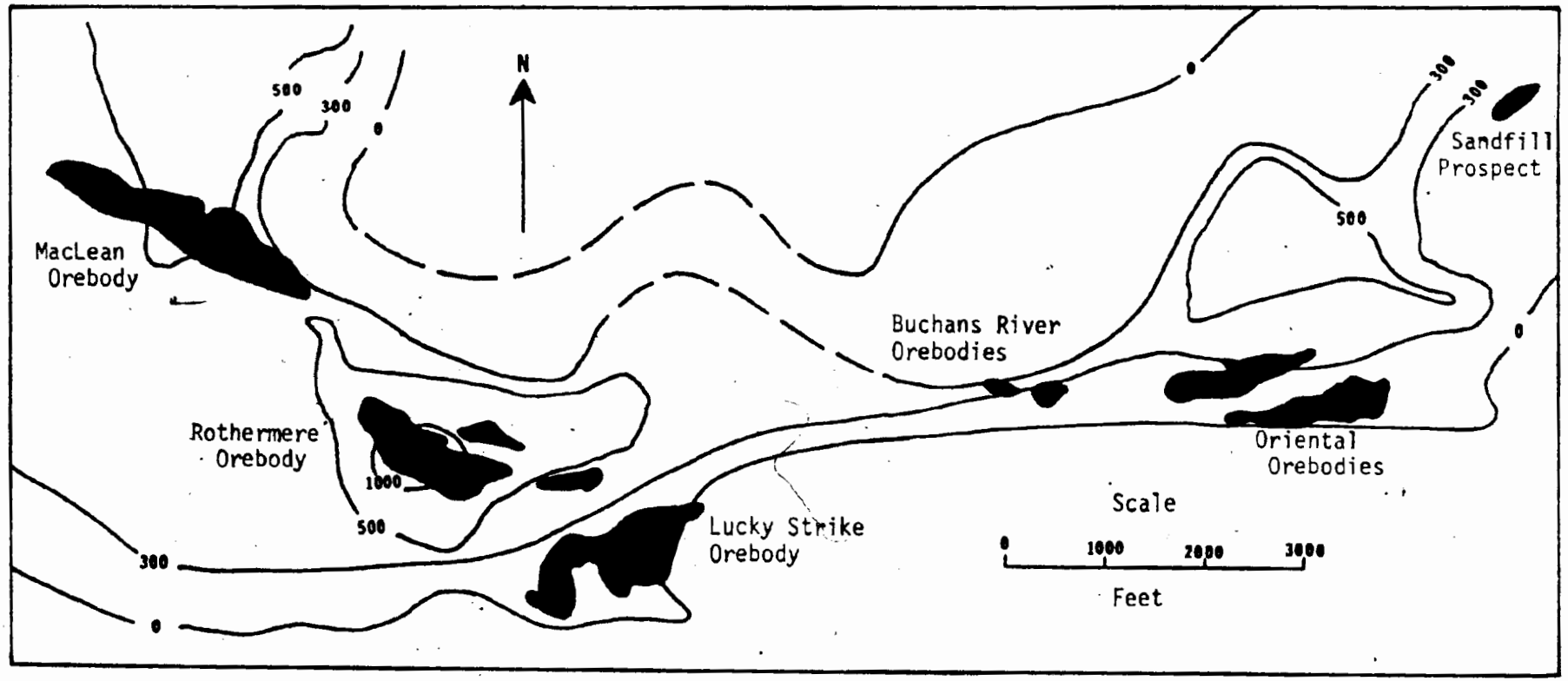

FIG. 4 - Isopach map of Dacite (modified after Relly, 1960)[4]

strongly resorbed. Plagioclase crystals (oligoclase-andesine) are generally slightly more abundant than quartz and are found in two distinct habits, i.e. as equant subhedral, untwinned and unaltered crystals or as twinned and altered laths, suggesting two different sources. Potassium feldspar forms a small portion of crystal fragments in some thin sections. Lithic dacite fragments are subordinate to crystals in most specimens and accessory basaltic fragments were seen in one thin section. Pumice fragments are not common.

The matrix consists of a mosaic of quartzo-feldspathic devitrification intergrowth with local spherulites. Original shards can be seen where devitrification is less intense. The shards are invariably flattened and bent plastically around crystal fragments (Plate 3), indicative of welding and providing evidence that the bulk of the Dacite was deposited subaerially as ash flows. Apatite and leucoxene are common accessory matrix minerals. Alteration of the matrix varies from slight to intense and consists of sericite, chlorite, epidote and calcite. Ragged prehnite crystals are a noteworthy matrix constituent of about 20% of the sections examined.

Following deposition of the initial ash flows in the MacLean depression there was a brief period of mafic volcanism, followed by renewed subsidence of the MacLean depression and initial subsidence of the Rothermere and Lucky Strike depressions. All depressions were then the site of subaqueous deposition of siltstone similar to the initial MacLean siltstones, with intermittent deposition of bedded, coarse, crystal-rich washed dacite tuffs. The massive sulphide orebodies occur in a stratigraphic horizon overlying these siltstones and washed dacites, and are associated with a distinct breccia zone.

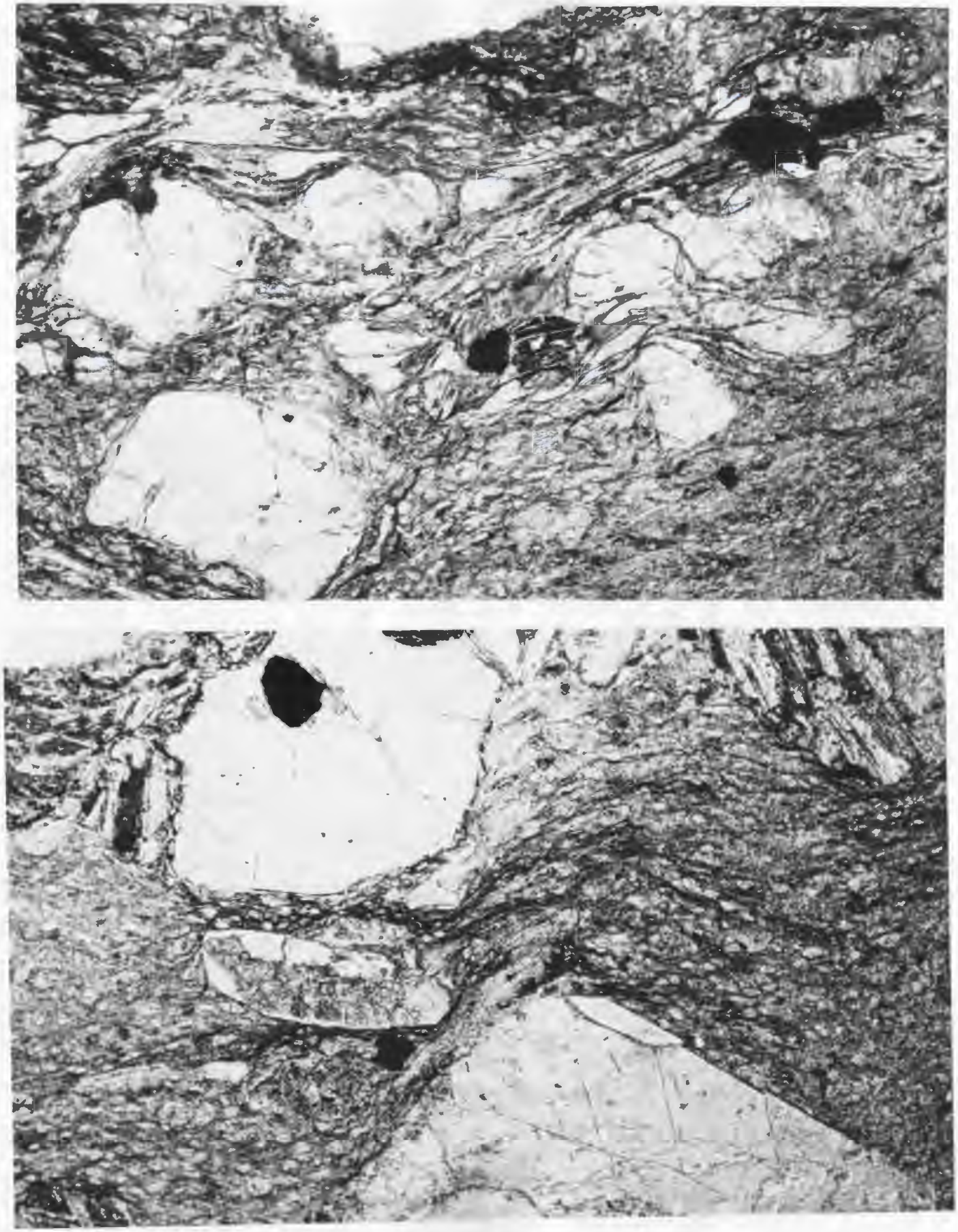

PLATE 3: Photomicrographs of welded Cycle One Dacite. Both samples from the hangingwall of MacLean Orebody. Plane polarized light. x35.

2.2.2.6. Breccia: The Breccia zone occurs as an elongate, discontinuous unit and fills an east-west paleo-trough which existed between the orebodies. A composite isopach map (Fig. 5) of Cycles One, Two and Three Breccias indicates that the zone has an average width of 1500 feet and varies in thickness up to a maximum of over 300 feet north of the Oriental orebodies.

The unit consists of a chaotic mixture of angular to subrounded sedimentary and volcanic fragments in an arenaceous breccia matrix of similar composition. Breccia fragments consist mainly of dacite, siltstone and rhyolite with less common mafic volcanic fragments similar to the Footwall Andesite and Intermediate Footwall, and rare granitic fragments. Massive sulphide and barite fragments are common near the orebodies. Most fragments range in size from three to five inches but all gradations exist from silt to boulders six or seven feet in diameter. The unit is generally unsorted and there is no tendency for larger fragments to be concentrated at the base of the unit. In some portions of the unit elongate fragments are aligned, defining a crude bedding, and the arenaceous fraction may also locally display a faint bedding. In many instances the footwall dacites and siltstones have been scoured immediately prior to breccia deposition. The massive sulphide orebodies variously occur at horizons at the top, within or at the base of the breccia zone, indicating influx of breccia at periods before, during and after ore deposition.

The linear distribution along a paleo-trough, thickness, heterolithic character and chaotic nature of the breccia zone strongly suggests that this unit represents a laharic breccia (terminology after Fisher, 1960a; 1960b).

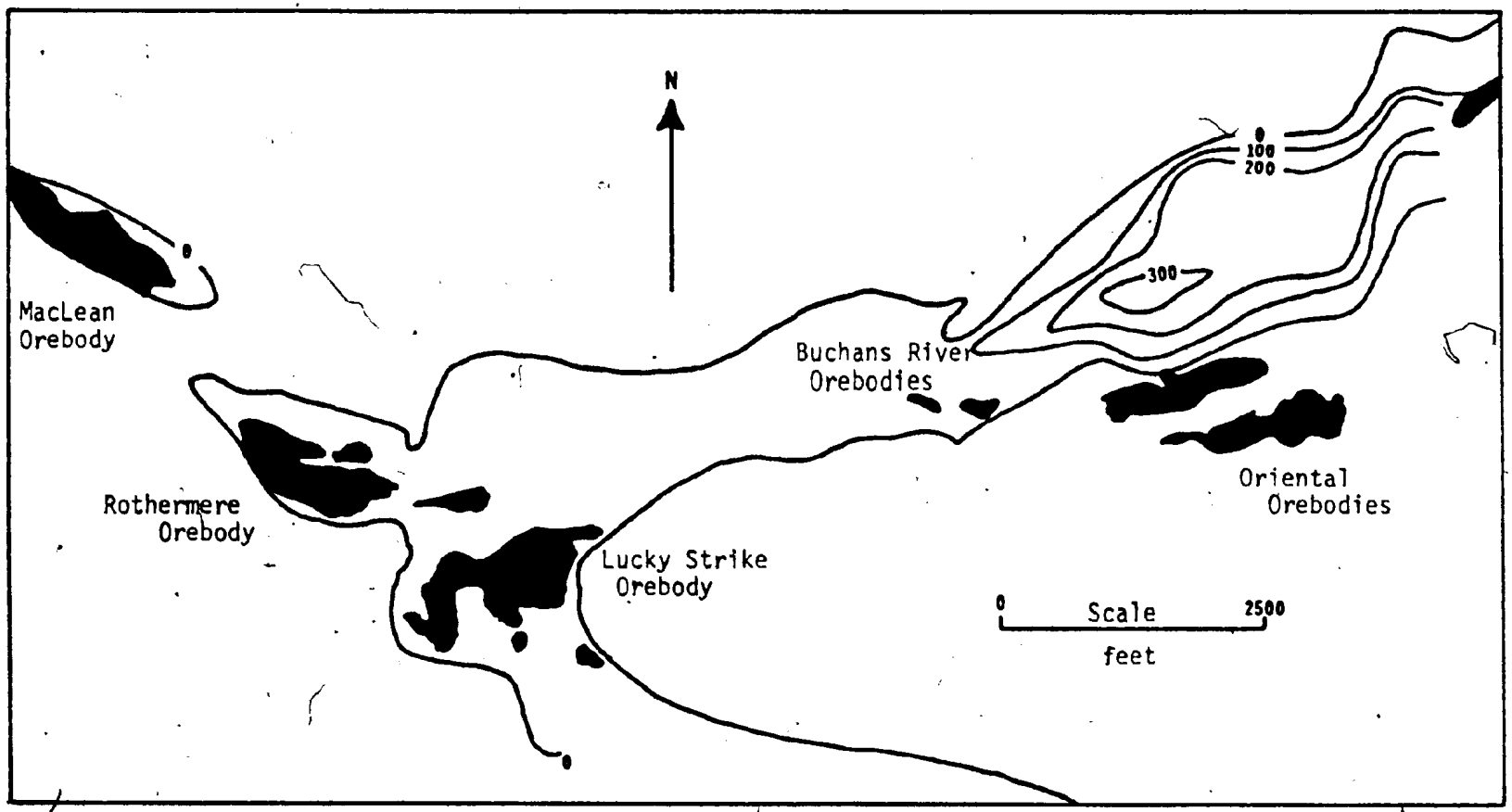

FIG. 5 - Isopach map of Breccia (after Relly, 1960)

There are numerous processes which could be responsible for the formation of the breccia zone, but in this case two mechanisms appear most probable: 1) dislodging of unconsolidated debris on the flanks of a volcanic dome,triggered by heavy rainfall, volcanic earthquakes, or release of water from a crater lake (or any combination of these); or 2) phreatic explosion on the flanks of a volcanic dome and subsequent debris flow down the slope.

Laharic breccias (like ignimbrites) characteristically follow topographic channels moving at speeds up to 60 miles per hour. Single flows may travel more than 100 miles although those of five to ten miles length are most common (Macdonald 1972). The Buchans Breccia has a minimum length of five miles from northeast of the Sandfill prospect to the vicinity of the Clementine prospect and was apparently channeled between a topographic high in the Sandy Lake area and the uplifted inlier of Footwall Andesite immediately south of the Oriental orebodies (Fig. 2). In this context, the source of the flow (and the previous and subsequent ignimbrites) may not be the area of the Sandy Lake "volcanic center" but an area northeast or east of Sandy Lake which is now largely underlain by granite.

The consanguinous relationship between Dacite, Breccia and ore has long been recognized, but the genetic reason for this association has not been clear. However this relationship may be explained in terms of topographically controlled ignimbrites and laharic breccias if the breccia moved rapidly along a topographic channel, was erosive in nature along local highs (explaining the heterolithic composition - e.g. see Fisher 1960a), and

was deposited in depressions within the channel. Similarly, the ore was deposited in the depressions but for somewhat different reasons (see section 2.4. "Origin of the Ore").

The recognition of the origin, source and distribution of the Breccia and Dacite and their relationship to ore is extremely important as it may provide insight into the location of potential exploration targets. After ore deposition there was renewed dacite ash flow activity which levelled the existing topography (Fig. 3).

2.2.2.7. Cycle Two: Cycle Two is characterized by a stratigraphic repetition of Cycle One lithologies. The basal mafic unit, the Cycle Two Andesite, ranges from basaltic to andesitic in composition as opposed to the first cycle Footwall Andesites which are almost entirely basaltic (see section 4.4.2.). The unit consists predominantly of grey-green to black tuffs, agglomerate, flow breccias and massive flows. Pillowed flows have not been recognized. It forms a sinuous east-west belt four miles long, one mile wide and approximately 2000 feet thick (Swanson and Brown, 1962) in the area north of the major orebodies.

The flows are generally feldsparphyric and normally contain 1%-10% augite phenocrysts set in a fine grained matrix of plagioclase microlites and less than 1% opaque oxides. Fluidal textures defined by aligned plagioclase laths are common (Plate 4). Circular and pipe amygdules are ubiquitous and are filled with quartz, prehnite, calcite and chlorite.

The matrix of the flow breccias and agglomerates generally consists of crystal-vitric tuffs composed of broken plagioclase and augite crystals. Quartzo-feldspathic spherulites and wisps of chloritic

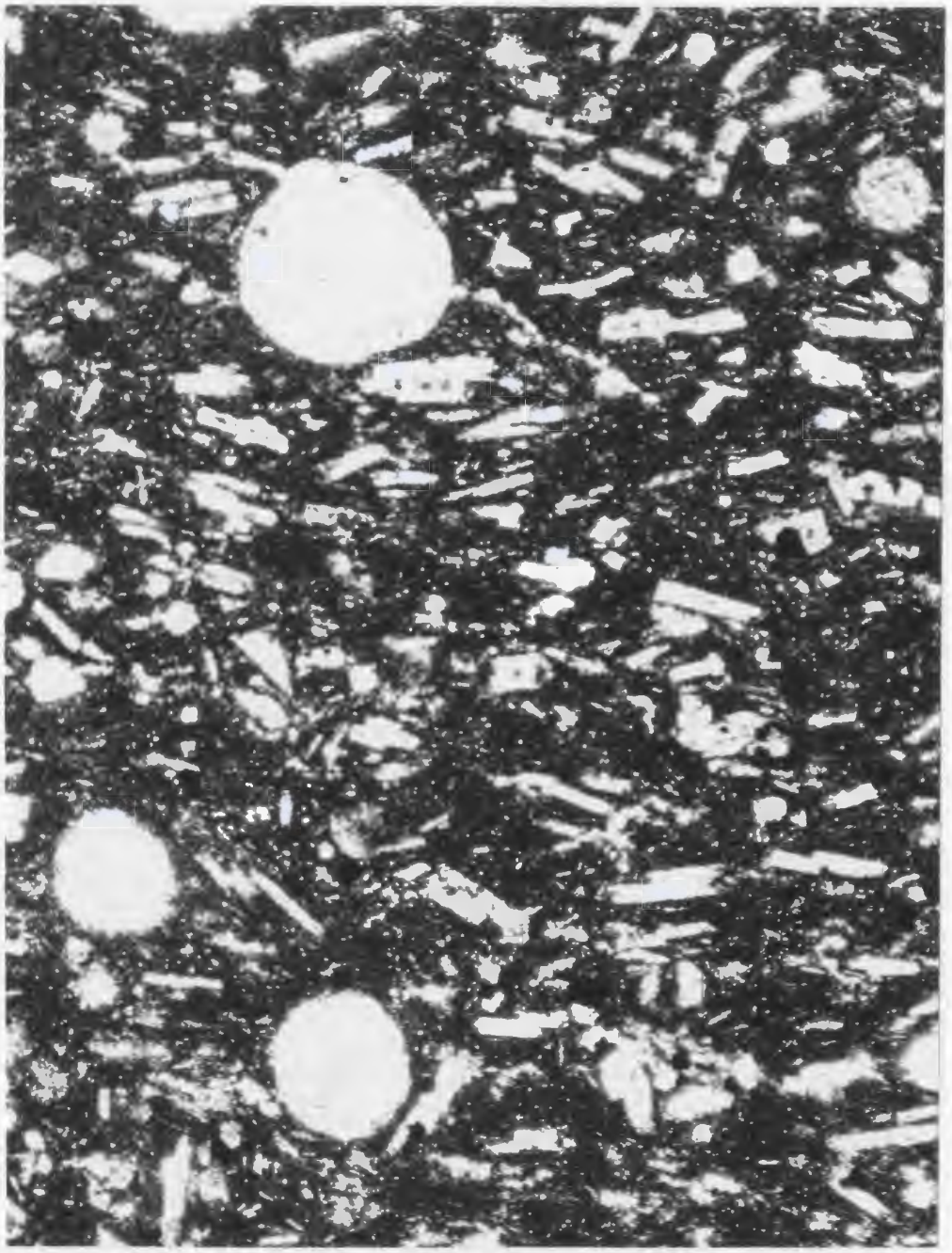

PLATE 4: Photomicrograph of Cycle Two Andesite flow showing aligned plagioclase laths in very fine grained groundmass. Vesicles are filled with quartz, calcite and prehnite. Plane polarized light. x35.

devitrification of original glass are common. Quartz-prehnite fracture filling is common throughout the unit.

The Cycle Two Arkose although not widespread is interbedded with the Cycle Two Andesite in much the same manner as the Cycle One Andesite and Arkose. The Cycle Two Arkose, like the Footwall Arkose, is the slightly reworked equivalent of a felsic crystal-lithic tuff.

The cycle two dacitic ash flows which contain the host breccias for the cycle two orebodies (Oriental and Buchans River) overlie the Cycle Two Andesite. A peculiar feature of the Cycle Two Breccia is the anomalous co-occurrence of well rounded granitic (actually granodiorite) cobbles and boulders with normal breccia. Granite conglomerate in a graded arenaceous matrix often overlies the main breccia zones. The boulders are probably derived from stream beds on the flanks of the volcano which had cut into a subvolcanic plug and subsequently formed a channelway for debris flows. Granite boulders are also present in the Cycle One Breccia but are less widespread than their Cycle Two equivalents.

Massive and flow banded red-brown quartz and feldsparphyric rhyolite flows (Plate 5) are locally voluminous in the upper portions of cycle two. It is possible that the Sandy Lake "volcanic center" was a rhyolite vent whose only product was these viscous rhyolite flows.

2.2.2.8. Cycles Three and Four: Cycles three and four underlie a large portion of the Buchans area (Fig. 2) but, due to a lack of associated mineralization, they have received relatively little attention. A noticeable feature of these cycles is the abundance of felsic volcanics (coarse crystal tuffs and ignimbrites) and the relative paucity of more mafic phases. It is the writer's opinion that, given the correct

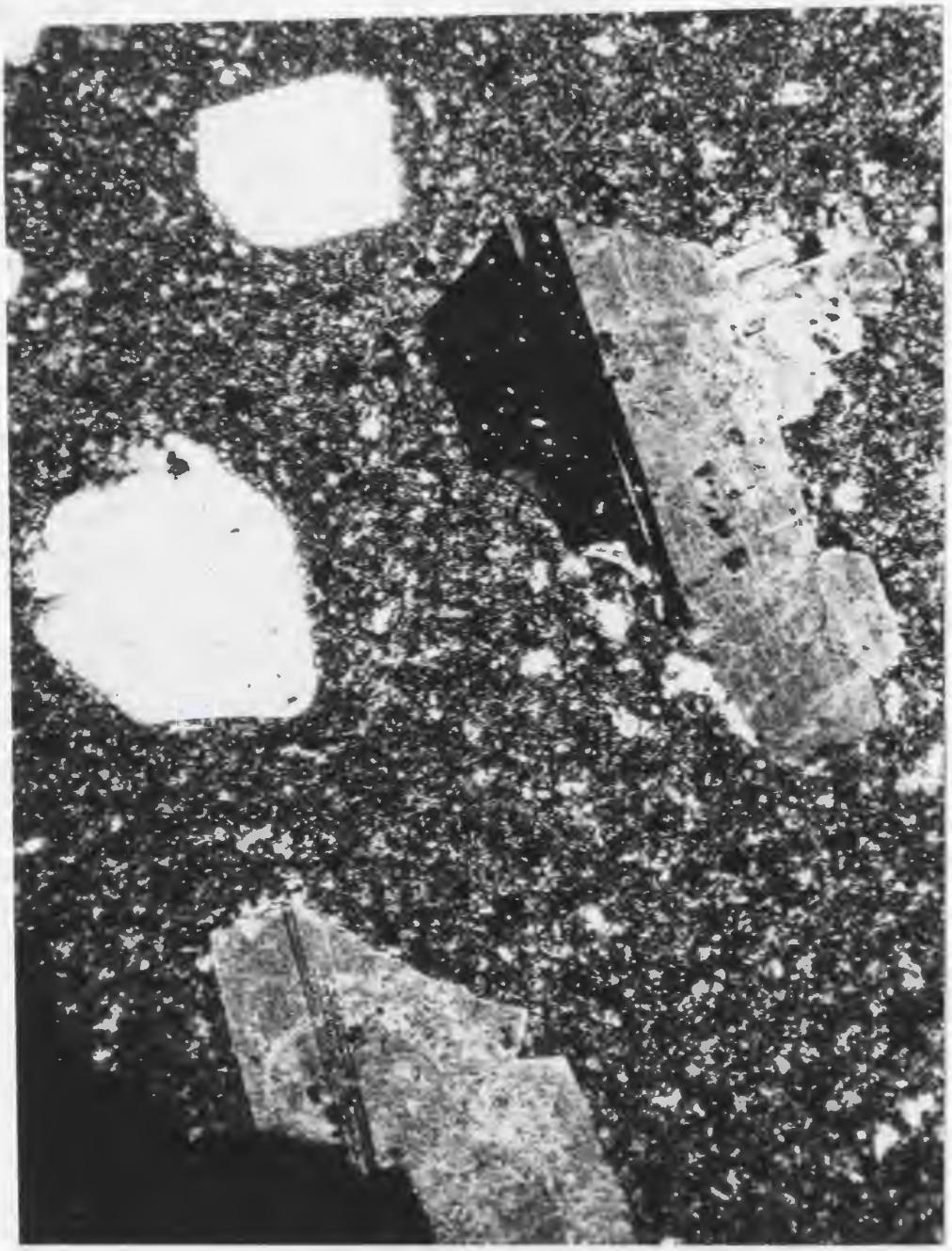

PLATE 5: Photomicrograph of Cycle Two Rhyolite flow. Altered plagioclase and partially resorbed quartz phenocrysts in a holocrystalline fine grained ground mass. Crossed nicols. x35.

environmental conditions in cycles three or four (i.e. depressions, etc.), these may contain significant mineralization. (Archean massive sulphides, for example, are generally best developed in the upper volcanic cycles). The investigation of this possibility might be included in future studies of the area.

2.2.2.9. Diabase: All units in the area are cut by fine to medium grained, dark green to black diabase dikes and sills (Fig. 3). These bodies range in size from small veinlets to several hundred feet thick and are characterized by sub-ophitic labradorite and augite (commonly titaniferous). Calcite-chlorite amygdules are common, indicating a shallow depth of emplacement. While the dikes themselves are genetically unrelated to ore, it has been postulated that they may have filled fractures which originally served as mineralizing conduits to the Intermediate Footwall (E.A. Swanson, personal communication). This hypothesis is the subject of geochemical investigation in section 5.2.

2.3. Description of Ore Deposits

The following descriptive summary of the nature of the ore occurrences at Buchans is based on underground observation, discussion with the mine staff, and from references to Relly (1960). For more detailed documentation the reader is referred to Relly (1960).

Two distinct but genetically related types of ore occur at Buchans, i.e., massive sulphide ore and footwall ore.

2.3.1. Massive Sulphide Ore

Massive sulphides associated with sedimentary horizons within dacitic volcanics occur at two distinct stratigraphic intervals. The MacLean, Rothermere, Lucky Strike, Two Level (Fig. 3) and North orebodies occur within the Cycle One Breccia and are enclosed by Cycle One Dacite. The Buchans River and Oriental orebodies are characterized by more prominent granite conglomerate and occur within Cycle Two Dacite. The major features of all the massive sulphide orebodies are similar, and subsequent discussion will be mainly concerned with these general unifying features.

The massive sulphide orebodies occur as conformable, tabular to lens-shaped bodies and are distributed along the south side and concentric around the Sandy Lake "volcanic center" (Fig. 2). The overall conformable nature of the deposits can be seen in cross section and on a detailed scale underground where primary features of the ore may be seen to parallel ore-host contacts and bedding in the host rocks.

The orebodies are invariably associated with the breccia horizon and/or the granite conglomerate, but are also locally in contact with dacite tuff, siltstone or diabase. Contacts between ore and host rocks are sharp, except where the ore rests on breccia or granite conglomerate where gradational contacts are seen.

The ore consists of a fine-grained mixture of sphalerite, galena and chalcopyrite with lesser pyrite and minor tetrahedrite. Bornite and covellite occur in trace quantities throughout. Enargite, native silver, argentite ruby silver and gold tellurides (?) are found as rare local occurrences. Fine

to coarse grained barite is the most abundant gangue mineral, averaging 26% of the ore. Quartz, calcite, sericite and chlorite are minor but ubiquitous constituents of the gangue.

Three major, mutually gradational, types of ore are generally recognized, i.e., massive structureless ore, baritic ore and breccia ore. The massive ore consists of a random aggregate of fine grained sulphides and contains no readily discernible textures or structures. Baritic ore contains abundant fine to coarse grained barite and is commonly concentrated near or at the top of the orebodies. This upward concentration of Ba constitutes the only zoning of any major ore constituent within the massive sulphide orebodies. Breccia ore contains a chaotic assortment of dacite, rhyolite, siltstone and less abundant Intermediate Footwall fragments suspended in massive or baritic ore.

A number of small-scale local textures and structures may be seen within each of the major ore types. Banded and 'streaky' ore, although not common, occur in all orebodies. Banding is consistently parallel to the margins of the ore body and bedding in the host rocks. 'Streaky' ore consists of discontinuous ore bands and wisps with irregular edges, and is probably a product of pre- and/or post-consolidation deformation of banded ore.

Interesting and important bedding sag structures are found where banded and breccia ore coincide. These structures are caused by the deposition of breccia fragments into a banded sulphide mud causing depression of the bands below the fragment. Since the sulphide is more dense than the

fragment, the fragment floats and subsequent sulphide layers are truncated against the side of the fragment. Further sulphide layering is deposited horizontally above the fragment.

Another interesting local feature of the ore is the occurrence of rounded fragments of ore in a massive ore matrix. Little is known of the extent of this feature due to difficulty in distinguishing fragments from matrix while underground, although several random polished slabs of ore contain ore fragments. The fragments are generally small (less than one inch) and isolated. Relly (1960) noted the presence of large (up to 8 feet) massive and baritic ore boulders in pyroclastic wallrock near the major orebodies. This suggests that large ore boulders might also occur within the main sulphide masses.

Small scale slump structures are seen locally in banded ore and, on a larger scale, portions of random chaotic breccia ore give the overall impression of large scale disruption and slumping of sulphide and contained breccia fragments.

Local scouring of the footwall rocks (siltstone, dacite or breccia), with subsequently deposited sulphides are features seen at the footwall contact of most orebodies. Thin, unmineralized siltstone beds intercalated with the ore are a minor occurrence in some orebodies.

Interpretation of all the above mentioned features will be discussed under the heading 'Origin of the Ore' (Section 2.4.).

2.3.2. Footwall Ore

It has been previously mentioned that the Intermediate Footwall consists of mineralized and unmineralized portions with a gradational contact. The former tends to occur near the top of the unit and consists of disseminated, stringer, vein and stockwork pyrite with minor Cu, Pb, and Zn sulphides. Moderate to intense silicification and/or chloritization of the host rocks is associated with this mineralization. The position of this mineralized Intermediate Footwall is shown in plan in Fig. 2 and in section in Fig. 3. From Fig. 2 it can be seen that the footwall mineralization is closely associated with the Oriental, Lucky Strike and Rothermere massive sulphides but not with MacLean or the Clementine prospect to the west.

The mineralized stockwork grades into concordant lenticular bodies of economic grade directly below or in close proximity to some of the massive sulphide orebodies (especially Lucky Strike). These footwall orebodies are considerably smaller than their massive counterparts and average grade is approximately one third that of the massive sulphides. (A notable exception is copper which is present in about the same abundance). Systematic internal textures and structures in the ore are generally absent. The ore mineralogy is essentially the same as the massive sulphides but grain size is normally medium to coarse. The chief gangue mineral is quartz with lesser carbonate and barite.

A brief summary contrasting footwall and massive sulphide occurrences is given in Table 1.

TABLE 1

SUMMARY OF CHARACTERISTICS OF MASSIVE SULPHIDE AND FOOTWALL ORE

Criteria	Massive Sulphide Ore	Footwall Ore
General description	Conformable tabular to lens shaped bodies.	Stringer and stockwork mineralization grading into higher grade irregular to lens shaped bodies. Two massive occurrences.
Stratigraphic position.	In depressions within Cycle One and Cycle Two Dacite.	Within Intermediate Footwall and generally closely associated with overlying massive sulphides.
Tonnage	Individually from 70,000 to 5,500,500 tons.	Up to 155,000 tons.
Grade	14.97% Zn, 7.73% Pb, 1.37% Cu, 3.73 oz. Ag, .046 oz. Au.	Approximately one third that of massive sulphides except Cu which is about the same in both.
Ore mineralogy	Mainly sphalerite, galena, chalcopyrite and tetrahedrite.	Same as massive sulphides.
Gangue mineralogy	Mainly barite.	Mainly quartz with minor barite and calcite.
Grain size	Fine grained.	Medium to coarse grained
Associated lithologies	Breccia, Granite Conglomerate and Siltstone.	Intermediate tuffs.
Contact relations with wallrock	Generally very sharp.	Generally diffuse.
Wallrock alteration	Variable from none to strong silicification and sericitization.	Moderate to strong silicification, sericitization, chloritization and pyritization.

It is interesting to note that nowhere has there been found any physical connection between footwall and massive ore types. They are invariably separated by 6 inches to several tens of feet of barren dacite and/or siltstone. However, the mineralized Intermediate Footwall was exposed at the time of deposition of the ore as indicated by fragments of this unit which are found within the ore.

2.4. Origin of the Ore

An integrated interpretation of the local geological environment and the nature of the orebodies compels one to ascribe the origin of the ore to a syngenetic volcanic exhalative process. Although Relly (1960) presented several arguments in favour of an epigenetic origin, virtually all these may be not only explained in terms of syngenesis, but may be used as evidence for a syngenetic origin.

All the previously mentioned descriptive textures and features of the deposits provide strong support for a syngenetic origin. The overall conformable nature of the ore, sharp contacts with wallrocks and the presence of banded (bedded) ore with sedimentary intercalations strongly suggest that the ore is a distinct sedimentary bed. Bedding sag structures provide unequivocal evidence that the ore formed at the (sea?) water-sediment interface as a plastic sulphide aggregate. Small scale slump structures, possibly triggered by earthquakes, volcanic explosions, or changes in slope due to activity in the subvolcanic magma chamber, give the impression of an uneasy quiescent phase in volcanism. The same unstable environment would be responsible for influx of Breccia and Granite Conglomerate into topographic lows. Instability would also cause local scouring of the footwall contact as well as horizons within the ore, thus forming ore fragments, pebbles and boulders, which were deposited within or outside the margins of the orebody.

The above features give insight into the type of environment and processes operative during ore formation but the sequence of events leading to ore deposition and the mechanism of deposition require further discussion.

Four major features appear to have exerted strong spatial control on mineralization:

1) The orebodies are situated along a linear zone between the Sandy Lake volcanic center and the footwall inlier to the south.

2) The ore is associated with sedimentary horizons enclosed in dacite.

3) The orebodies occur in paleotopographic depressions.

4) Most deposits are closely associated with epigenetic stockwork mineralization in the footwall.

Within the confines of these controlling factors, the following sequence of events may be postulated:

1) an initial stockwork mineralization of the Intermediate Footwall by fluids emanating from a parasitic fumarole on a temporarily inactive volcanic center.

2) formation of the MacLean pit crater and subsequent partial filling with siltstone followed by terrestrial dacite.

3) slight renewed subsidence of the MacLean depression and initial subsidence of Lucky Strike, Rothermere, etc. depressions.

4) shallow water deposition of siltstone and minor crystal-rich washed dacite tuffs in the depressions.

5) a second period of stockwork mineralization in the Intermediate Footwall with expulsion of metal-bearing fluids into sea water and subsequent deposition as sulphide in topographic depressions.

6) influx of Breccias and Conglomerate into depressions at various periods before, during and after sulphide deposition.

7) slight uplift and, with the onset of more oxidizing conditions, more prominent deposition of barite.

8) emergence above water and inundation by dacitic ignimbrites.

9) a complete repetition of the above sequence in Cycle Two.

2.5. Buchans as Compared to other Massive Sulphide Deposits

The Buchans deposits are massive volcanogenic sulphides and, as such, display numerous characteristics similar to other such deposits throughout the world. This group of deposits can be broadly divided into two genetic types, i.e. those formed at accreting plate margins and those formed at consuming plate margins (Strong, 1973b). The former includes the cupreous pyrite deposits of ophiolite affinity (Troodos, Betts Cove, etc.) while the best examples of the latter are the Japanese Kuroko deposits. The Archean deposits are also included in the latter on the basis of numerous similarities. The Buchans deposits show little environmental similarity to the ophiolite type mineralization but show strong similarities to the Archean and Kuroko deposits.

Generally speaking the Archean, Kuroko and Buchans deposits are all similar in the following respects:

1) The deposits occur as stratabound lenses associated with breccia horizons within felsic volcanics.

2) They generally have sharp boundaries with wallrock and display numerous internal submarine sedimentary structures and textures.

3) Stringer and stockwork mineralization is characteristic of the footwall of most deposits.

4) The ores owe their origin to submarine volcanic exhalative activity.

The Buchans deposits differ from either one or both of the Archean and Kuroko deposits in several respects. Both Archean and Kuroko deposits are situated on the summit or flanks of domal rhyolite or dacite bodies characterized by coarse agglomerates and various volcanic breccias in the Archean case (e.g. Sangster, 1972) and by steam explosion breccias in the Kuroko case (e.g. see Horikoshi, 1969; Tatsumi, 1970). At Buchans, neither agglomerate nor extensive volcanic breccia are widespread. The Buchans breccia zones may, however, represent the product of local, near surface steam explosion. The felsic volcanic host rocks at Buchans are more sheet-like than domal in aspect although a small original dome may have subsided within the Sandy Lake volcanic center.

Sediments closely associated with both Buchans and Kuroko deposits tend to be of the fine grained volcaniclastic type whereas sedimentation associated with Archean deposits is dominantly chemical, consisting of chert and iron formation.

The Buchans deposits and some Kuroko deposits are associated with depressions in the immediate footwall rock whereas no such relationship is seen in the Archean. This may be a function of more widespread reducing conditions in the Archean, obviating the necessity of a specialized local reducing environment.

The ore mineralogy at Buchans is similar to Kuroko ore per se and unlike the Archean assemblages which tend to be considerably more Fe

sulphide rich, somewhat richer in copper, proportionately poorer in zinc and rarely contain significant lead. Precious metal content at Buchans is intermediate between the high Au, low Ag Archean and lower Au, high Ag Kuroko deposits. Gangue mineralogy at Buchans is again more akin to the Kuroko type and unlike the barite-free Archean type. Neither gypsum nor anhydrite occur at Buchans.

Zoning at Buchans is neither exactly similar to that in typical Archean nor typical Kuroko deposits although it shows more similarity to the latter. Archean deposits are characterized by a chloritizted, silicified, sericitized and pyritized copper rich stockwork which grades upward into a pyrrhotitic Cu-Au-rich base of the massive sulphide. The upper portions of the orebody are generally pyritic and Zn-Ag-rich. Pyritic cherts and/or iron formation often overlie the orebodies.

Zoning in the Kuroko deposits is roughly similar to the Archean type but is somewhat more complex. Disseminated and stockwork Cu bearing siliceous ore (Keiko) generally forms the base of mineralization and grades upward into chalcopyrite-pyrite yellow ore (Oko). This is in turn generally overlain by black Kuroko (sphalerite) ore with a baritic cap. A (pyritic) hematite-quartz bed commonly overlies baritic ore. Both Ag and Au tend to be concentrated mainly in the Kuroko.

At Buchans, host rocks to the stockwork mineralization are both silicified and chloritized, i.e. akin to both Kuroko and Archean types. Stockwork ore is pyritic but contains abundant Zn and Pb unlike the Kuroko type. Copper, while volumetrically subordinate to Zn and Pb is relatively

enriched on a metal ratio basis compared to the massive ore. The base of the Buchans orebodies is not Cu-rich nor is there any gradation from stockwork ore to massive sulphides as in the Archean or Kuroko types. Massive Buchans ore is similar to black Kuroko ore and grades upward to baritic ore. Unlike the Archean and Kuroko, no silica-iron sediments overlie the Buchans orebodies.

A final point of comparison is the abundance of terrestrial volcanics associated with the Buchans deposits as opposed to the entirely submarine Archean and Kuroko types.

CHAPTER 3

FIELD, LABORATORY, AND STATISTICAL METHODS

3.1. Sample Collection and Preparation

Diamond drill core samples of about one pound were obtained from the core sheds at Buchans. It was originally planned that samples be taken from three intersecting cross sections and that these be supplemented by additional underground and surface samples. Towards this end, 1600 drill core samples, 145 underground samples and 40 surface samples were taken. Core samples were taken at a maximum interval of 25 feet and additional samples were taken where added detail was necessary in order to gain coverage of all important units.

From the 1600 core samples, 625 were chosen for analysis. The basis for this choice depended mainly on the desired sample density for each section of core and the degree to which the sample was representative of the section of core involved. Samples selected for analysis were washed, logged and put into clean sample bags prior to crushing. One half to two thirds of each sample was subjected first to a coarse crush and then a fine crush on a Denver steel jaw crusher. Representative portions of the crushed samples were placed in vials and sent to ASARCO's geochemical laboratory in Salt Lake City for trace element analysis. Duplicate sets are on file at Buchans, one in vials and one in sample bags.

Ten grams of the fine crushed material was pulverized to -100 mesh in Coors alumina ball mills mounted in a paint shaker. Care was taken throughout the procedure to ensure that contamination was held to an absolute minimum.

During the crushing and grinding program it was decided that, for a variety of reasons, it would not be wise to attempt to analyse and interpret the results of all 625 samples within the scope of this thesis. It was consequently decided to focus attention on the N60W section for the reasons outlined earlier. The 293 pulverized samples from this section were shipped to St. John's for analysis for major elements.

3.2. Analytical Procedures

Preparation for major element analysis was similar to that described by Langmhyr and Paus (1968). All major elements were determined by the author at Memorial University on a Perkin Elmer model 303 atomic absorption spectrophotometer equipped with a recorder readout.

Samples were first dried overnight at 100^{o} C and subsequently shaken to ensure homogeneity. Precisely 0.2000 grams were then weighed into a plastic cap and placed in a polycarbonate digestion bottle. Digestion was effected by the addition of 5 ml. HF and heating on a water bath for 30 minutes. The samples were then allowed to cool and 50 ml. of saturated Boric acid was added in order to complex undissolved fluorides. The solution was again heated on the water bath until the entire sample was digested and finally removed, cooled and diluted with 145 ml. distilled and de-ionized water to yield 200 ml. of 1000 ppm solution.

For samples containing sulphides it was first necessary to add 5 ml. aqua regia, heat for 20 minutes and then follow the same procedure as above except for the addition of 5 ml. less water.

Standards were prepared in a manner similar to that described by Abbey (1968).

Phosphorus was determined on a Bausch and Lomb Spectronic 20 colorimeter according to a method somewhat modified after Shapiro and Brannock (1962).

Loss on ignition was determined by weighing an amount of sample in a porcelain crucible, heating to 1050° C for two hours, cooling in a dessicator, and weighing to determine the percent weight loss of volatiles (principally CO_2, H_2O and SO_2).

Samples totalling between 98% and 101.5% were considered acceptable. Those totalling outside these limits were subjected to scrutiny for errors. If no apparent errors were found, the sample was reweighed and a total analysis was repeated. In some cases the subsequent analysis showed a weighing error in the original attempt or an error in analysis for one element. In other cases the replicate analysis was nearly identical to the original, indicating 1) that some element(s) (usually Ba) was present in addition to the analysed major elements, and/or 2) that there had been oxidation of ferrous iron during heating for loss on ignition causing the net loss on ignition to be low. (This effect was especially noticeable on sulphide samples).

Analytical precision was determined by choosing a sample intermediate in composition within the expected range, and preparing 13 separate solutions of this sample together with the regular samples. One precision sample was included in each analytical batch. The results of the precision test are shown in Table 2.

TABLE 2

PRECISION OF ATOMIC ABSORPTION MAJOR ELEMENT DETERMINATIONS

Element	Number of Determinations	Mean (Weight %)	Standard Deviation	Coefficient of Variation (%)
SiO_2	13	65.4	.82	1.25
TiO_2	13	.40	.01	2.50
Al_2O_3	13	14.29	.21	1.47
Fe_2O_3	13	4.59	.10	2.18
MnO	13	.11	.01	9.09
MgO	13	1.71	.03	1.76
CaO	13	3.47	.05	1.44
Na_2O	13	1.88	.03	1.60
K_2O	13	3.40	.05	1.47
P_2O_5	13	.05	.03	60.0
Loss Ig.	13	3.89	.14	3.60

Accuracy was determined by comparison to the United States Geological Survey standard BCR-1. The results of the accuracy test are shown in Table 3.

Rock chips sent to the ASARCO laboratory at Salt Lake City for trace element analysis were ground at -50° C to prevent loss of Hg vapour. Hg was subsequently determined on a modified Perkin Elmer 303 using a flameless method. Zn, Mo, Cu, Pb, Ni, Co, V and Ag were determined by conventional atomic absorption methods using a background correction for non-specific absorption (L.D. James, personal communication).

Precision of trace element analyses was determined by replicate analysis of every tenth sample. The results of the precision test are given in Table 4.

Rb, Ba, Sr, Zr, and Cr were determined at Memorial University by X-ray fluorescence on pressed powder discs using a Phillips 1220-C Automatic X-ray fluorescence spectrometer. Typical precision and accuracy data are given in Tables 5 and 6 respectively.

TABLE 3

ACCURACY OF ATOMIC ABSORPTION MAJOR ELEMENT DETERMINATIONS

Wt. %	A*	Mean	Standard Deviation	Number of Determinations
SiO_2	54.36	55.38	0.37	4
TiO_2	2.24	2.35	0.18	4
Al_2O_3	13.56	13.50	0.27	5
Fe_2O_3	13.40	13.00	0.28	5
CaO	6.94	6.63	0.07	4
MgO	3.46	3.57	0.06	5
Na_2O	3.26	3.23	0.05	5
K_2O	1.67	1.73	0.05	4
MnO	0.19	0.18	0.01	5

* Proposed values after Abbey (1968).

TABLE 4

PRECISION OF ATOMIC ABSORPTION TRACE ELEMENT DETERMINATIONS

Element	Number of Determinations	Range of Analysed Samples (ppm)	Average Coefficient of Variance (%)
Cu	25	2 - 9700	2.39
Pb	23	1 - 23000	5.30
Zn	26	10 - 115000	4.74
Mo	9	3 - 124	14.57
Ag	12	0 - 140	4.37
Hg	24	4 - 3466 (ppb)	11.21
Co	24	2 - 48	3.35
Ni	26	0 - 80	1.74
V	23	0 - 520	6.31

TABLE 5

PRECISION OF X-RAY FLUORESCENCE TRACE-ELEMENT DETERMINATIONS (N = 45)

Element	Mean	Standard Deviation	95% Confidence Interval for Mean
Zr	156 ppm	6.7 ppm	154.1 - 158.1 ppm
Sr	232	6.3	230.5 - 234.1
Rb	180	3.0	178.7 - 180.4
Ba	3668	236	3800 - 3937
Cr	362	2.0	361.1 - 362.9

TABLE 6

ACCURACY OF X-RAY FLUORESCENCE TRACE ELEMENT DETERMINATIONS

AT ONE STANDARD DEVIATION

Element	Accuracy	Number of Samples	Range of Analysed Samples
Zr	± 12.8 ppm	16	80 - 540 ppm
Sr	18.3	19	66 - 850
Rb	6.4	23	5 - 250
Ba	33.4	18	120 - 1950
Cr	18.7	15	20 - 650

3.3. Statistical Procedures and Methods of Data Presentation

Upon completion of the analytical program, the major and trace element results were punched on separate computer cards according to the format shown in Fig. 6. The individual samples were subsequently assigned to the major lithologic groups to which they belong (e.g. Footwall Andesite, Cycle One Dacite, etc.) and means, standard deviations and coefficients of variance (100x standard deviation/mean) were calculated for all elements in each group. Samples were also arranged according to drill hole number and lithologic groups in each drill hole were defined. Means, standard deviations and coefficients of variance were computed for each sub-group in order to study lateral geochemical variations within each major lithologic unit.

A standard statistical program was then employed to plot variation diagrams, histograms and calculate Pearson correlation coefficients for all elements in each major lithologic group.

Another program was designed to plot the concentration of individual elements against depth on the N60W section as an aid in recognizing vertical geochemical trends through the sequence. The coordinates of each sample point and the corresponding chemical analyses were fed on magnetic tape to a PDP-12 computer which relayed plotting instructions to a Calcomp plotter. These diagrams are described and interpreted in section 5.2.

The non-parametric Mann-Whitney U test, as described by Siegel (1956), and successfully used by Davenport & Nichol (1972), was used to statistically compare various groups of data. The U test was chosen because of the generally non-Gaussian distribution of the elements, the small number of samples in each group and, in some cases, the widely

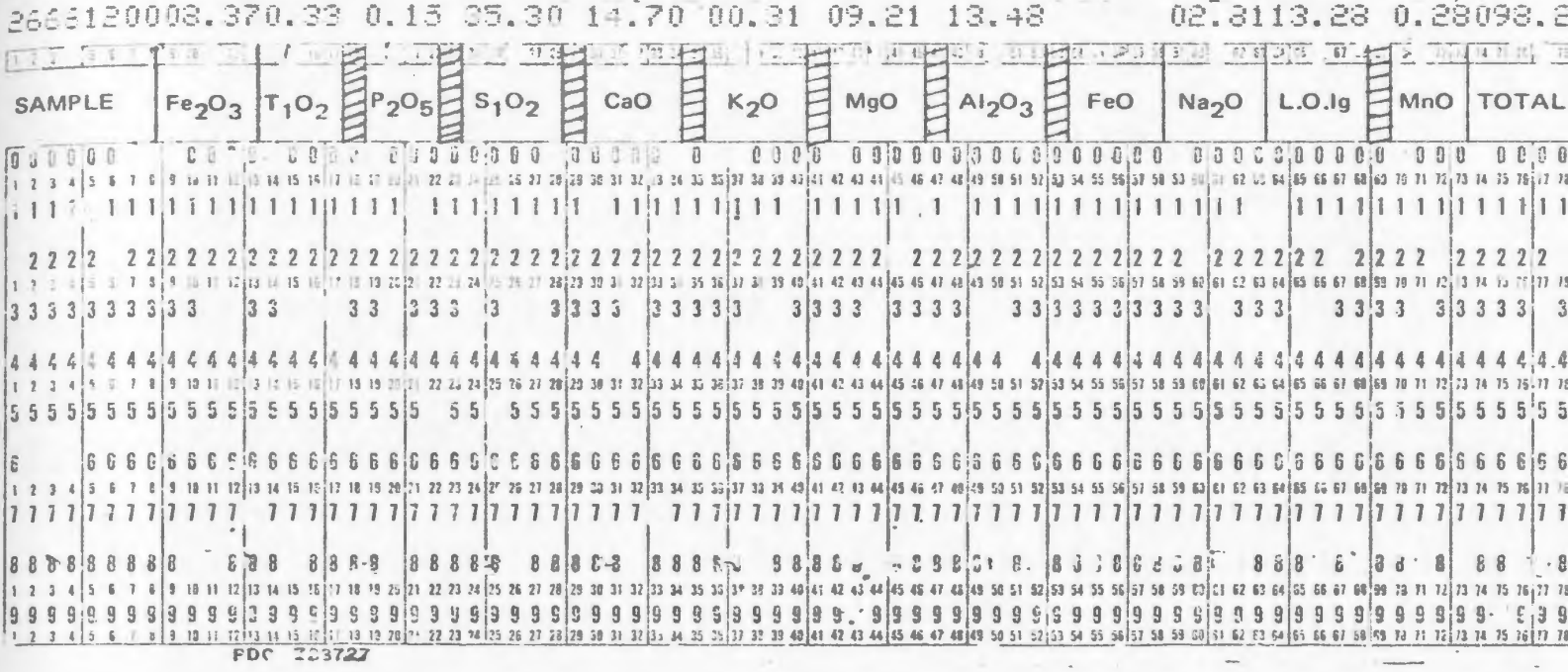

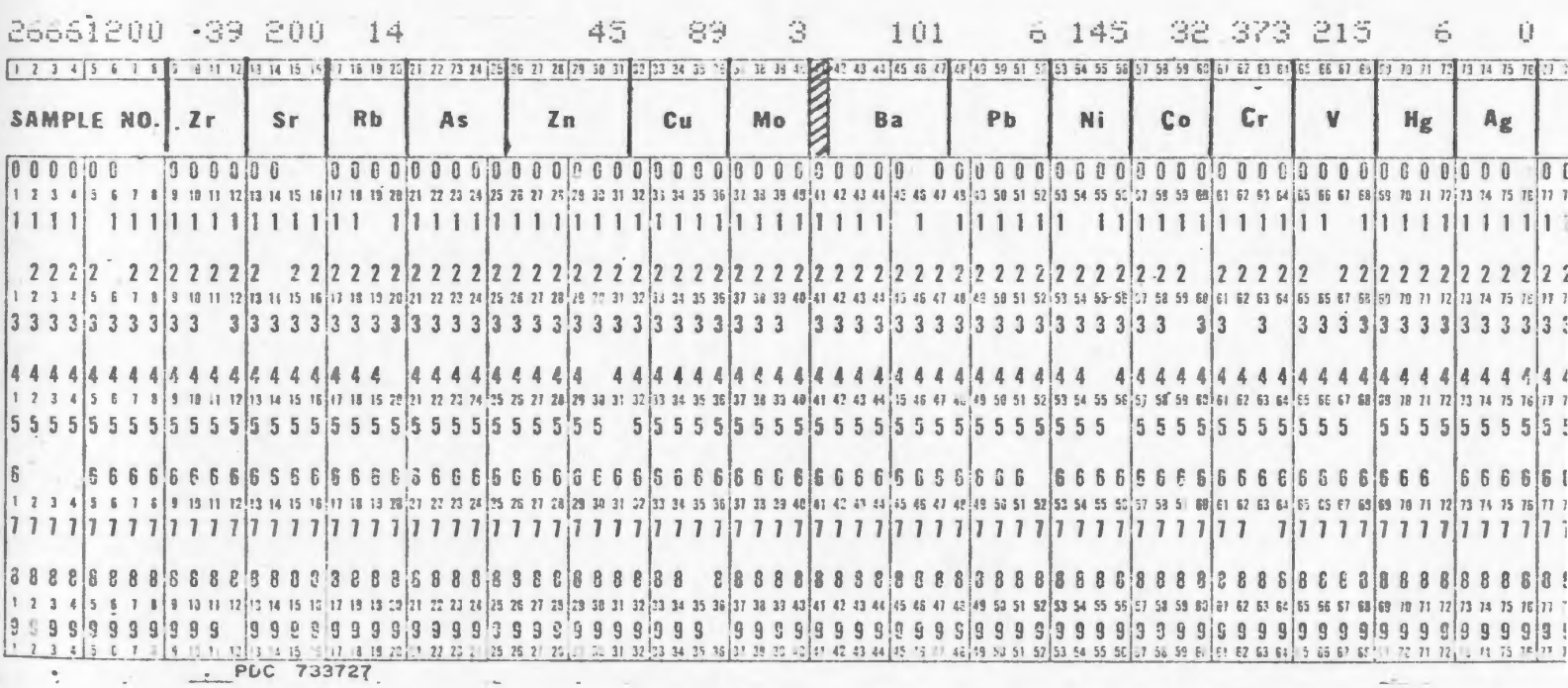

Fig. 6. Major and trace element computer format.

differing variances of some elements between groups. The Mann-Whitney U test, like the Students t test, determines the probability that two groups of data were drawn from the same population.

CHAPTER 4

GENERAL PETROCHEMICAL SETTING

4.1. Introduction

It is of both academic and practical exploration interest to gain an understanding of the petrochemical setting of the host rocks of the Buchans orebodies. Such knowledge is of academic significance in that it enables a more detailed and accurate reconstruction of the geological processes which have been responsible for the development of the Central Mobile Belt of the province. An understanding of this evolution is of critical importance to the exploration geologist in defining metallogenic characteristics of an area and in choosing specific exploration targets.

A major proportion of Phanerozoic massive volcanogenic sulphide deposits is formed at consuming plate margins within volcanic rocks of calc-alkaline magmatic affinity. In the subsequent sections of this chapter, the writer describes the general petrochemistry of the Buchans Group and demonstrates the island arc-type, calc-alkaline nature of the volcanic rocks. The regional extent of this island arc-type volcanism is not known, but should be investigated in future studies.

4.2. The Effect of Secondary Processes on Chemical Compositions

Before discussion of the chemistry of the volcanic rocks of the Buchans area, a comment on the effects of geochemical changes due to secondary processes is in order. The writer is of the opinion that the sub-greenschist to low greenschist metamorphism of the Buchans area has

caused little or no bulk introduction or removal of elements from the volcanic rocks, as similar conclusions have been reached by numerous other authors (e.g. Jolly and Smith, 1972; Thompson, Esson and Dunham, 1972). However local redistribution of some elements has undoubtedly taken place, causing widespread scatter on several of the variation diagrams. Ca and, to a lesser extent Si, have been mobile in the mafic lavas, as evidenced by calcite, prehnite and quartz filling vesicles and fractures. The alkalis have undoubtedly also been redistributed during the formation of these minerals. Samples containing abundant vesicle and fracture filling have been omitted from most geochemical discussion. Substitution of Na for K, and vice versa, has been widespread in the glassy portions of the ash flows as demonstrated by a strong negative correlation between these elements, but total alkali content remains essentially constant indicating only local re-adjustments, a feature also noted in the Pilleys Island region to the north of Buchans (Strong, 1973a). Dispersion of very mobile elements such as Hg from the orebodies possibly provides an indication of the extent of secondary migrations. In the case of Hg, diagenetic and metamorphic processes have caused dispersion only on the scale of a few feet (see section 5.2.). If this is the case, then elements much less mobile than Hg have probably migrated proportionally shorter distances.

Nevertheless, it is apparent that varying degrees of depositional enrichment of certain elements has occurred primarily due to subaqueous precipitation, particularly in the basaltic and andesitic tuffs. Fine grained vitric and crystal tuffs, especially in the Footwall Andesite,

locally display strong concordant hematization which was presumably developed at deposition. The fine grained pyrite present in the matrix of several specimens is probably the product of syngenetic deposition from volcanically charged waters under reducing conditions. There is also evidence (see Chapter 5) that other elements, notably Ba, have also undergone depositional enrichment in parts of some units.

With respect to the elemental abundances discussed in this section, it is apparent that an average of a large number of samples will tend to nullify the effects of local migrations as the population will presumably include samples at all phases of migration. In this regard, the averages are probably a reasonable approximation of the original composition. However, the effects of depositional enrichment are superimposed on the averages and quantitative estimates of their contribution are difficult if not impossible.

4.3. General Magmatic and Geochemical Characteristics of Island Arcs

Studies of recent island arcs during the past decade have revealed a distinct spatial relationship between island arc magmatism and the dipping subduction zone beneath the arc. Seismic, gravity and heat flow data (e.g., Sykes, 1966; Isacks et al., 1968; Gorshkov, 1970) are consistent with the hypothesis that oceanic crust is consumed beneath island arcs. Geochemical evidence indicates that the resultant magmatism is related to partial melting of the upper portions of the descending slab and not to contamination or fractional crystallization of a parent basaltic magma (e.g., Taylor, 1968).

Within island arcs there exists a continuous spatial and temporal variation of magma types directly related to the depth to the Benioff zone (e.g., Kuno, 1966; Sugimura, 1968). Mature island arcs consist dominantly of island arc tholeiite (approximately 85%) with considerably less abundant calc-alkaline (12.5%) and shoshonitic (2.5%) magmatic types (Jakeš and White, 1971) which are distributed from trench to continent side of the arc respectively (Fig. 7). Superimposed on this spatial variation is a less pronounced temporal variation from tholeiitic to progressively younger calc-alkaline to shoshonitic magmatism.

Several other consistent geochemical variations have been shown to parallel the major magmatic variations (e.g., Dickinson and Hatherton, 1968; Jakeš and White, 1969, 1970, 1971, 1972). Island arc tholeiites are geochemically intermediate in composition between abyssal tholeiites (from which they appear to be derived by high degrees of partial melting at shallow depth) and the more evolved calc-alkaline and shoshonitic suites with which they are associated (Table 7). They display a moderate degree of iron enrichment at intermediate compositions (moderate FeO/MgO) and Ni and Cr abundances between that of abyssal tholeiitic and calc-alkaline high alumina basalt. The degree of iron enrichment and Ni and Cr abundances decreases systematically from island arc tholeiite to calc-alkaline to shoshonitic magma types (Table 7). However the large cations (K, Rb, Cs, Sr, Ba, Pb) display the most significant variations across island arcs and show a consistent increase from island arc tholeiite to calc-alkaline to shoshonitic magmatic associations. Na/K and K/Rb ratios exhibit corresponding decreases.

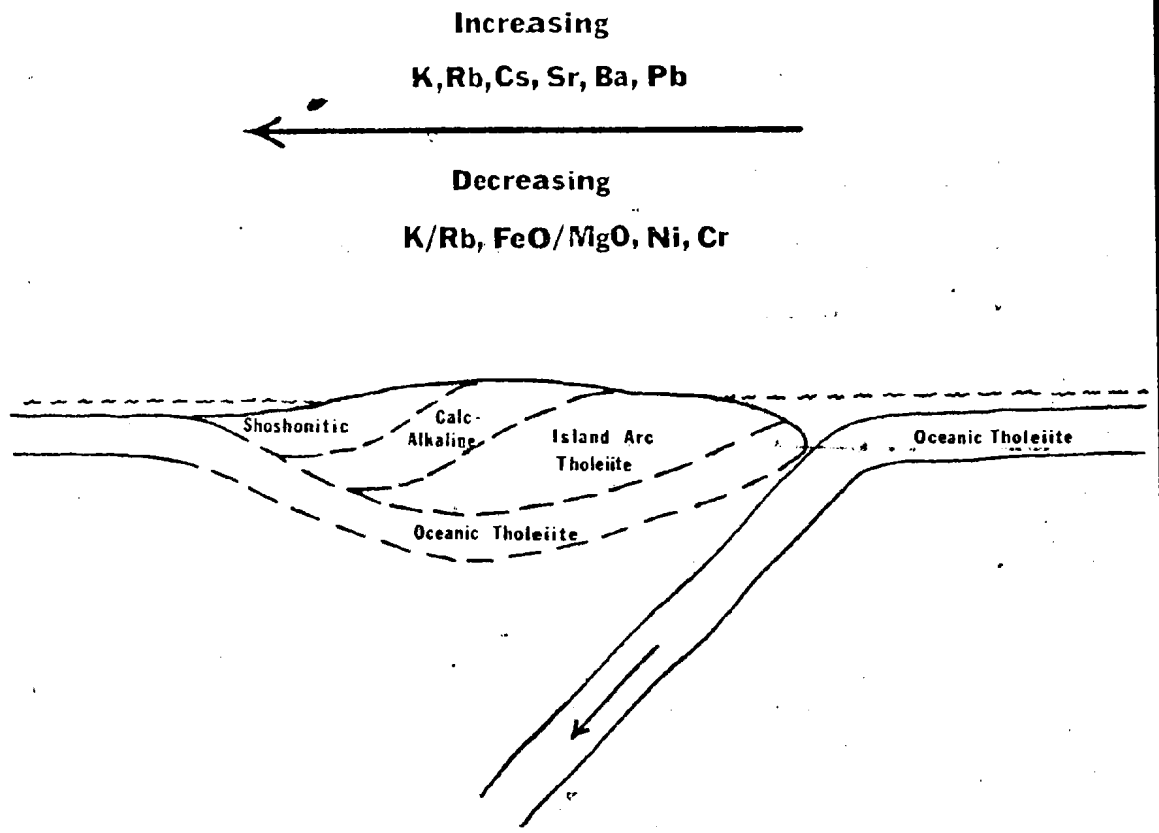

Fig. 7. Schematic diagram showing spatial & temporal relationships between the various suites comprising modern island arcs and geochemical variations across the arc.

TABLE 7

TYPICAL AVERAGE CHEMICAL ABUNDANCES OF SOME VOLCANIC SUITES COMPARED TO BUCHANS VOLCANIC ROCKS

Weight Percent	Abyssal Tholeiite	Island Arc Tholeiite		High Al Basalt	Low Si Andesite	Low K Andesite	Andesite	High K Andesite	Dacite	Rhyolite	Shoshonite	High Ti Diabase	Low Ti Diabase	Footwall Andesite	Cycle Two Andesite	Intermediate Footwall	Dacite	
		Basalt	"Andesite"														Hanging Wall	Footwall
	(i)	(ii)	(ii)	(ii)	(ii)	(ii)	(ii)	(ii)	(ii)	(iii)	(ii)	(17)****	(8)	(20)	(47)	(23)	(50)	(24)
SiO_2	49.34	51.57	57.40	50.59	54.54	59.05	59.64	58.52	66.80	74.22	53.74	46.7	47.4	52.46	57.58	58.74	73.43	73.67
TiO_2	1.49	.80	1.25	1.05	1.13	.69	.76	.76	.23	.28	1.05	2.00	.83	.89	.63	.47	.23	.23
Al_2O_3	17.04	15.91	15.60	16.29	16.26	17.07	17.38	16.20	18.24	13.27	15.84	15.52	15.82	17.81	16.95	16.86	14.15	13.32
Fe_2O_3*	8.81	9.78	8.49	8.74	7.71	6.47	5.26	6.21	2.27	1.80	8.10	11.71	10.49	11.95	9.49	9.79	2.14	2.37
MnO	.17	.17	-	.17	.12	.15	.09	.09	.06	.05	.11	.20	.18	.16	.16	.36	.09	.08
MgO	7.19	6.73	3.38	8.96	6.97	3.25	3.95	4.14	1.50	.28	6.36	6.25	7.28	5.93	4.31	7.08	.93	1.69
CaO	11.72	11.74	6.14	9.50	7.50	7.09	5.92	5.59	3.17	1.59	7.90	8.95	8.73	6.52	6.47	.99	2.33	1.99
Na_2O	2.73	2.41	4.20	2.89	3.64	3.80	4.40	3.64	4.97	4.24	2.38	3.06	2.35	2.18	2.87	1.98	2.93	2.78
K_2O	.16	.44	.43	1.07	1.49	1.27	2.04	2.67	1.92	3.18	2.57	.45	.91	1.89	1.62	2.10	2.99	2.57
P_2O_5	.16	.11	.44	.21	.23	.20	.28	.25	.09	.05	.54	.36	.23	.14	.14	.11	.05	.07
Loss Ig.**	-	.45	-	.81	1.31	.64	1.08	1.47	.26	-	1.09	4.95	5.87	-	-	-	-	-
ppm																		
Rb	1.2	5	6	10	-	-	30	-	45	108	75	19	28	37	30	40	74	51
Ba	14	75	100	115	-	-	270	-	520	870	1000	460	933	1261	941	1290	1684	1463
Sr	130	200	220	330	-	-	385	-	460	125	700	349	298	252	281	91	226	188
Zr	95	70	70	100	-	-	110	-	100	160	40	169	86	72	71	86	125	103
Nb	-	-	-	-	-	-	1.1(iv)	-	-	2.6	-	3	3	3	3	3	3	3
Ni	97	30	20	25	-	-	18	-	5	n.d.	20	49	57	29	19	13	2.6	2.5
Co	32	-	-	-	-	-	24(iv)	-	-	n.d.	-	32	31	30	21	18	2.8	3.9
V	292	270	175	255	-	-	175	-	68	8.5	200	271	353	384	225	208	17	23
Cr	297	50	15	40	-	-	25	-	13	1.7	30	73	146	90	76	56	25	32
Cu	77	-	-	100(iv)	-	-	54(iv)	-	-	6	-	39	56	78	53	52	5.0	6.5
Zn	-	-	-	-	-	-	-	-	-	-	-	100	88	91	83	268	37	29
Pb	-	-	-	-	-	-	-	-	-	18	-	25	24	25	24	93	19	14
Ag	-	-	-	-	-	-	-	-	-	-	-	.49	.51	.55	.26	.93	.20	.23
Hg***	-	-	-	-	-	-	-	-	-	-	-	22	16	21	35	47	17	16
K/Rb	1300	1000	890	340	-	-	430	-	380	250	200	197	270	424	448	436	313	454

* - Total Fe as Fe_2O_3
** - Loss on Ignition
*** - Hg in ppb
**** - Number of samples
n.d. - not detected

(i) Engel et al., 1965
(ii) Jakes & White, 1971, 1972.
(iii) Ewart et al., 1968.
(iv) Taylor, 1968.

The recognition of a distinctive island arc suite of volcanic rocks and their inherent geochemical variations has been a major contribution to modern geologic thought and allows for sophisticated re-interpretations of ancient volcanic sequences.

4.4. General Elemental Abundances

4.4.1. Introduction

The average chemical compositions of all lithologic units represented on the N60W section are given in Tables 7 and 8. Altered samples have been omitted from these averages except where the alteration is characteristic of the unit as a whole.

The volcanic rocks of the Buchans Group display little or no alkaline affinity. Neither olivine nor feldspathoids are present in the mode or the norm and pyroxenes are neither sodic nor titaniferous. Phosphorus and Ti are present in abundances well below normal for any alkaline suite and the Buchans volcanics are generally sub-alkaline on the alkali:silica diagram of Macdonald and Katsura (Fig. 8).

Similarly, the volcanic rocks of the Buchans Group bear little lithologic or chemical resemblance to oceanic tholeiites. The environment of deposition varies from subaerial to shallow water marine and pillowed flows and chemical sediments are rare. There is no known association in the area of ultramafic rocks, gabbros or sheeted dikes, the rocks generally taken as associated with oceanic volcanism. Chemically, the Buchans volcanics display abundances of K, Rb, Ba, and Sr which are much greater than those of oceanic tholeiites (Table 7) and have correspondingly lower Ni, Cr and K/Rb.

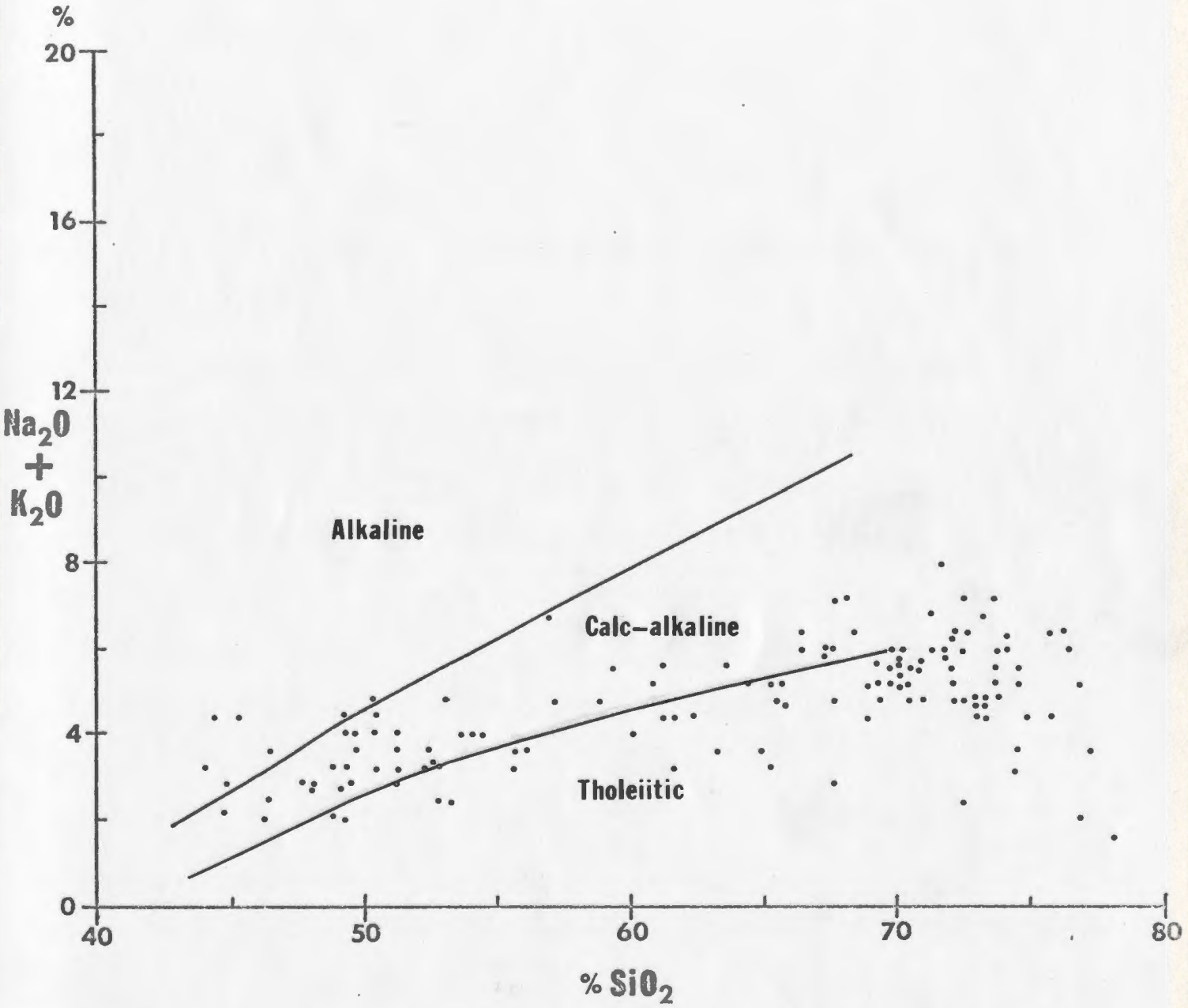

Fig. 8. Alkali:silica diagram for Buchans volcanic rocks. Dividing line between alkaline and calc-alkaline fields after Irvine and Baragar, 1972. Dividing line between calc-alkaline and tholeiitic fields after Kuno, 1968.

TABLE 8

AVERAGE CHEMICAL ABUNDANCES - MINERALIZED AND SEDIMENTARY UNITS

Weight Percent	Mineralized Intermediate Footwall	Ore	Breccia	Cycle One Siltstone	Cycles Two and Three Siltstone
	(14)****	(6)	(4)	(18)	(11)
SiO_2	47.22	11.50	61.65	65.38	67.10
TiO_2	.21	.13	.28	.34	.35
Al_2O_3	8.61	3.19	12.86	13.58	13.25
Fe_2O_3*	17.16	5.74	4.12	3.86	4.83
MnO	.35	.06	.10	.11	.17
MgO	7.17	1.27	1.88	3.18	2.46
CaO	2.09	1.80	2.27	2.13	2.39
Na_2O	.29	.45	2.36	2.87	2.16
K_2O	.79	.34	2.30	2.10	3.34
P_2O_5	.09	.00	.10	.08	.09
Loss Ig.**	11.78	8.39	5.74	4.07	3.18
ppm					
Rb	28	30	40	34	63
Ba	1898	98300	31600	1848	760
Sr	68	748	625	219	130
Zr	59	146	116	129	97
Mo	92	55	3	3	3
Ni	27	15	5.3	4.7	4.6
Co	19	2.3	6.0	6.6	7.4
V	136	52	65	54	50
Cr	122	43	33	28	39
Cu	1670	11160	596	21	20
Zn	11700	134600	1323	364	48
Pb	5470	17830	559	88	19
Ag	4.1	91	5.3	.43	.16
Hg***	234	2579	99	67	30

* - Total Fe as Fe_2O_3
** - Loss on Ignition
*** - Hg in ppb
**** - Number of samples

However, the Buchans Group exhibits numerous chemical characteristics similar to the suite of rocks found in modern island arcs, a point which is emphasized in this chapter.

4.4.2. Volcanic Rocks

The average chemical compositions of the various suites of island arc volcanic rocks are given in Table 7 together with the averages for the Buchans extrusives. The Footwall and Cycle Two Andesite are characterized by basaltic and andesitic silica abundances respectively and both contain high alumina and K_2O. According to the nomenclature of Mackenzie and Chappell (1972), the Footwall Andesite may be termed "High alumina basalt" whereas the Cycle Two Andesite generally falls in the range between "High alumina basalt" and "Dacite" (Fig. 9). The chemistry of both the Footwall and Cycle Two Andesites is similar to that found in island arcs, except for somewhat higher iron content and lower Ca, Mg and Na. Most trace element abundances are directly comparable to those of island arc volcanic rocks except for higher Ba and Cr and somewhat lower Sr and Zr.

All samples of the Intermediate Footwall on the N60W section were mildly to moderately silicified, sericitized and chloritized, but this visually recognizable alteration is represented chemically by only slight additions of Mg, Fe and Cr. Without knowledge of the original composition it is difficult to judge whether silica or K_2O have actually been added. TiO_2 and Al_2O_3, which generally remain inert during such alteration (Cann, 1970; Hart, 1970), show no effects of dilution, and the abundances present

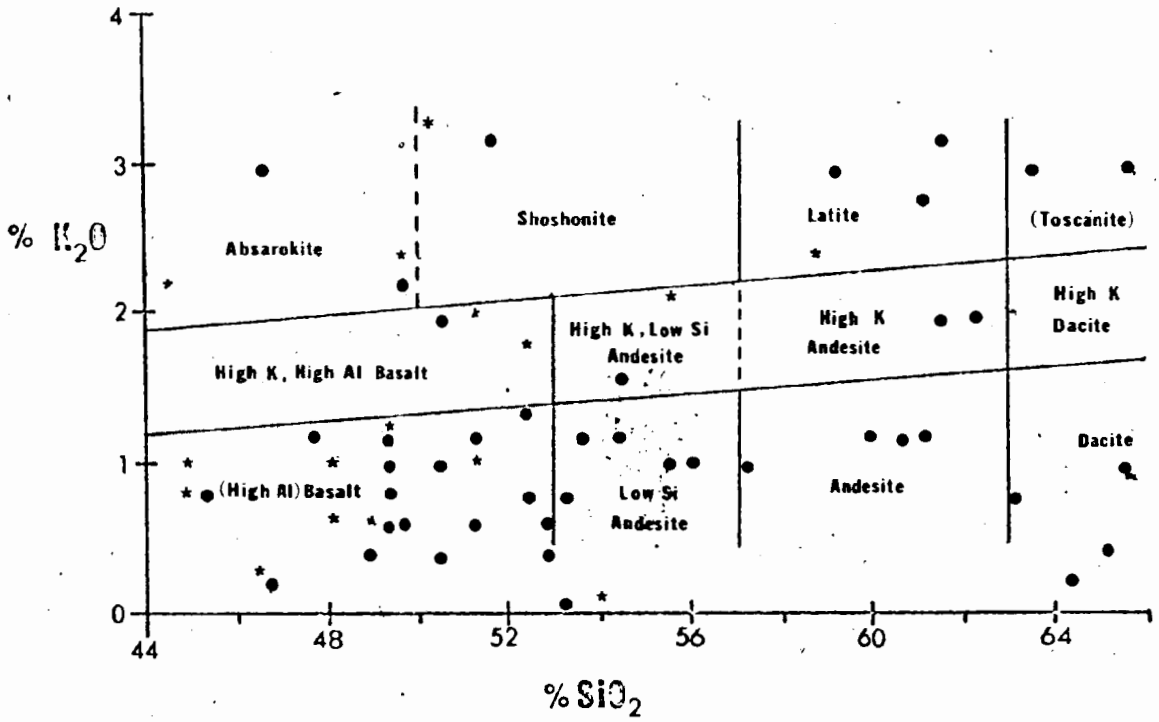

* Footwall Andesite

• Cycle Two Andesite

Fig. 9. K_2O:SiO_2 classification of Buchans mafic volcanic rocks. Nomenclature and divisions after Mackenzie and Chappell, 1972.

are those of an intermediate volcanic rock. This suggests that SiO_2 and K_2O have been redistributed but not added during alteration. The most profound effect of the alteration of the Intermediate Footwall was the extensive removal of Ca and Sr and the addition of Mn, Zn, Pb, Ag and Ba. The chemistry of the mineralized Intermediate Footwall is dominated by widespread epigenetic introduction of Zn, Pb, Cu, Ag, Hg, Ba, Mo, Ni and Cr. Compared to the "unmineralized" Intermediate Footwall (and holding alumina constant) the alteration also consists of large additions of Si, Fe, Ca, Mg and volatiles with strong depletion of Na and to a lesser extent K. It is thus apparent that Ca, which was removed from the lower levels of the Intermediate Footwall, was in part redeposited in the upper mineralized portion.

Both the major and trace element content of the Dacite is more akin to that of rhyolite. Compared to rhyolitic ignimbrites from New Zealand (Table 7), the Dacite contains high Ba and Cr abundances which parallel the enrichment of these elements in the Footwall and Cycle Two Andesites.

4.4.3. Sediments

The abundances of most major and trace elements in the Cycle One Siltstone are intermediate between those of the Dacite and the Intermediate Footwall, lending support to the hypothesis that this unit was derived from both these sources. Zn and Hg are present in abundances greater than those of the Intermediate Footwall, confirming petrographic evidence that the mineralized Intermediate Footwall also contributed detritus.

The abundances of Ca and Na in the Siltstone are similar to those of the Dacite and are not intermediate between the Dacite and Intermediate Footwall. The excess Na in the Siltstone may represent the equivalent of that which was leached from the mineralized Intermediate Footwall and escaped deposition in the overlying mineralized Intermediate Footwall. These data suggest chemical additions to the Siltstone during deposition.

Although only four samples of Breccia were analysed (two from Rothermere and two from MacLean), these suggest that the unit displays homogeneous chemistry. This may seem somewhat surprising in view of the heterolithic nature of the unit and the widely spaced sample locations, but seems to be an expression of the chaotic, homogeneous, unstratified nature of the unit. The chemical similarity of the MacLean and Rothermere breccias supports the hypothesis that they had a similar source and were deposited simultaneously as a single, discontinuous unit.

The major element chemistry of the Breccia is similar to that of the Siltstone and, like the Siltstone, represents a mixture of mafic and felsic volcanic fragments. However, the trace element chemistry of the Breccia is distinctive, consisting of high abundances of Zn, Pb, Cu, Ba, Hg and Ag, a reflection of their proximity to ore.

4.4.4. Ore

Geochemically speaking, the ore consists of an abnormal enrichment of S, Ba, Zn, Pb, Cu, Ag, Au, Hg and (to a lesser extent) Mo above normal

crustal abundances. The remainder of the elements determined are neither abnormally depleted nor enriched over the range of normal crustal abundances.

4.4.5. Diabase

It is evident from the analyses that two chemically distinct types of diabase dikes occur at Buchans. The first is characterized by consistently low Ti and Zr and relatively low P and Na, with higher K, Ba and Cr, while the second type exhibits correspondingly high Ti and Zr and relatively higher P and Na with lower K, Ba and Cr. The latter type outnumbers the former by about two to one. The distribution of the two types on the N60W section is random and displays no relation to ore. The high-Ti dikes exhibit mildly alkaline characteristics and are possibly post-orogenic and not associated with the Buchans Group volcanism. The low-Ti dikes show a degree of consanguinity with the Footwall Andesite as evidenced by their lower K/Rb and overall similarity of most major and trace elements. As such, they may represent feeders to the Cycles Three and Four mafic volcanics. However, the lower K content of the dikes and their higher Ni and Cr are possibly evidence against this hypothesis.

4.5. Harker Variation Diagrams and Correlation Matrix

Harker variation diagrams are presented in this section for the entire suite of extrusive rocks sampled during this study. For discussions of individual units the reader is referred to section 5.1. Included in the diagrams (Fig. 10) are the least altered samples from the Footwall and Cycle

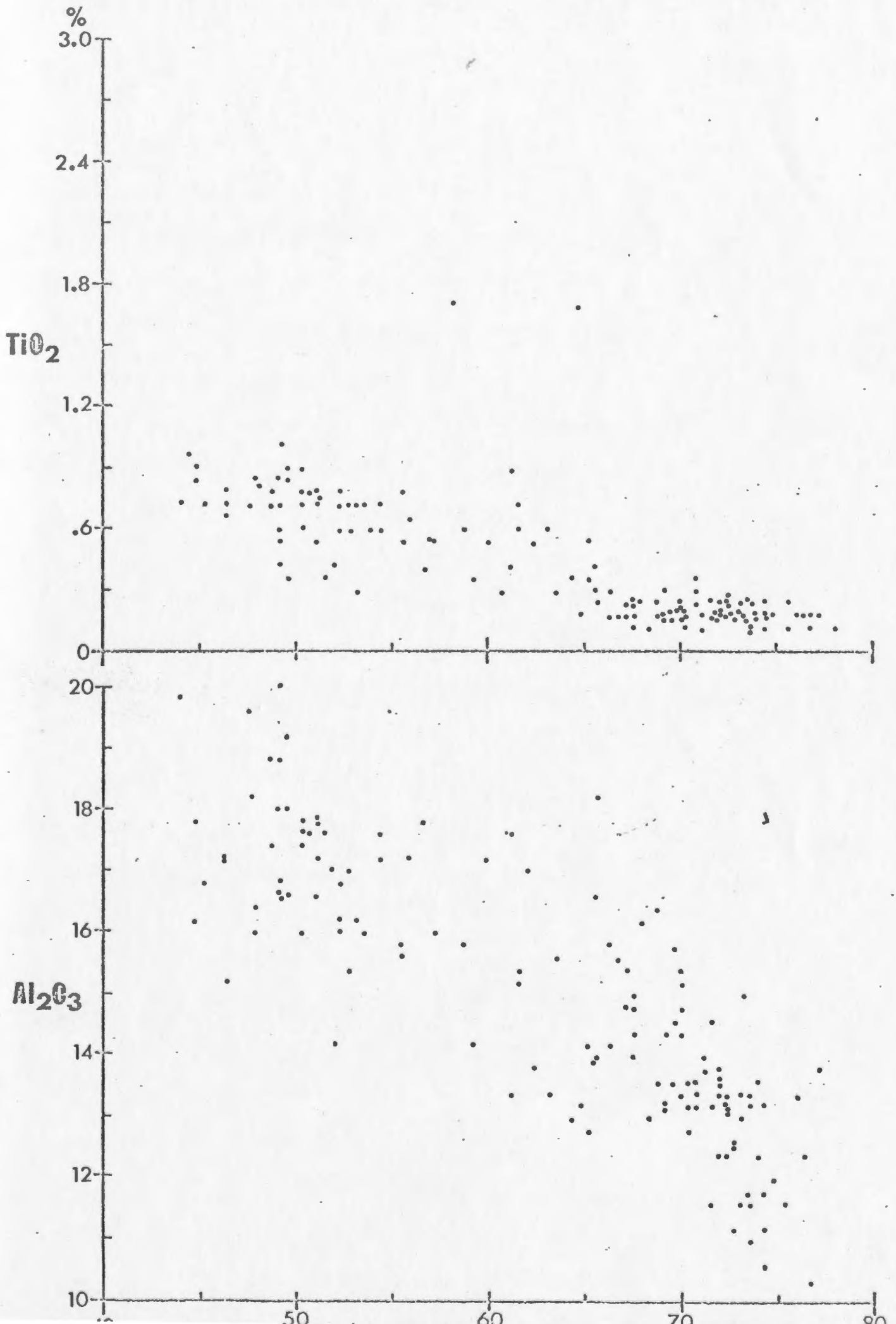
%
3.0
2.4
1.8
TiO_2
1.2
.6
0
20
18
16
Al_2O_3
14
12
10
50
60
70
80

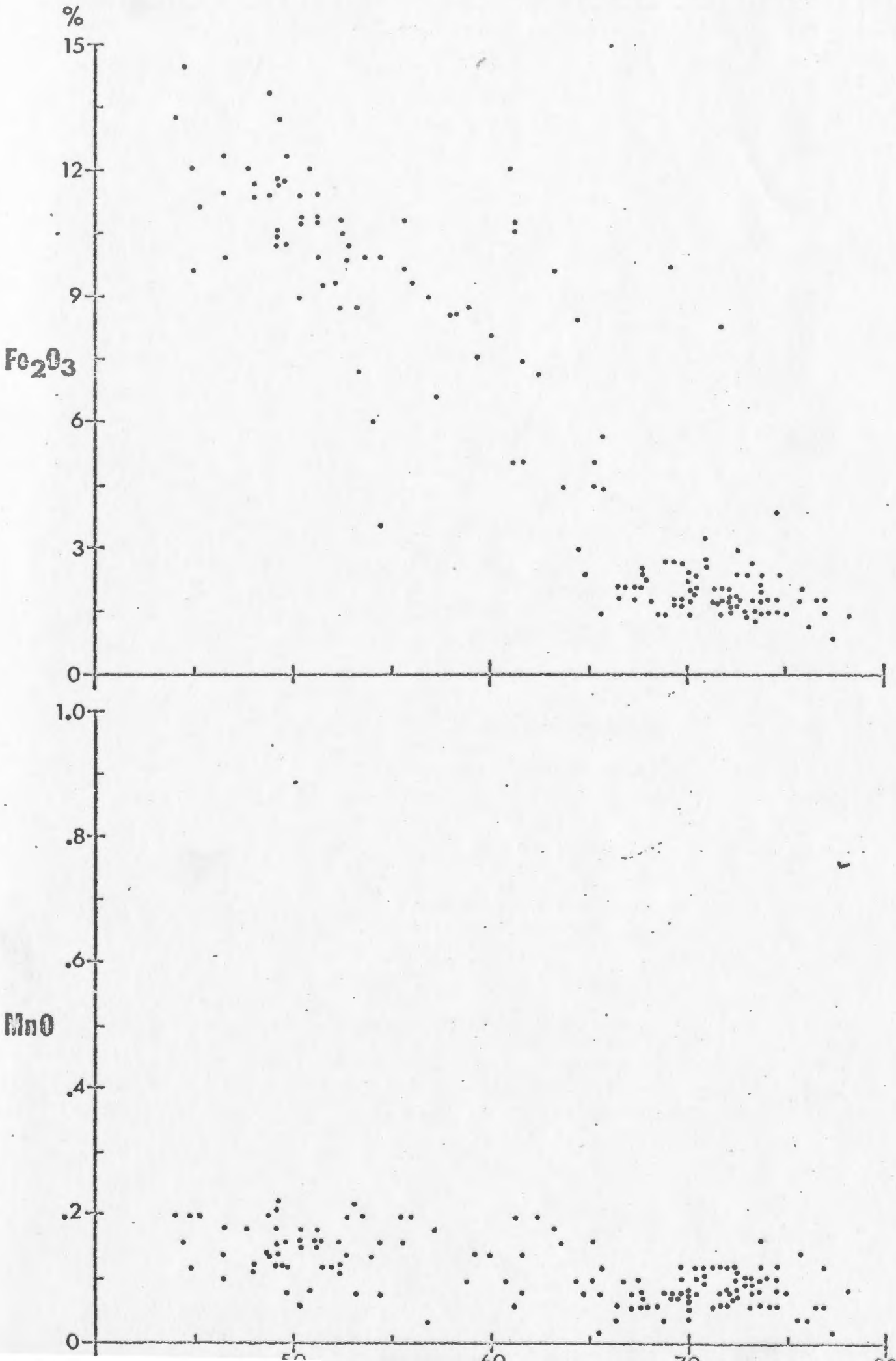
%
15
12
9
Fe_2O_3
6
3
0
1.0
.8
.6
MnO
.4
.2
0

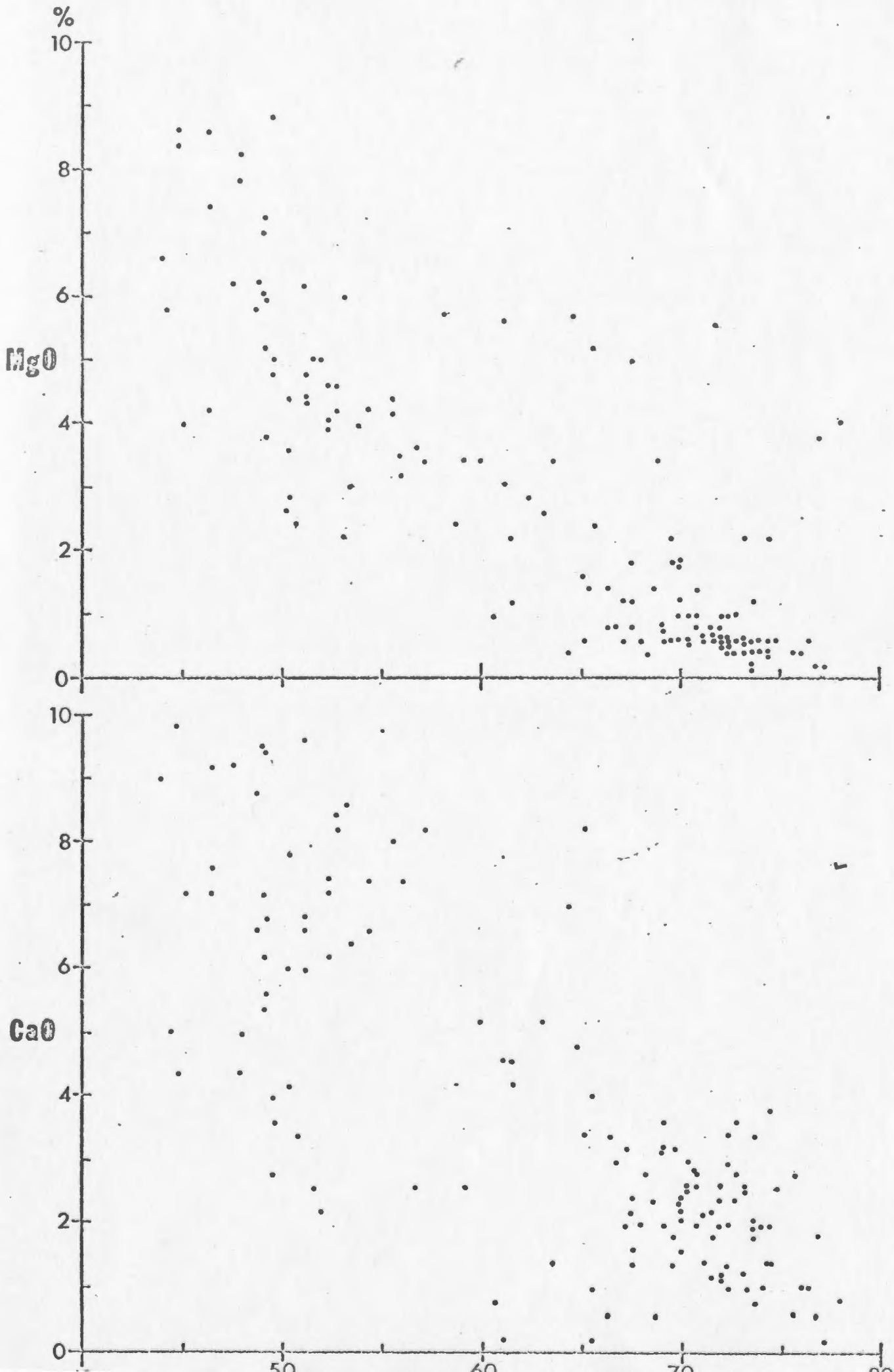
%
10
8
6
MgO
4
2
0
10
8
6
CaO
4
2
0

Fig. 10 (Cont'd.)

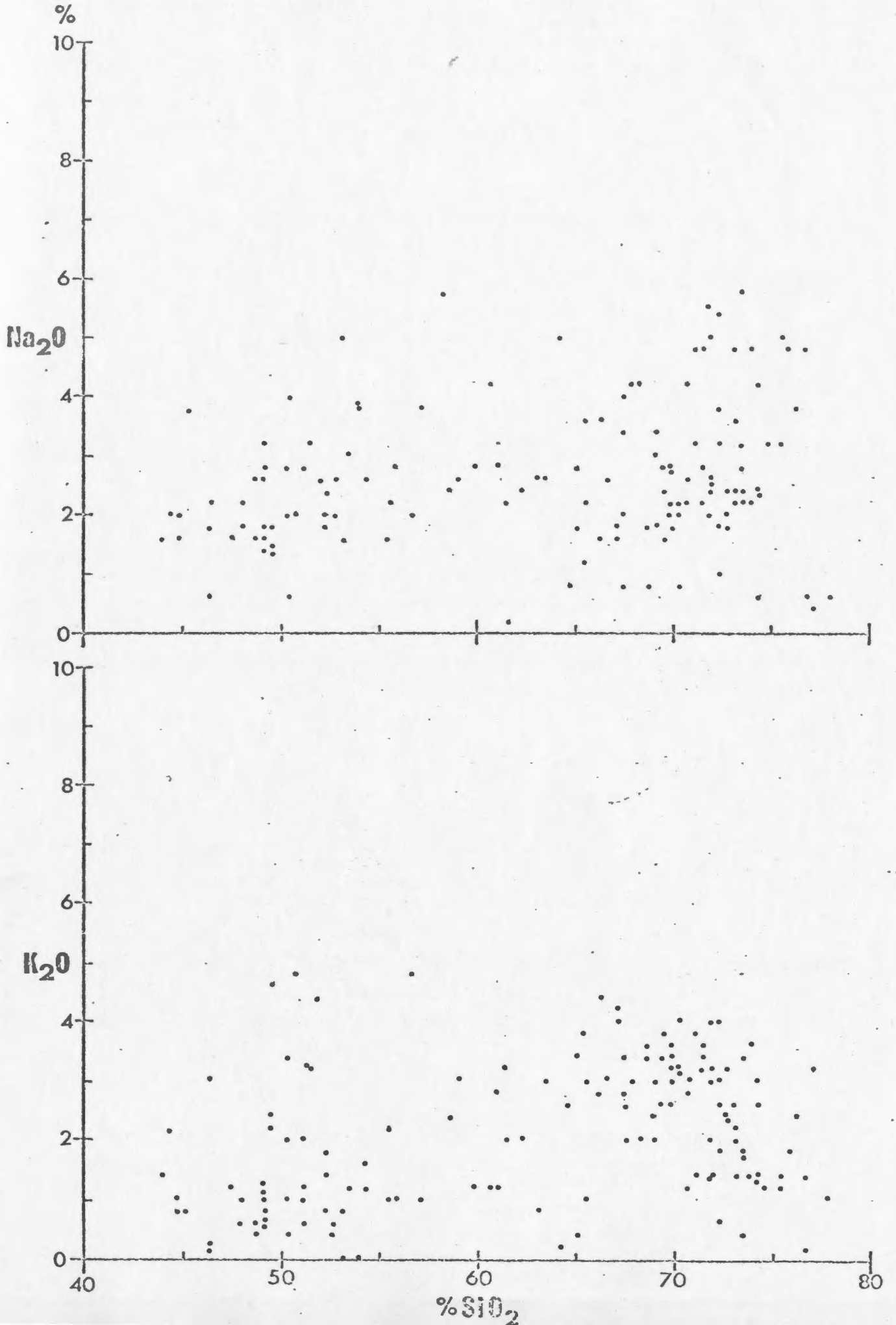

Fig. 10 (Cont'd.)

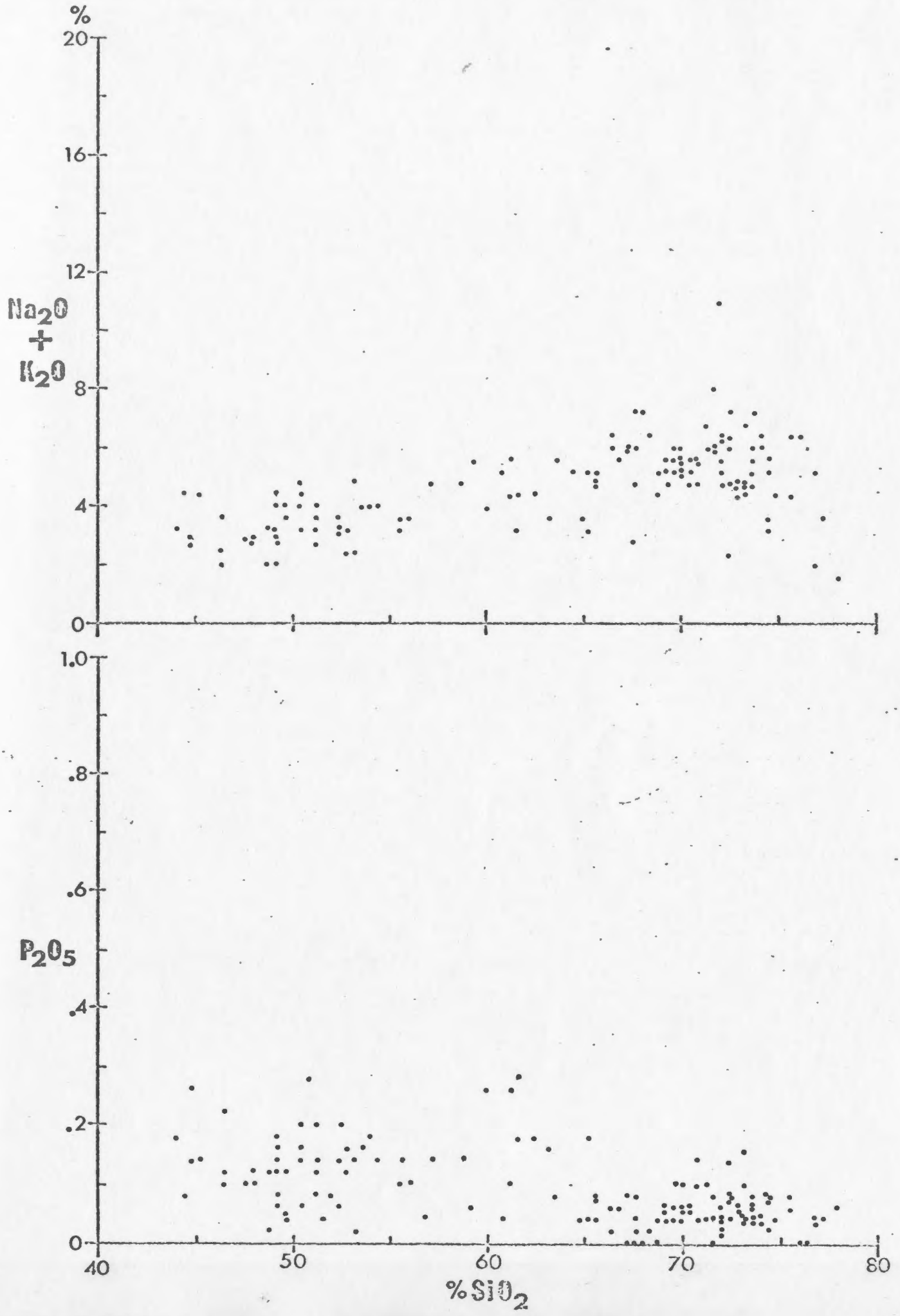

Fig. 10 (Cont'd.)

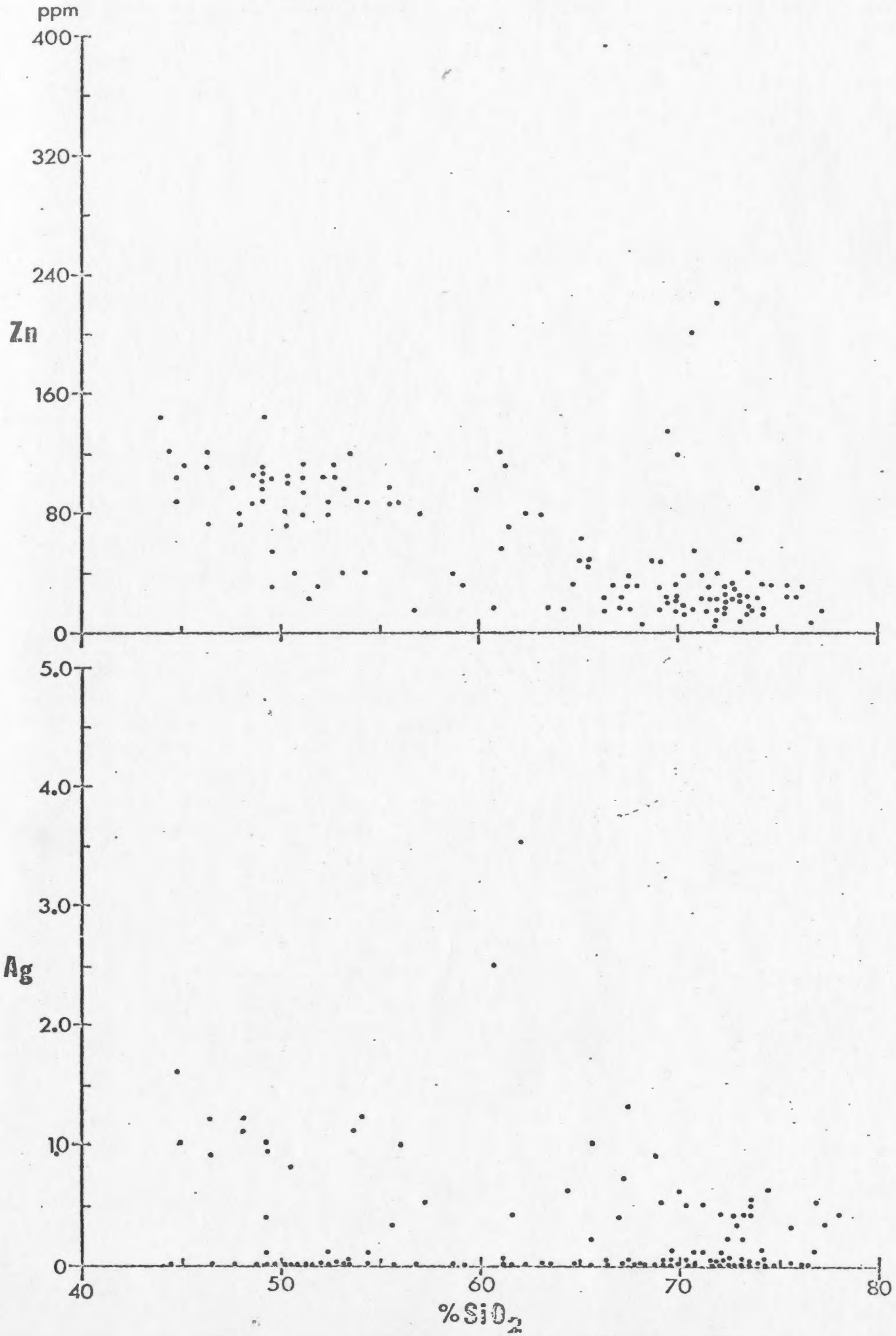

Fig. 10 (Cont'd.)

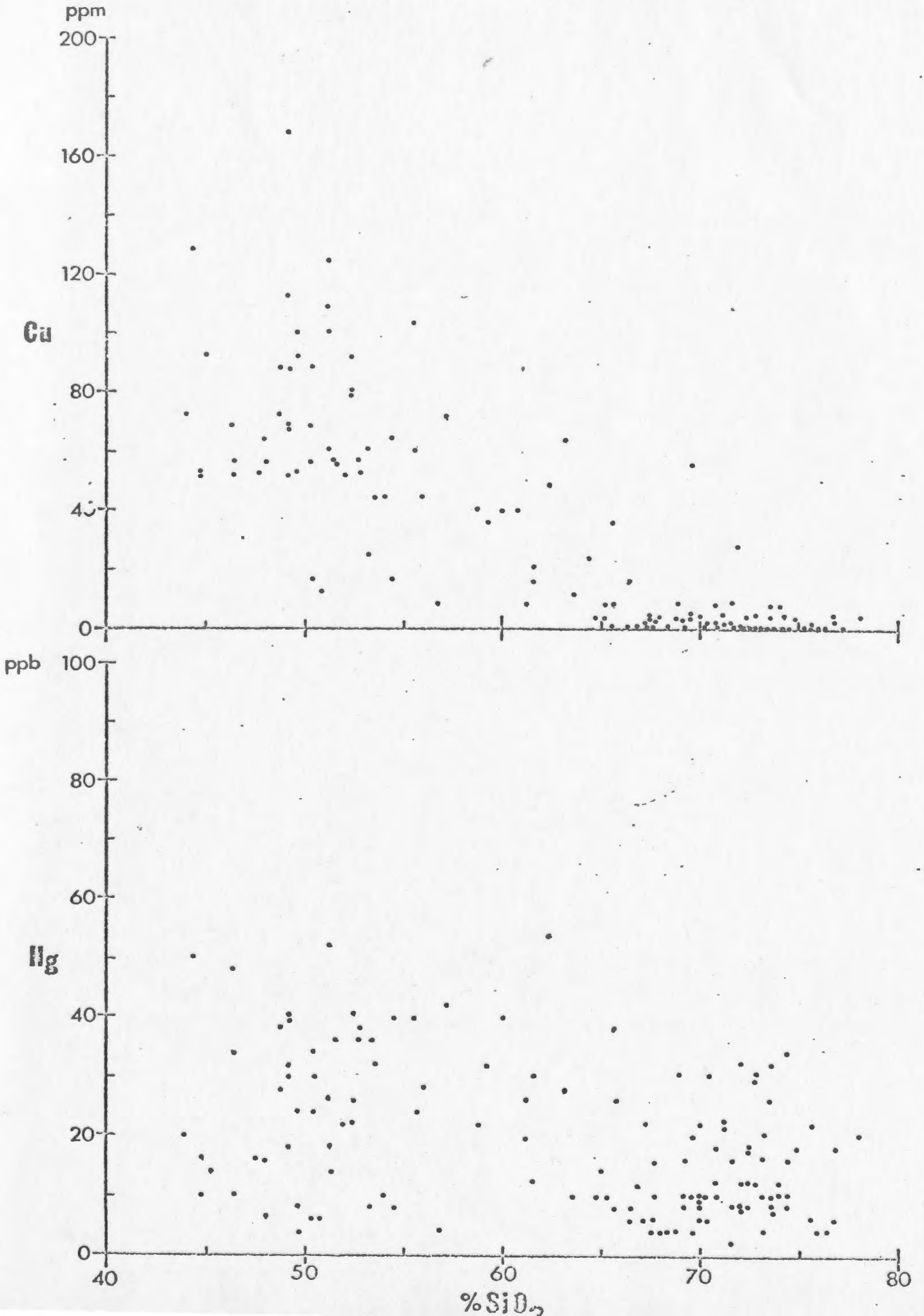
ppm
200
160
120
Cu
80
40
0
ppb
100
80
60
Hg
40
20
0
40
50
60
70
80
%SiO2

Fig. 10 (Cont'd.)

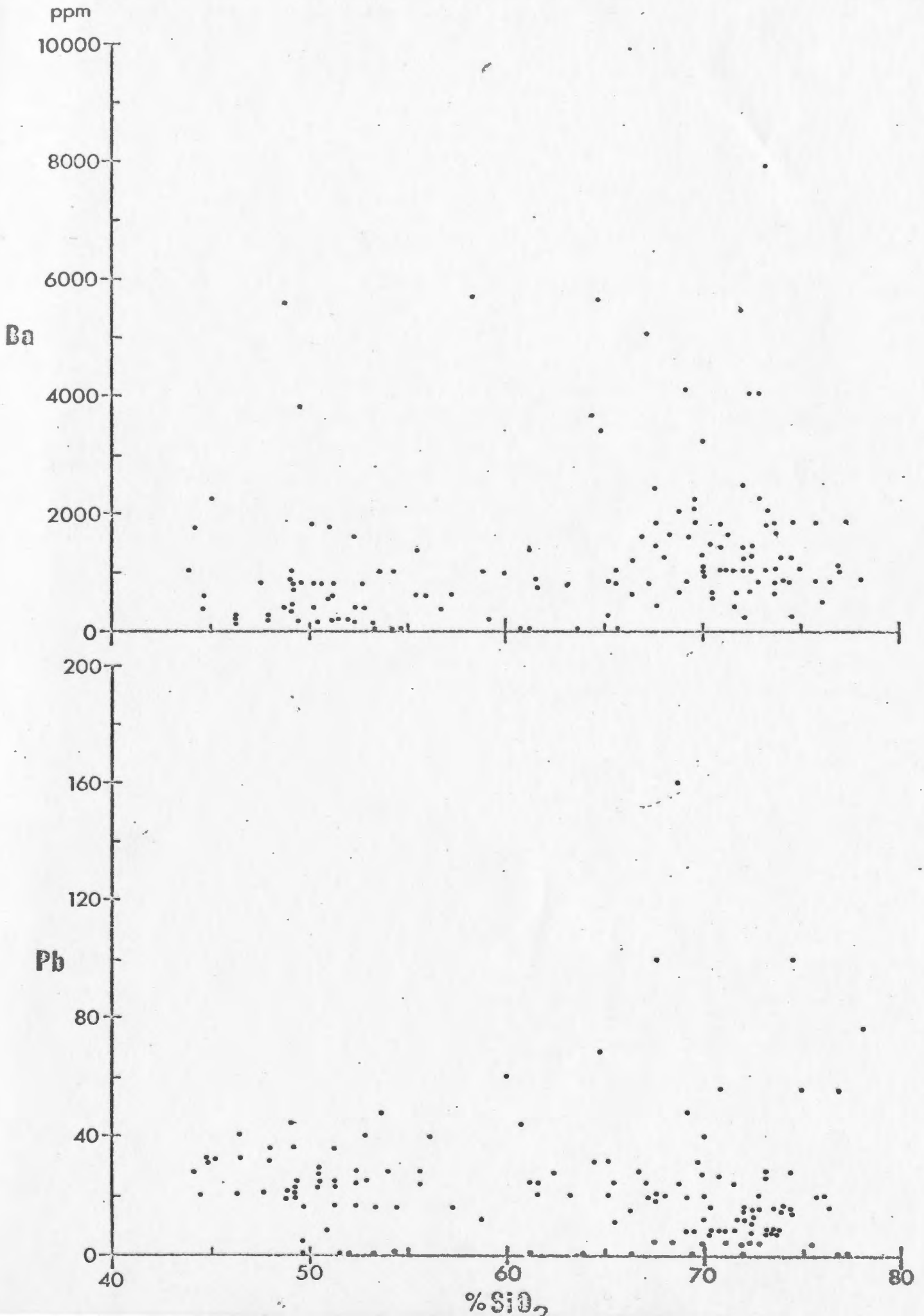
ppm
10000
8000
6000
Ba
4000
2000
0
200
160
120
Pb
80
40
0
40
50
60
70
80
%SiO2

Fig. 10 (Cont'd.)

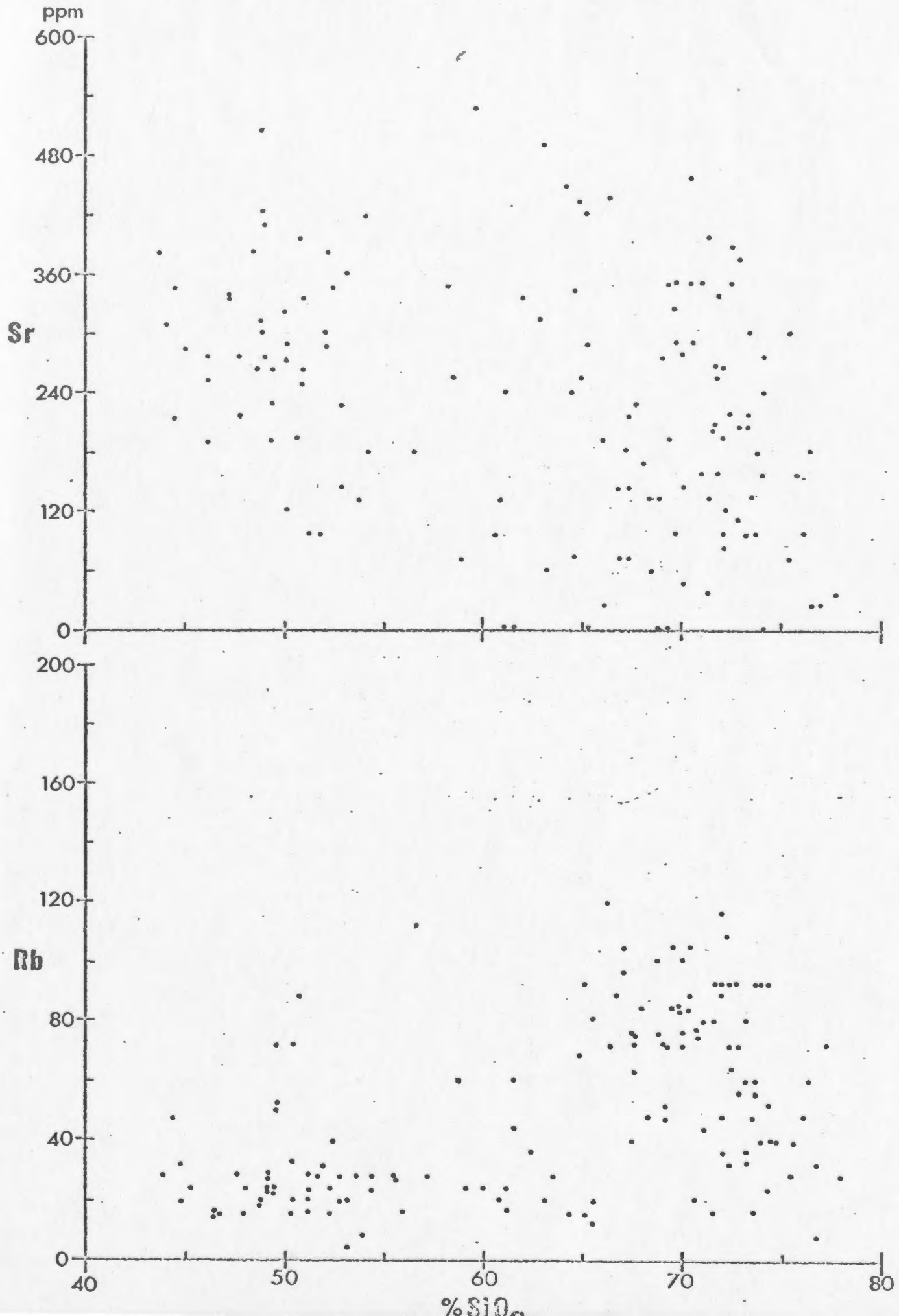
ppm
600
480
360
Sr
240
120
0
200
160
120
Rb
80
40
0
40
50
60
70
80
%SiO2

Fig. 10 (Cont'd.)

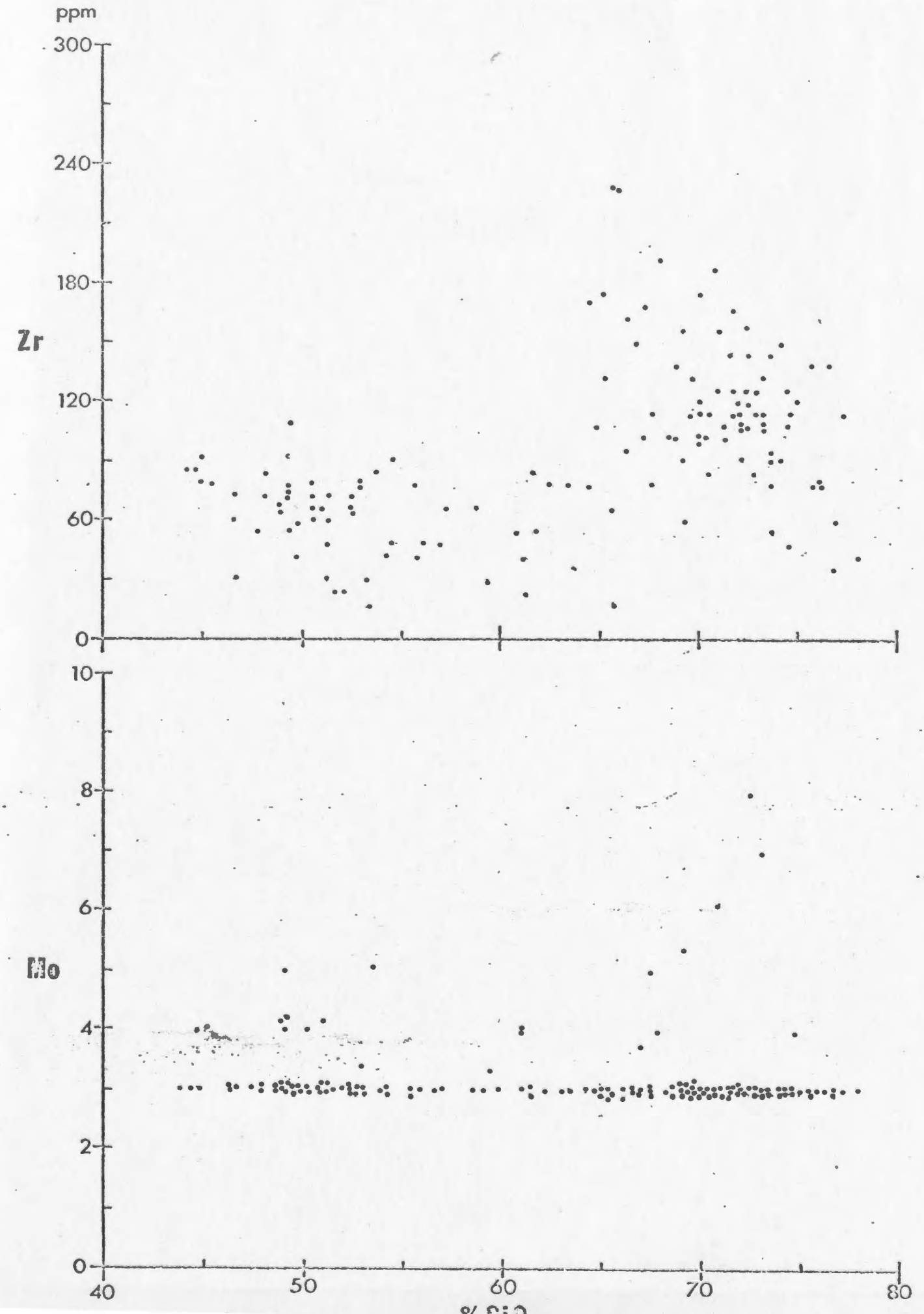

Fig. 10 (Cont'd.)

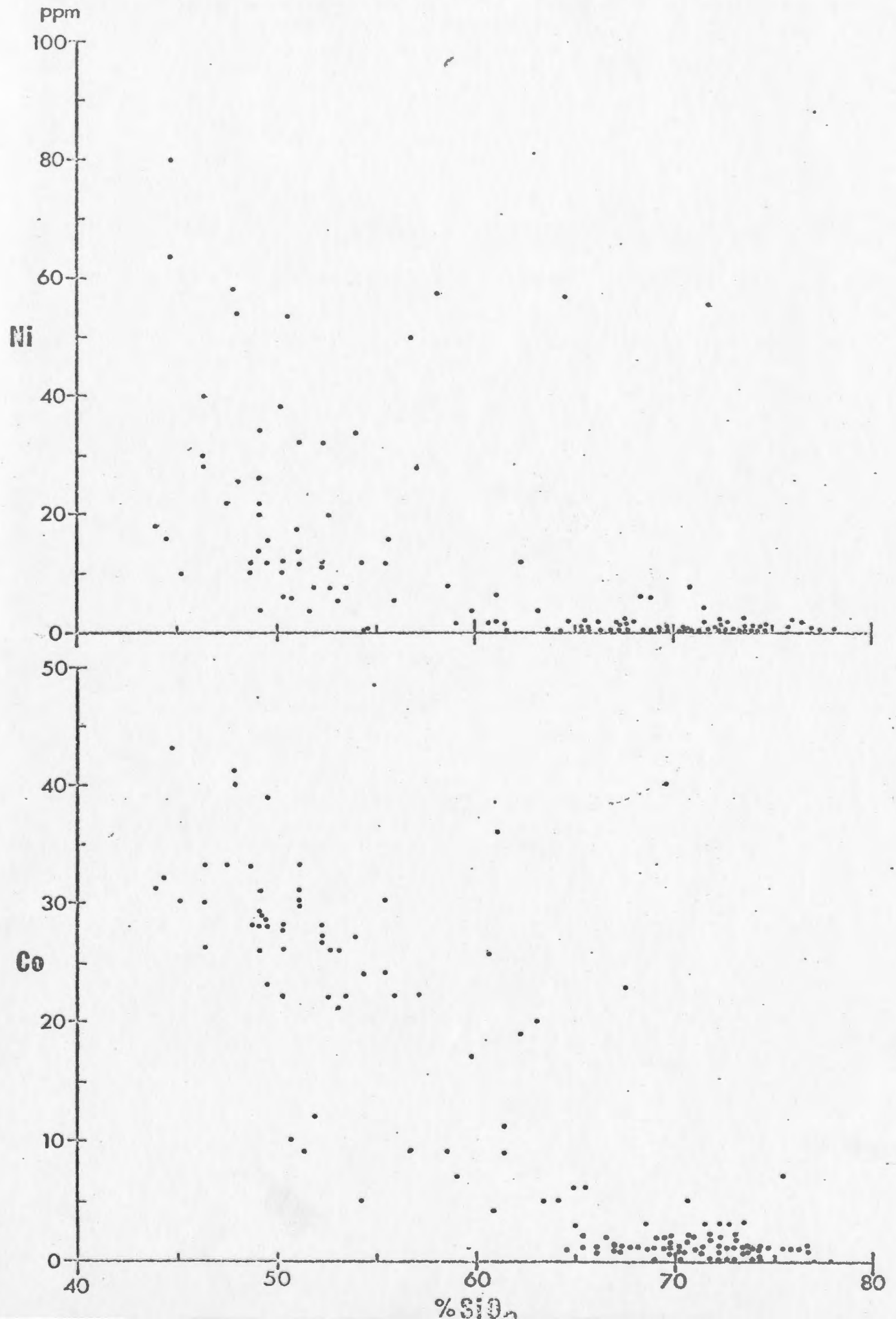

Fig. 10 (Cont'd.)

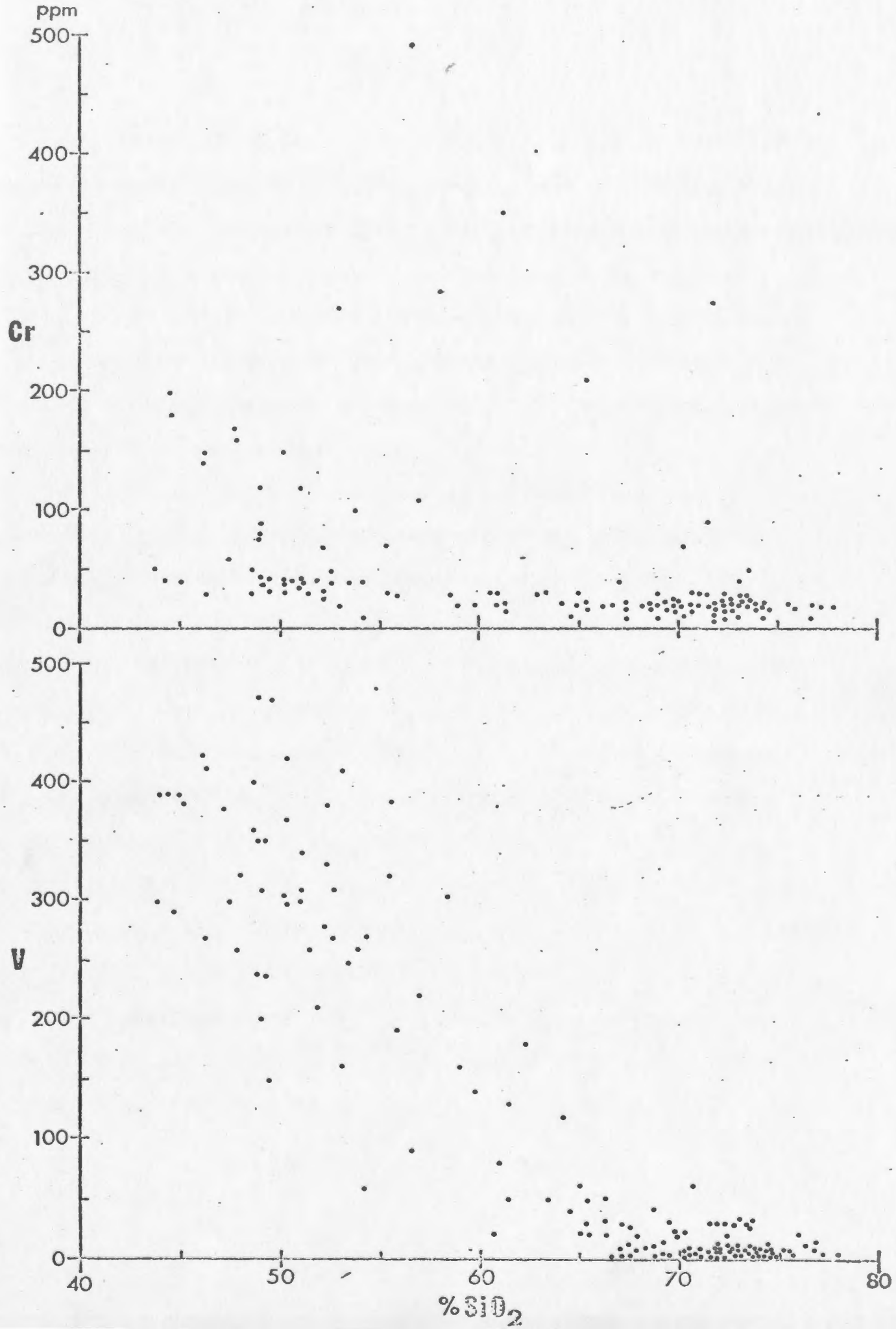
ppm
500
400
300
Cr
200
100
0
500
400
300
V
200
100
0
40
50
60
70
80
%SiO2

Two Andesites and the Cycle One and Three Dacites. Samples from the Intermediate Footwall have been omitted because of extensive alteration.

A feature common to all the diagrams is an apparent compositional gap in the intermediate silica range. It must be emphasized at this point that this apparent gap is a function of a lack of intermediate volcanic rocks on the N60W section and not in the Buchans area as a whole. The effect of the gap is enhanced by the omission of the altered Intermediate Footwall rocks from these and subsequent diagrams.

Although the scatter of all elements reflects varying degrees of alteration, it is evident that the extrusives of the Buchans Group form a consanguinous mafic to felsic sequence. This is perhaps best demonstrated by elements such as Fe, Ti, P, Mn, Zn, Cu and Ni. The distribution of Mg, Na, K, Rb, Ca, Sr, Ba, Pb, Hg and Ag is considerably more scattered as a result of local redistributions during alteration.

The behaviour of all elements is predictable on standard petrological grounds and no element exhibits anomalous trends. For example, most elements decrease with increasing silica while Zr, Na, K, Rb and Ba generally increase with silica. Omitting anomalous samples, Pb, Ag and Hg decrease very slightly with increasing silica. Mo was below the limits of detection (3 ppm) for most samples.

The value of Peacock's alkali-lime index (Peacock, 1931) is somewhat obscure due to scatter, but falls somewhere between 56% and 61% SiO_2, in the calc-alkaline field.

A correlation matrix tabling Pearson correlation coefficients for all elements determined for all the volcanic rocks as a whole is shown in Table 9. Correlation matrices for individual lithologic units (see section 5.1.) show considerable variation from that presented in Table 9 and, as such, only general comments may be derived from this table.

Fe, Ti, Ca, Mg, Cu, Co and V all exhibit strong mutual correlations (greater than + .70) and equally strong negative correlations with silica. Cr and Ni are strongly correlative although they display only a weak to moderate affinity with the above mentioned group. Among the base metals, only Zn and Pb exhibit moderate coherence while Ag and Hg vary independently of most elements. Ba varies independently of all other elements including the base metals and K, a curious feature that will be discussed in a later section.

4.6. Other Variation Diagrams

4.6.1. FMA Diagram

A triangular FMA diagram plotting the least altered volcanic samples is presented in Fig. 11, and the trend of the Buchans volcanics is compared to that of other well documented suites in Fig. 12. From Fig. 12 it can be seen that the Buchans trend shows little overlap with the mildly tholeiitic suite from the New Guinea-New Britain arc and shows no relation to the moderately tholeiitic Hawaiian and Icelandic trends. On the other hand, the Buchans field largely encloses the modern calc-alkaline trends from the Solomon Islands, Bougainville and East Papua.

Table 9

Correlation matrix for Buchans extrusive rocks.

Significance = .001 @ .23
= .01 @ .18

	Fe_2O_3	TiO_2	P_2O_5	SiO_2	CaO	K_2O	MgO	Al_2O_3	Na_2O	L.O.I.	MnO	Zr	Sr	Rb	Zn	Cu	Mo	Ba	Pb	Ni	Co	Cr	V	Hg
TiO_2	92																							
P_2O_5	58	67																						
SiO_2	-93	-89	-54																					
CaO	70	71	59	-79																				
K_2O	-43	-41	-41	39	-61																			
MgO	81	72	41	-85	61	-43																		
Al_2O_3	71	72	35	-78	46	- 3	62																	
Na_2O	-19	-16	1	19	- 8	-30	-36	-24																
L.O.I.	46	43	17	-58	37	-10	52	38	-36															
MnO	69	66	63	-64	72	-54	50	-39	3	13														
Zr	-51	-40	-34	50	-38	32	-52	-24	12	-46	-37													
Sr	26	27	26	-25	42	-32	16	25	6	-14	37	24												
Rb	-53	-49	-47	49	-53	78	-50	-16	-30	-21	-56	60	-16											
Zn	2	2	3	- 2	- 4	- 7	24	7	-33	18	- 4	-20	-11	-17										
Cu	86	82	47	-81	66	-43	71	66	-14	35	67	-46	30	-52	10									
Mo	2	- 7	5	3	- 5	- 5	- 7	-10	0	12	1	0	2	6	- 1	- 3								
Ba	-17	-12	- 6	20	-13	15	-19	-12	- 7	-14	1	17	15	16	3	- 8	- 1							
Pb	- 5	- 2	- 1	0	- 4	0	9	12	-24	18	- 9	- 3	10	-13	68	5	5	5						
Ni	46	37	17	-53	42	-23	66	29	-21	40	18	-31	12	-22	- 1	39	- 5	-18	- 6					
Co	89	85	53	-88	72	-49	82	62	-20	45	64	-46	28	-52	5	85	1	-14	- 1	64				
Cr	37	28	12	-44	30	-11	55	28	-19	32	5	-30	8	-13	3	24	- 5	-19	12	84	45			
V	88	87	57	-84	65	-33	68	68	-19	40	58	-47	22	-41	4	81	- 8	-11	- 5	38	82	25		
Hg	29	18	16	-18	13	-24	9	9	1	13	21	-25	6	-28	7	26	38	4	9	- 7	22	- 6	14	
Ag	17	15	8	-22	15	-21	27	0	-15	36	14	-20	- 5	-20	31	8	32	-13	35	19	26	21	3	41

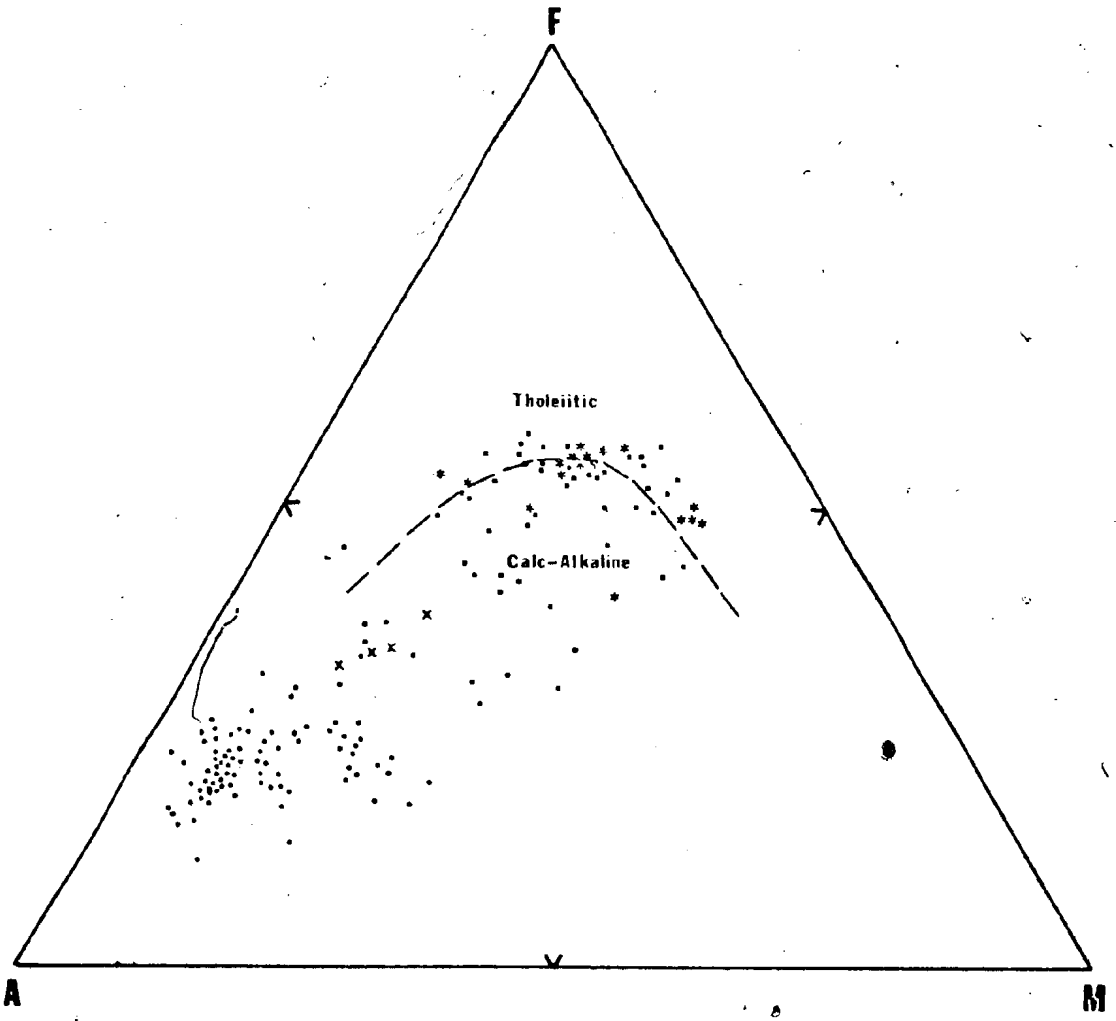

* Footwall Andesite

• Cycle Two Andesite

× Intermediate Footwall

• Dacite

—·— Dividing line between tholeiitic and calc-alkaline suites (after Irvine and Baragar, 1972)

Fig. 11. FMA diagram for Buchans volcanic rocks. F = total Fe as FeO, M = MgO, A = $Na_2O + K_2O$.

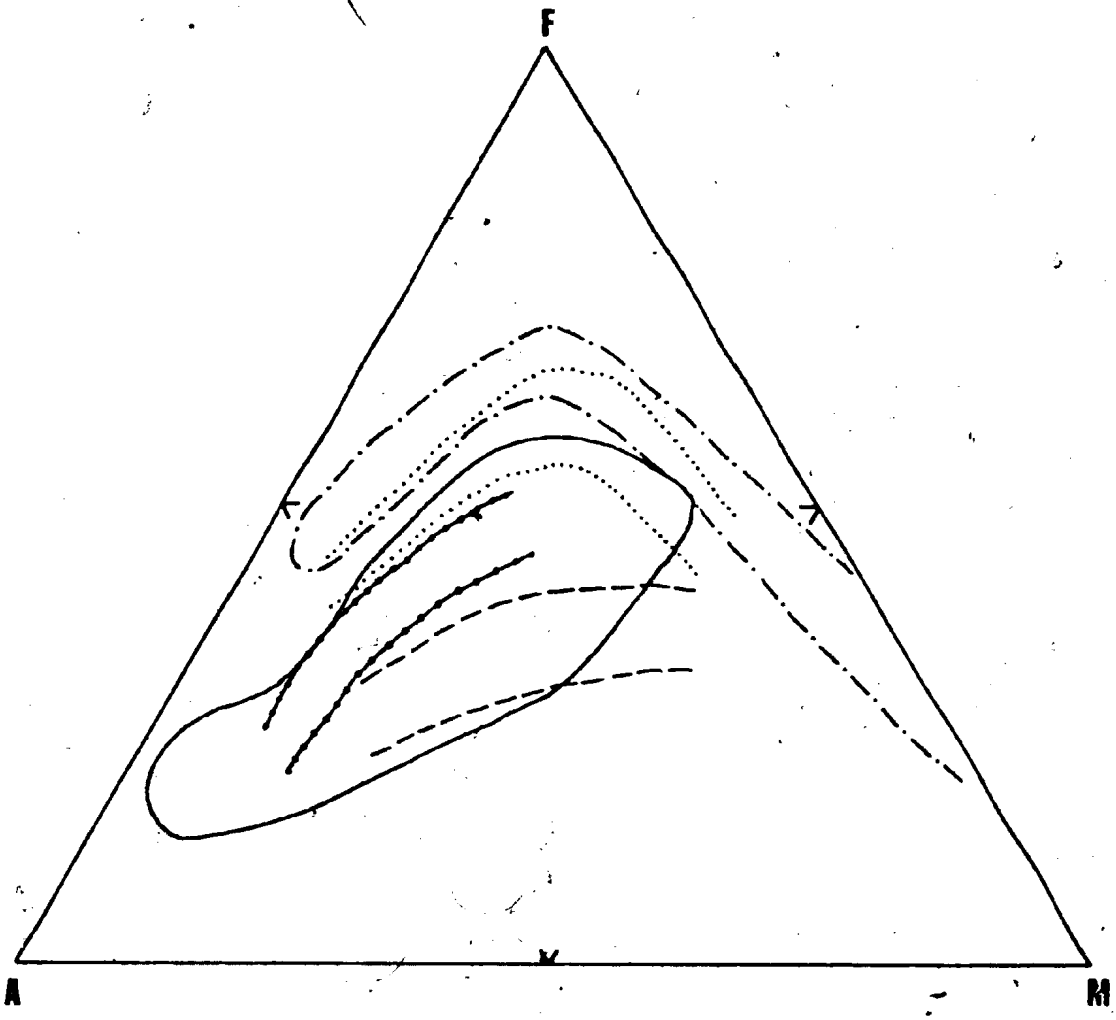

Fig. 12. FMA diagram outlining field of Buchans volcanic rocks as compared to other well documented suites.

The empirical dividing line between tholeiitic and calc-alkaline suites (after Irvine and Baragar, 1971) is also plotted in Fig. 11 and from this it can be seen that a number of the Footwall and Cycle Two Andesite samples fall in the vicinity of or above the dividing line, i.e. in the tholeiitic field. This iron enrichment may reflect a slight island arc tholeiitic tendency or may be a result of post-depositional iron enrichment (e.g., precipitation of iron oxide or sulphide from sea water or addition of Fe due to submarine weathering (Hart, 1970)). Despite this slight enrichment, the overall trend may be termed calc-alkaline.

The apparent compositional gap present on the FMA diagram is a function of omission of the altered samples from the Intermediate Footwall. Only four samples from this unit are plotted and these may be seen to bridge the gap between the mafic and felsic end members. Had this unit been represented volumetrically, the compositional gap probably would not exist.

4.6.2. K:Rb Ratios

The alkali metals K and Rb are the focus of considerable attention in many petrochemical studies. Both elements have similar electronegativity, ionization potential and valence allowing camouflage of Rb by K. However, Rb has a slightly larger ionic radius and consequently lower bond strength, causing a progressive Rb increase with respect to K with magmatic differentiation (Taylor, 1965). As such, the K/Rb ratio should be a useful geochemical parameter in distinguishing "primitive" magmas (with high K/Rb) from more differentiated magmas (with

progressively lower K/Rb). The K/Rb ratio is of special interest in island arcs where K increases and K/Rb decreases from trench to continent side of the arc.

K/Rb data must be interpreted with caution in older volcanic suites due to the mobility of these elements in secondary environments. The slightly more ionic nature of the Rb-O bond causes preferential adsorption of Rb onto clay minerals (Heier and Adams, 1964) probably causing K/Rb to decrease during hydrothermal alteration and surface weathering. Metamorphism has little or no effect on whole rock K/Rb ratios except at upper amphibolite and higher grades (Jakeš and White, 1970; Heier and Adams, 1964).

The average K/Rb ratios of the Buchans extrusives are compared to typical values from island arcs in Table 10. The K/Rb ratios from Buchans compare favourably with modern calc-alkaline values although they display a slight island arc tholeiitic tendency. There is no apparent decrease in K/Rb with stratigraphic position in the mafic volcanics but the K/Rb ratio decreases systematically from Footwall to Hangingwall to Cycle Three Dacite. The similarity of K/Rb ratios between related mafic and felsic volcanics in the early cycles and a similar relationship between the Cycle Three Dacite and the low-Ti diabase dikes suggests that the dikes may represent feeders to the cycle three mafic lavas. The very low K/Rb of the high-Ti diabase suggests extreme fractionation and late stage emplacement. It is interesting to note that the K/Rb ratios in the Intermediate Footwall are apparently little affected despite considerable alteration.

TABLE 10

K/Rb RATIOS FROM BUCHANS COMPARED TO TYPICAL VALUES FROM OTHER VOLCANIC SUITES

(All K/Rb ratios except Buchans after Jakeš and White, 1970)

Rock Type	K/Rb
Oceanic Tholeiite	800-2000
Hawaiian Tholeiites	500
Continental Tholeiites	150-1000
Island Arc Tholeiites	440-1160 (New Britain) 450 (South Sandwich Is.) 1070 (Fiji)
Calc-alkaline	
Low K Andesite	236-540 (New Zealand) 236-540 (Izu Peninsula) 590 (Siapan) 515-563 (Bougainville)
Medium K Andesites	300 (Asama, Japan)
High K Andesites	297-330 (Bougainville)
Shoshonites	200-320 (New Guinea)
Buchans	
High Ti Diabase	197
Low Ti Diabase	270
Cycle Three Dacite	299
Cycle Two Andesite	448
Hangingwall Dacite	313
Footwall Dacite	454
Intermediate Footwall	436
Footwall Andesite	424

A K vs. Rb plot outlining the fields of the various lithologies at Buchans is presented in Fig. 13. The plot demonstrates the overall coherence of K and Rb, especially in the dacites, whereas the Footwall and Cycle Two Andesites generally exhibit more widespread scatter. The K/Rb ratio remains essentially constant in all units except the Cycle Two Andesite in which K/Rb increases with increasing K, causing a slightly discordant trend for this unit.

4.6.3. Ti:Zr Diagram

The elements Ti, Zr, Y, and Nb have recently received attention because their abundances are little affected by alteration (Cann, 1970). In addition, various binary and ternary diagrams involving these elements allow a reasonable geochemical distinction between modern ocean floor basalts, island arc tholeiites, calc-alkaline andesites and alkali basalts (Pearce and Cann, 1971).

A Ti:Zr diagram for the Buchans extrusives, including the empirical fields of Pearce and Cann (1971), is presented in Fig. 14. Most samples of Footwall and Cycle Two Andesite fall in an area transitional between the field of ocean floor basalt and island arc andesite. Dacite samples plot in a lower Ti, higher Zr portion of the diagram as would be expected. The Footwall Andesite is generally more Ti-rich than the Cycle Two Andesite but, despite the generally higher Si content of the Cycle Two Andesite, Zr is approximately the same in both groups causing a slightly anomalous distribution. The diagram illustrates the similarity of the low-Ti diabase to the Footwall and Cycle Two Andesites, and the alkaline tendencies of the high-Ti diabase dikes.

Fig. 13. K vs Rb plot for Buchans volcanic rocks.

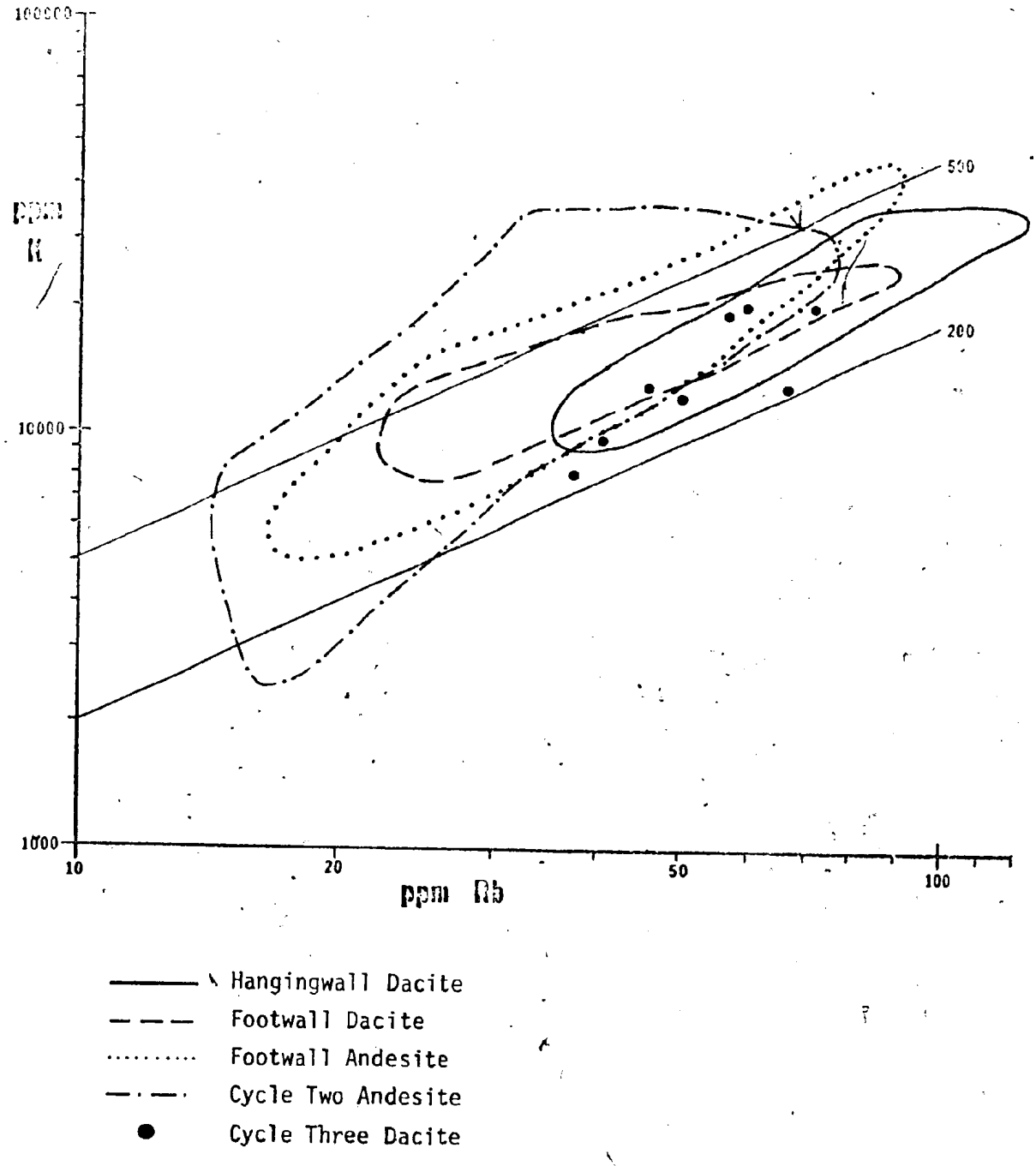

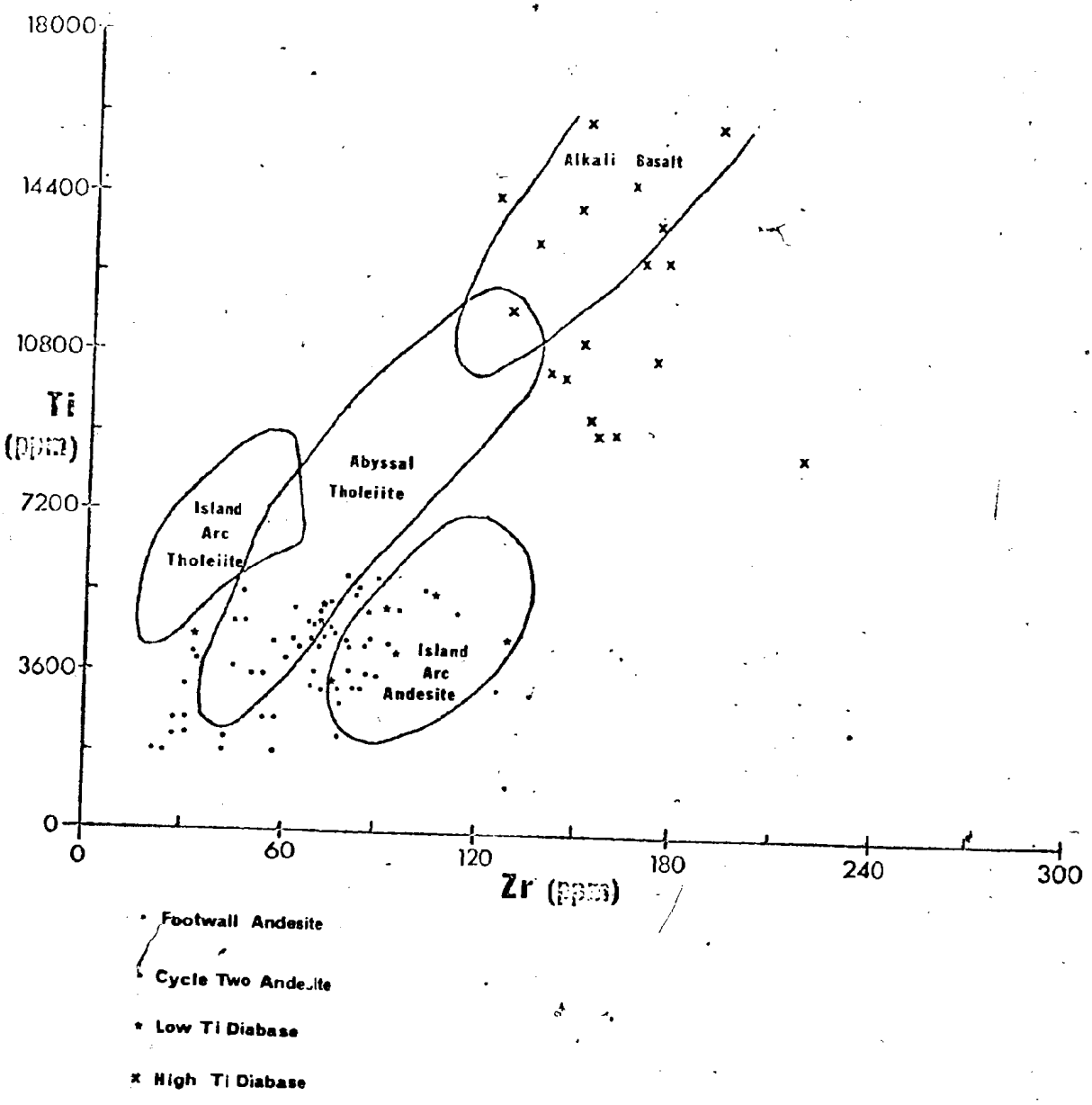

Fig. 14. Ti:Zr diagram for Buchans mafic volcanic rocks. Outline of fields after Pearce and Cann, 1971.

With respect to the fields outlined by Pearce and Cann (1971), the writer suggests that one should use caution in their interpretation as they are empirically derived from relatively few samples from selected areas. Furthermore, the conclusions reached from this diagram often conflict with those reached from other more fundamental geological and geochemical criteria (e.g., Ewart and Bryan, 1972). Consequently, the author suggests that little emphasis be placed on interpretations gained from this diagram.

4.7. Summary with Respect to Petrochemical Setting

In summary, the bulk of the petrochemical evidence suggests that the suite of rocks present at Buchans are calc-alkaline in character and similar to those found in modern island arcs. Both the FMA diagram and the K/Rb ratios, while dominantly calc-alkaline, suggest a weak island arc tholeiitic tendency, but the abundances of large cations and the metallogenic association dictate strongly against this possibility. The alkali-lime index and the alkali:silica diagram also suggest a calc-alkaline character. The Ti:Zr diagram implies both calc-alkaline and ocean floor tholeiitic tendencies but the shallow water to subaerial environment of deposition, the lack of rocks of ophiolitic association and all the above mentioned criteria eliminate the latter possibility. The presence of abundant intermediate and felsic volcanic rocks in the Buchans area and the preponderance of clastic sediments are also suggestive of an island arc, calc-alkaline association.

The recognition of a calc-alkaline suite (with slight island arc tholeiitic tendencies?) at the base of the Buchans Group, while not surprising,

is important from an exploration standpoint. It implies that the upper volcanic cycles are also calc-alkaline in character (although shoshonites may be found in the extreme upper portions) and thus empirically represent a favourable exploration target. On a larger scale, the delineation of the extent of calc-alkaline volcanism in the Central Mobile Belt of Newfoundland in effect would outline the area in which polymetallic massive sulphides are probable.

CHAPTER 5

THE RELATIONSHIP BETWEEN GEOCHEMISTRY AND MINERALIZATION

5.1. Scattergrams and Correlation Matrices

The purpose of this section is to discuss scattergrams and correlation matrices for the individual lithologic units with emphasis placed on the behaviour of the ore metals. Lithologic units will be discussed in pairs in order to identify differences which may exist between the units. A summary of the characteristic correlations within each lithologic unit is presented in Table 11.

5.1.1. Intermediate Footwall and Mineralized Intermediate Footwall

The Intermediate Footwall is characterized by a widespread scatter for most elements on the Harker variation diagrams (Fig. 15) undoubtedly caused by alteration. The scatter for the mineralized portions of the unit is generally similar (except for the base metals) despite more pervasive alteration. The removal of Na from the mineralized Intermediate Footwall is readily apparent from the diagrams.

The Intermediate Footwall displays distinct bimodal tendencies for Mn, Cu, Pb, Zn, Co and Hg reflecting variations in intensity of alteration. However, inspection of the correlation matrix (Table 12) reveals that of these elements, only Pb and Zn are significantly correlative indicating that the type of alteration as well as its intensity is widely variable.

Base metal correlations in the mineralized Intermediate Footwall also show similar variations. Zn, Pb and Hg exhibit strong mutual correlations but show no correlation to Ba and Ag which are themselves

TABLE 11

SUMMARY OF CHARACTERISTIC CORRELATIONS

Unit	Correlations
Footwall Andesite	Very low correlations between Fe and Mg, Ni, Co, Cr, & V. Pb-Ag-Mg-Ni-Cr especially Ag-Ni-Cr. Cu-Zn-Hg
Intermediate Footwall	Zn-Pb
Mineralized Intermediate Footwall	Zn-Pb-Hg Ba-Ag
Cycle One Siltstone	Ba-Hg
Footwall Dacite	Cu-Pb-Cr Zn-Ag-Mg Zn-Pb-Hg
Hangingwall Dacite	Very low correlations between Fe and Ni, Co, Cr, V and Mg. Ni-Co-V-Cu-Zn
Cycle Two Andesite	Fe-Co-V-Cu-($\pm$Zn) Hg-Ag-Mo
Cycles Two and Three Siltstones	Mg-Ti-P-Fe-Ca-Sr-Cr Zn-Co-V Zn-Pb-Ag Co-Pb-Ni
Cycle Three Dacite	Fe-Ti-Ni-Co-Cr-V Ba-K-Rb

Fig. 15. -Harker diagrams comparing Intermediate Footwall and Mineralized Intermediate Footwall.

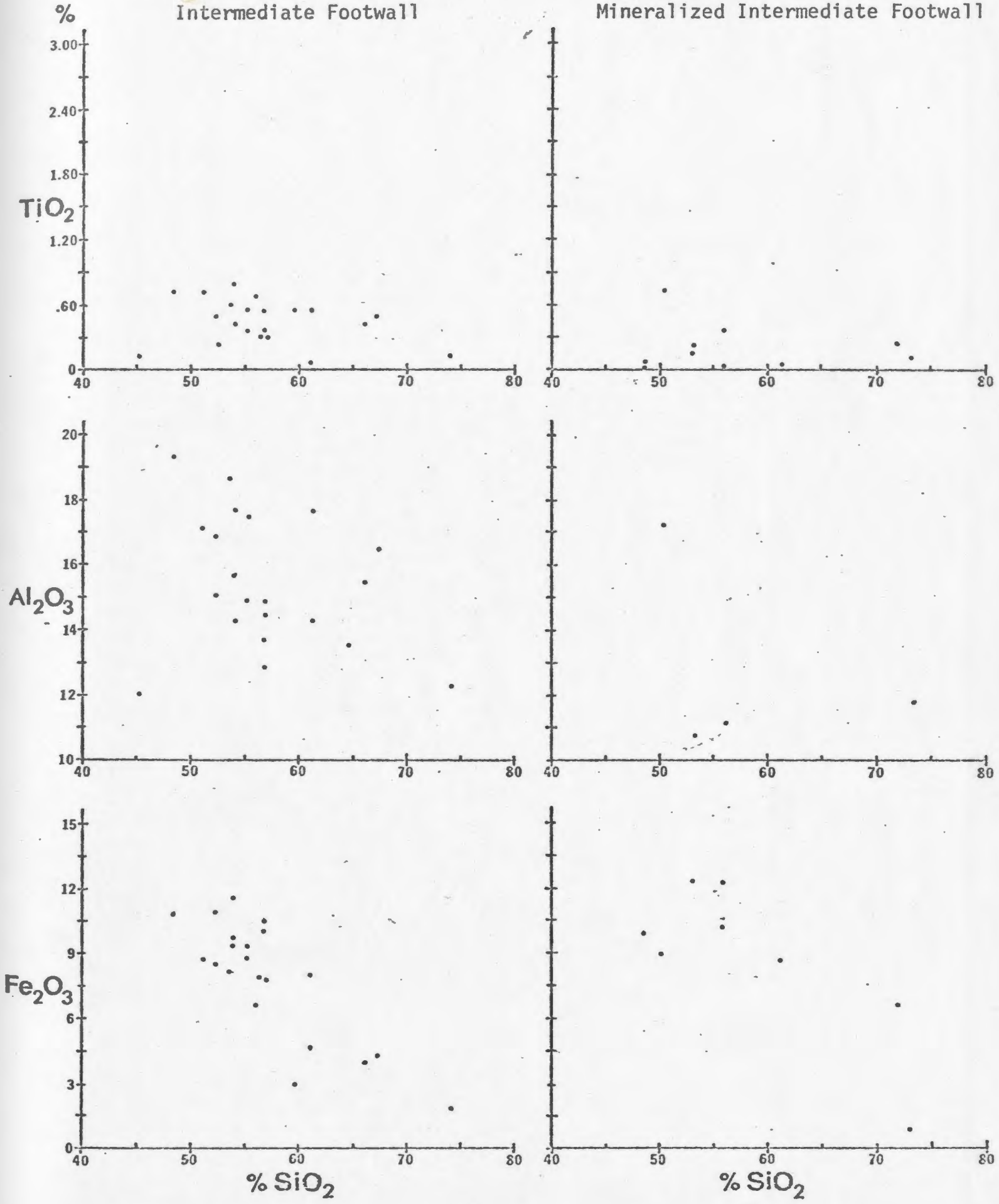

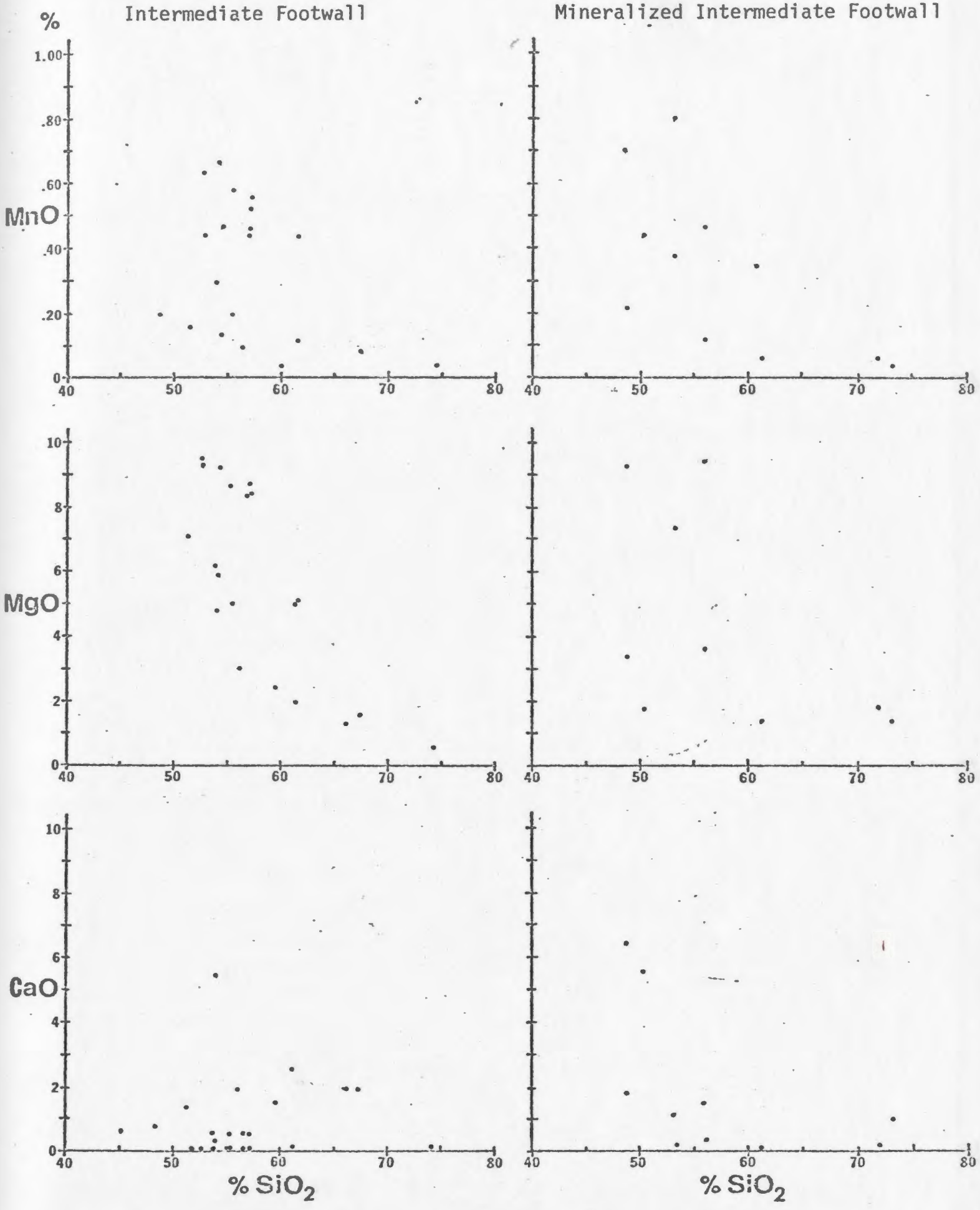
%
Intermediate Footwall
Mineralized Intermediate Footwall
MnO
MgO
CaO
% SiO2
% SiO2

Fig. 15 (Cont'd.)

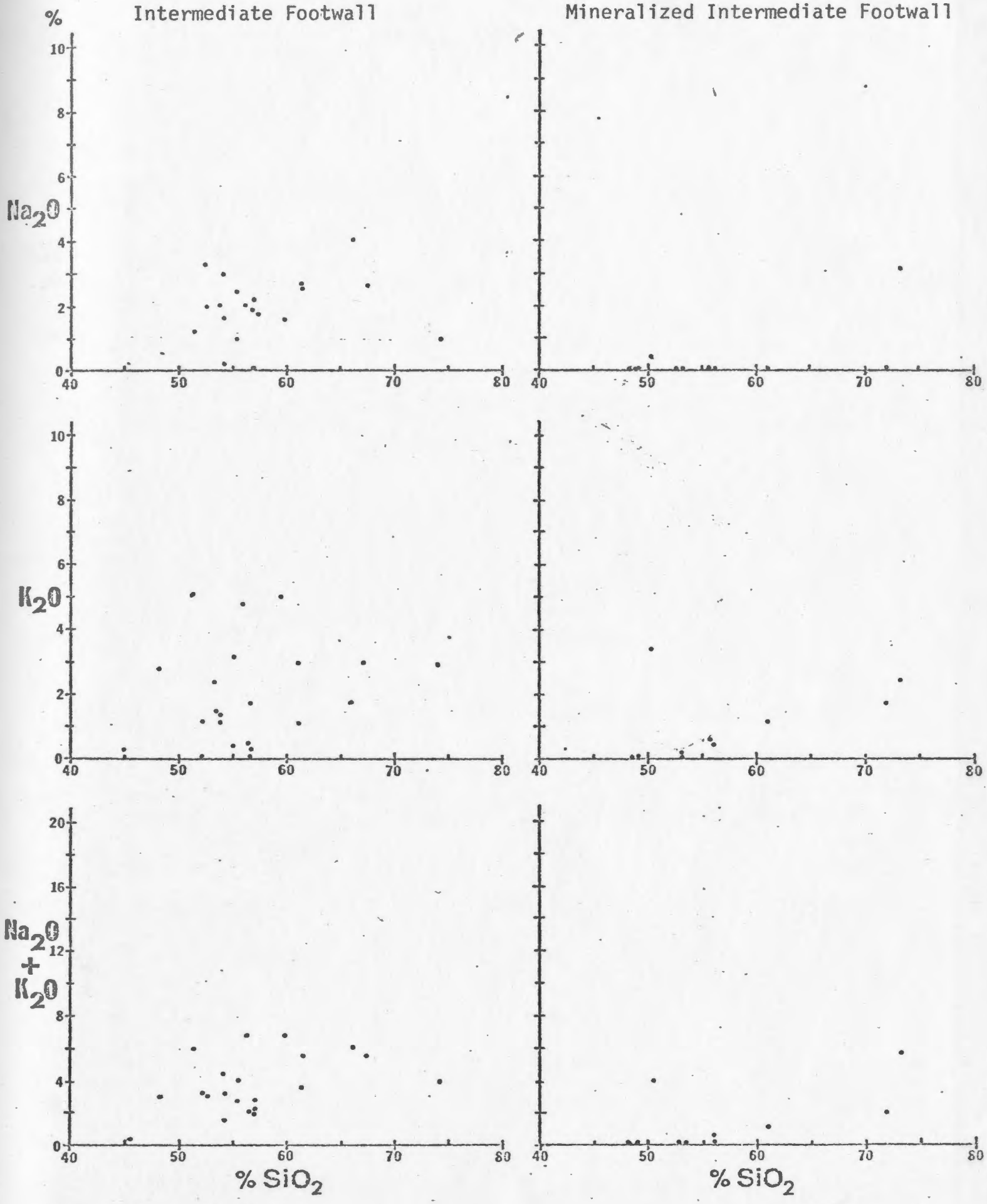
%
Intermediate Footwall
Mineralized Intermediate Footwall
Na_2O
K_2O
$Na_2O + K_2O$
% SiO_2
% SiO_2

Fig. 15 (Cont'd.)

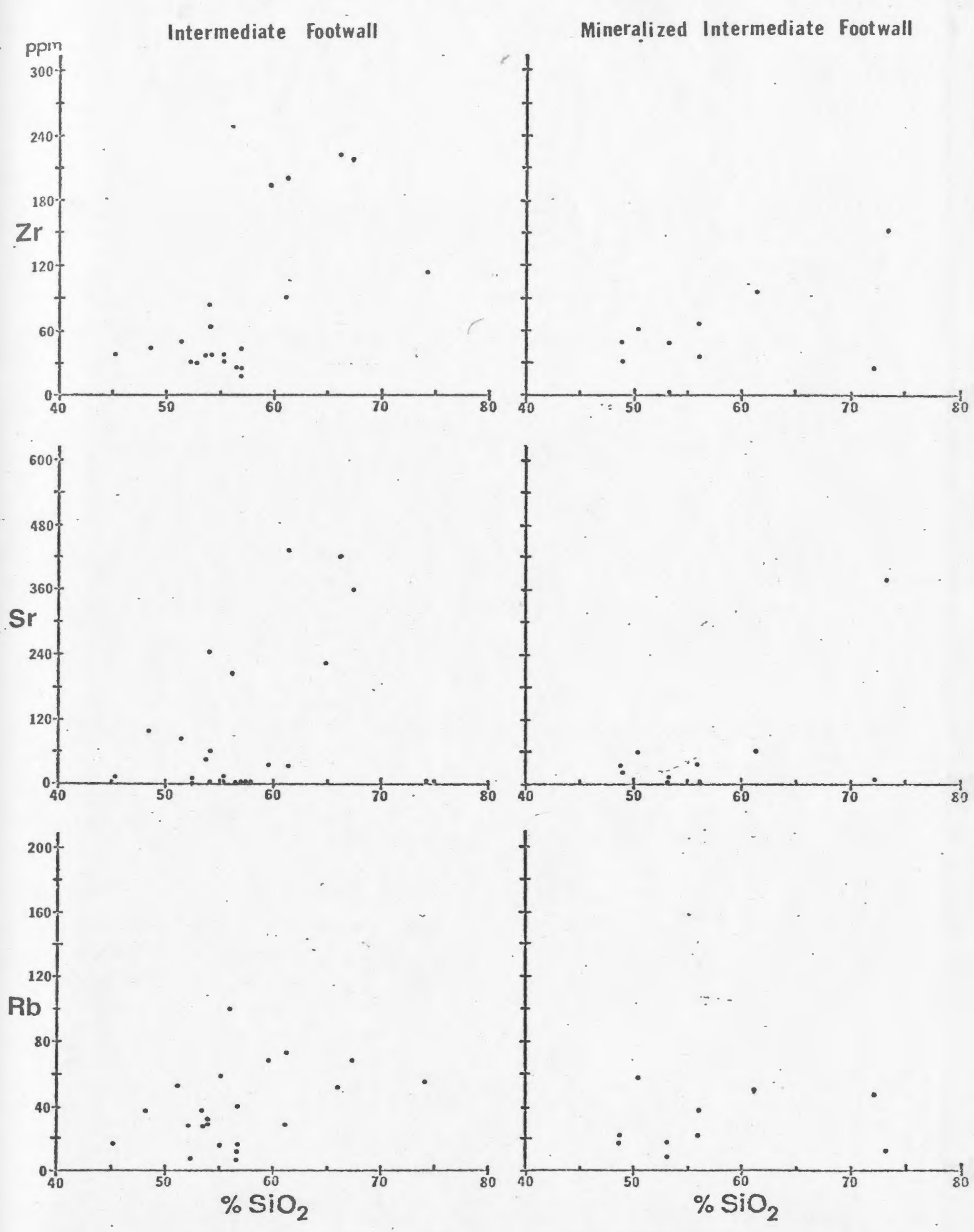
Intermediate Footwall
Mineralized Intermediate Footwall
ppm
Zr
Sr
Rb
% SiO2
% SiO2

Fig. 15 (Cont'd.)

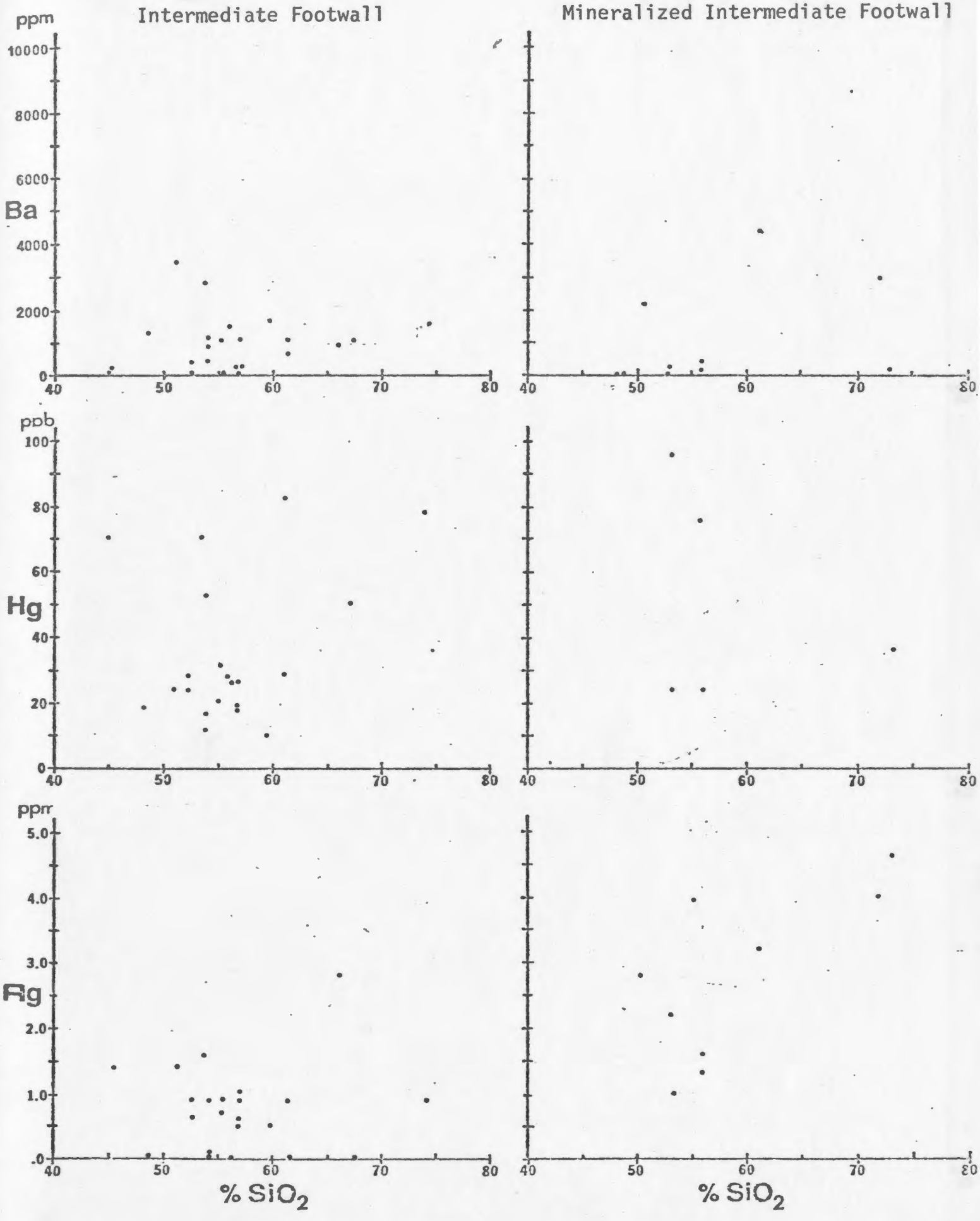
Intermediate Footwall
Mineralized Intermediate Footwall
ppm
Ba
10000
8000
6000
4000
2000
0
ppb
Hg
100
80
60
40
20
0
ppm
Ag
5.0
4.0
3.0
2.0
1.0
.0
40
50
60
70
80
% SiO2

Fig. 15 (Cont'd.)

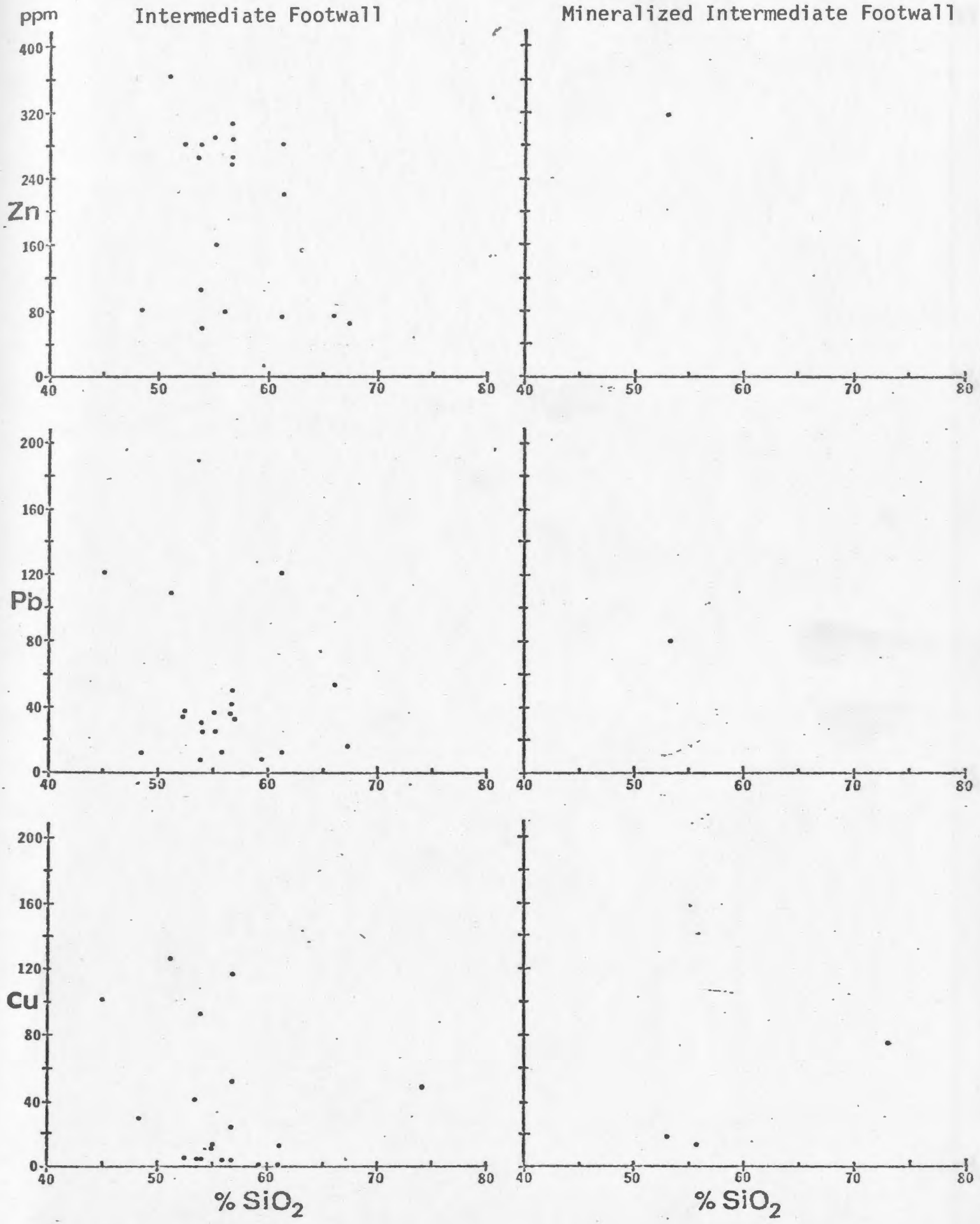
ppm
Intermediate Footwall
Mineralized Intermediate Footwall
Zn
Pb
Cu
400
320
240
160
80
0
200
120
40
50
60
70
80
% SiO2

Fig. 15 (Cont'd.)

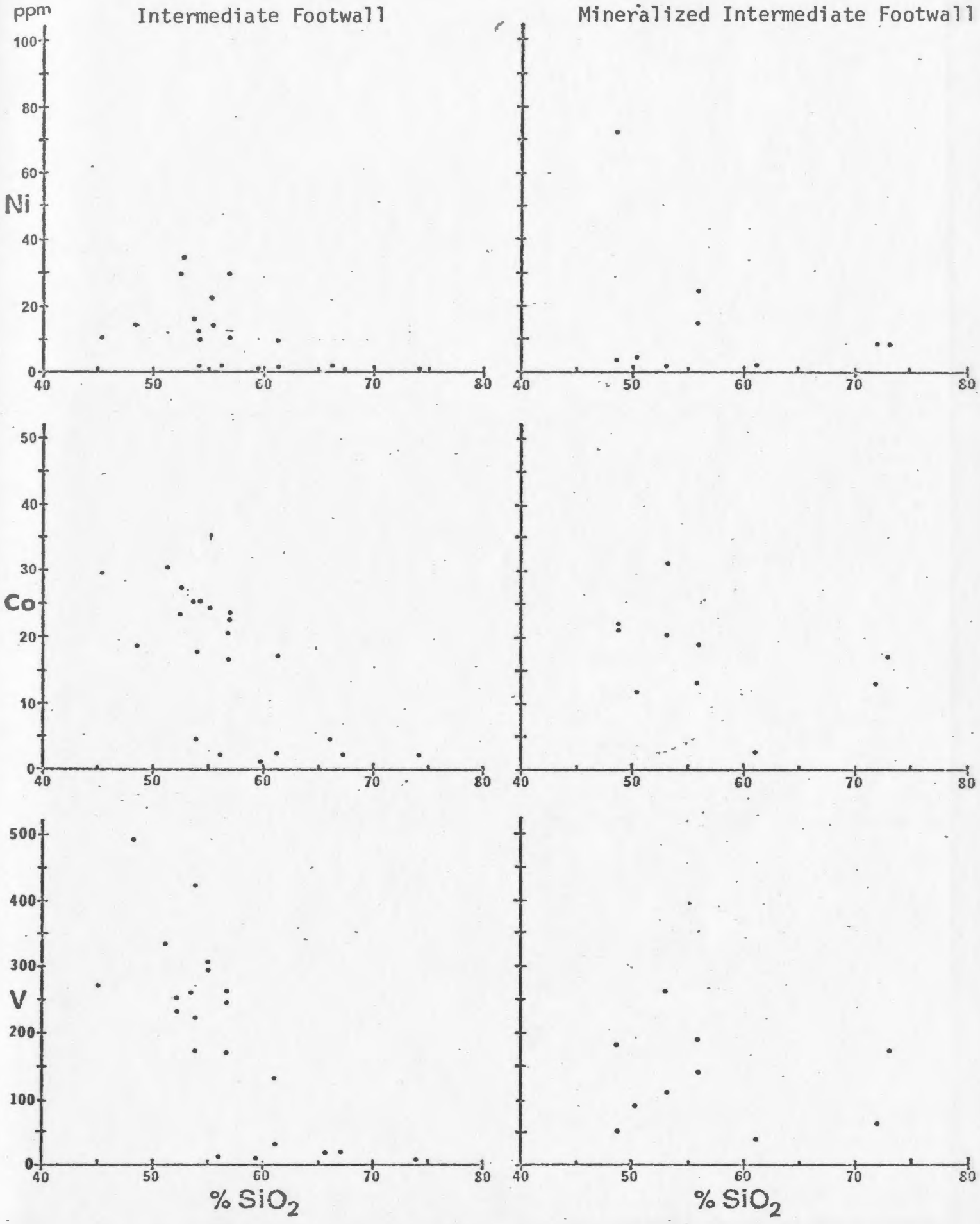
ppm
Intermediate Footwall
Mineralized Intermediate Footwall
Ni
Co
V
% SiO2
% SiO2

Fig. 15 (Cont'd.)

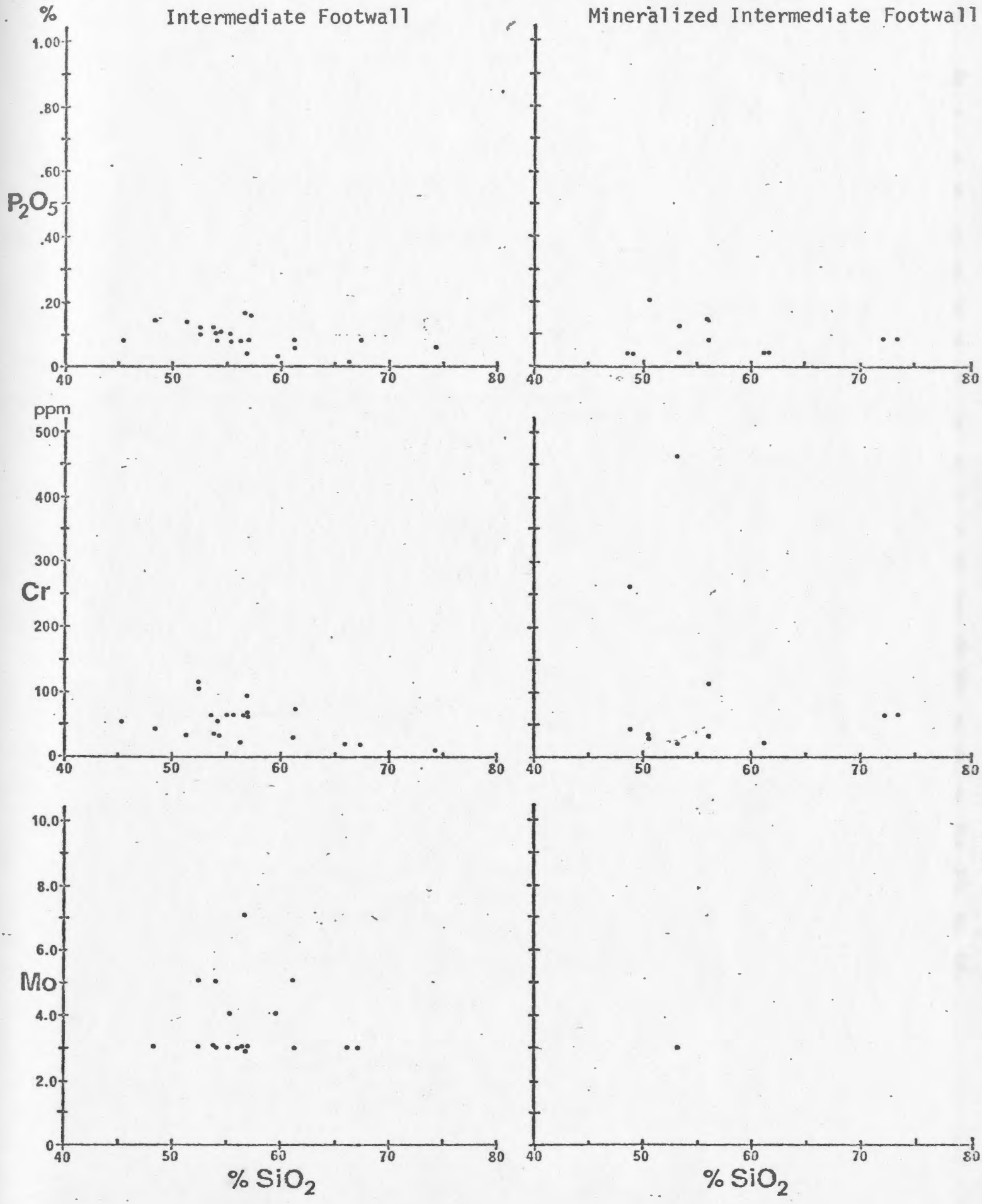
Intermediate Footwall
Mineralized Intermediate Footwall
%
P_2O_5
1.00
.80
.60
.40
.20
0
ppm
Cr
500
400
300
200
100
0
Mo
10.0
8.0
6.0
4.0
2.0
0
40
50
60
70
80
% SiO_2

Table 12

Correlation matrix comparing Intermediate Footwall and Mineralized Intermediate Footwall.

Upper Figures: Intermediate Footwall
Significance = .001 @ .56
= .01 @ .46

Lower Figures: Mineralized Intermediate Footwall
Significance = .001 @ .70
= .01 @ .60

	Fe_2O_3	TiO_2	P_2O_5	SiO_2	CaO	K_2O	MgO	Al_2O_3	Na_2O	L.O.I.	MnO	Zr	Sr	Rb	Zn	Cu	Mo	Ba	Pb	Ni	Co	Cr	V	Mg
TiO_2	-32 -35																							
P_2O_5	- 4 -27	44 89																						
SiO_2	-86 -87	- 2 13	-25 9																					
CaO	-14 25	55 4	-21 - 7	12 -30																				
K_2O	-55 56	59 62	1 55	34 59	31 4																			
MgO	61 7	- 7 14	56 10	-75 -42	-43 -30	-59 -55																		
Al_2O_3	-51 -51	73 86	39 75	- 7 19	26 -17	60 51	-11 41																	
Na_2O	-42 -39	1 8	-15 11	33 42	19 - 5	- 7 56	-29 -30	36 31																
L.O.I.	16 2	25 13	48 33	-43 4	-28 9	-15 29	49 -41	24 -16	0 -19															
MnO	41 8	-37 22	32 2	-44 -34	-51 33	-74 -41	77 63	-20 32	3 -36	-22 -45														
Zr	-55 -23	16 - 6	-50 12	53 21	46 -13	61 43	-80 -31	37 11	40 78	-46 10	-64 -62													
Sr	-29 -13	31 -11	-40 - 5	32 19	71 8	33 43	-61 -37	22 7	43 94	-40 -13	-57 -45	76 84												
Rb	-56 -27	44 43	-20 40	45 27	37 - 3	88 62	-75 -41	51 15	6 -20	-30 66	-76 -42	83 6	56 -27											
Zn	8 -23	-49 24	7 9	6 12	-41 -16	-22 15	18 22	-35 22	-23 -19	-33 2	33 -13	-34 -12	-47 -23	-29 43										
Cu	10 49	- 1 1	- 4 2	5 -41	8 -31	-19 -14	4 13	-23 6	6 -24	-17 -14	6 -17	- 8 -12	14 -18	-14 12	20 29									
Mo	26 22	-17 - 1	18 - 2	-28 - 2	-13 13	- 3 18	35 -38	-16 32	-29 -15	-43 49	31 -40	-24 -17	-25 - 6	-20 40	55 34	29 15								
Ba	47 41	- 7 -18	-27 -31	-35 -31	4 62	20 2	-17 -44	-33 -46	-39 -12	6 25	-40 -13	2 0	10 14	15 15	-13 - 7	16 -22	- 6 39							
Pb	-28 -23	-35 7	-18 - 3	47 14	-19 -33	14 10	-35 16	-25 6	-16 -14	-33 12	-26 -34	4 0	-19 -14	11 43	73 92	2 29	12 51	6 - 2						
Ni	25 -24	4 2	59 -23	-39 0	-32 - 7	-43 -34	62 64	5 31	13 -15	49 -54	52 79	-67 -47	-47 -29	-54 -41	15 5	30 -27	10 -44	-22 -29	-25 - 7					
Co	75 - 7	-11 14	27 4	-71 -25	-24 -16	-45 -44	62 86	32 40	-28 -10	33 -54	44 60	-78 -28	-46 -19	-60 -51	21 35	26 1	28 -33	30 -37	-22 20	66 68				
Cr	25 -18	-22 6	52 -20	-33 -12	-49 - 8	-62 -39	66 76	- 8 37	18 -16	48 -57	71 78	-67 -44	-53 -27	-67 -43	20 16	15 -18	4 -40	-24 -27	-25 5	91 97	56 79			
V	64 -31	21 21	49 17	-24 0	- 4 -32	-40 -24	76 80	- 5 61	-29 11	50 -47	41 60	-78 -13	-40 - 8	-63 -48	5 - 2	- 9 -17	18 -63	9 -62	-28 -13	88 77	79 77	45 80		
Mg	-20 1	-17 6	-42 - 3	35 -33	18 1	- 5 -26	-40 55	-15 15	41 -23	-41 -18	-23 13	40 - 2	51 -15	11 3	1 78	51 22	- 2 0	2 2	16 66	-28 18	-22 62	75 35	33 20	
Ag	35 68	-45 -38	-33 -33	-19 -51	-26 46	-29 -19	4 -32	-44 58	12 2	- 8 25	14 -26	-36 14	- 5 31	-31 -11	22 - 8	47 10	20 61	49 69	14 6	3 -44	42 -24	6 -37	6 -61	63 7

strongly correlative. Cu behaves independently of both these two groups. On this basis, it appears that three mutually independent types of mineralization have operated on the mineralized Intermediate Footwall, i.e. Zn-Pb-Hg, Ba-Ag and Cu. None of these types of mineralization bear any consistent relationship to silicification, sericitization or chloritization (represented by Si, K and Mg respectively). The existence of these distinct types of mineralization does not necessarily indicate numerous episodes of mineralization but merely demonstrates the inhomogeneous nature of the mineralization of the Intermediate Footwall.

5.1.2. Footwall and Cycle Two Andesites

In general the scatter for most elements on the Harker variation diagrams (Fig. 16) is more compact for the Cycle Two Andesite than for the Footwall Andesite. Ca, K and Na distributions are diffuse for both groups reflecting the mobility of these elements. Zr distribution is more compact for the Footwall Andesite and displays a well defined decreasing trend with silica as opposed to increasing trends for all other units. Among the base metals, Zn and Cu decrease with silica in the Cycle Two Andesite but show no consistent trend in the Footwall Andesite. Pb, Hg, Ag and Ba vary independently of silica in both groups.

The correlation matrix (Table 13) reveals some unexpected metal associations within the Footwall Andesite. Fe has anomalously low (less than .30) correlations with Mg, Ni, Co, Cr and V. However the group Pb, Ag, Mg, Ni and Cr exhibit mutual correlations greater than .70 and within this group Ag, Ni and Cr exhibit mutual correlations greater than .90. Cu, Zn

Fig. 16. Harker diagrams comparing Footwall Andesite to Cycle Two Andesite.

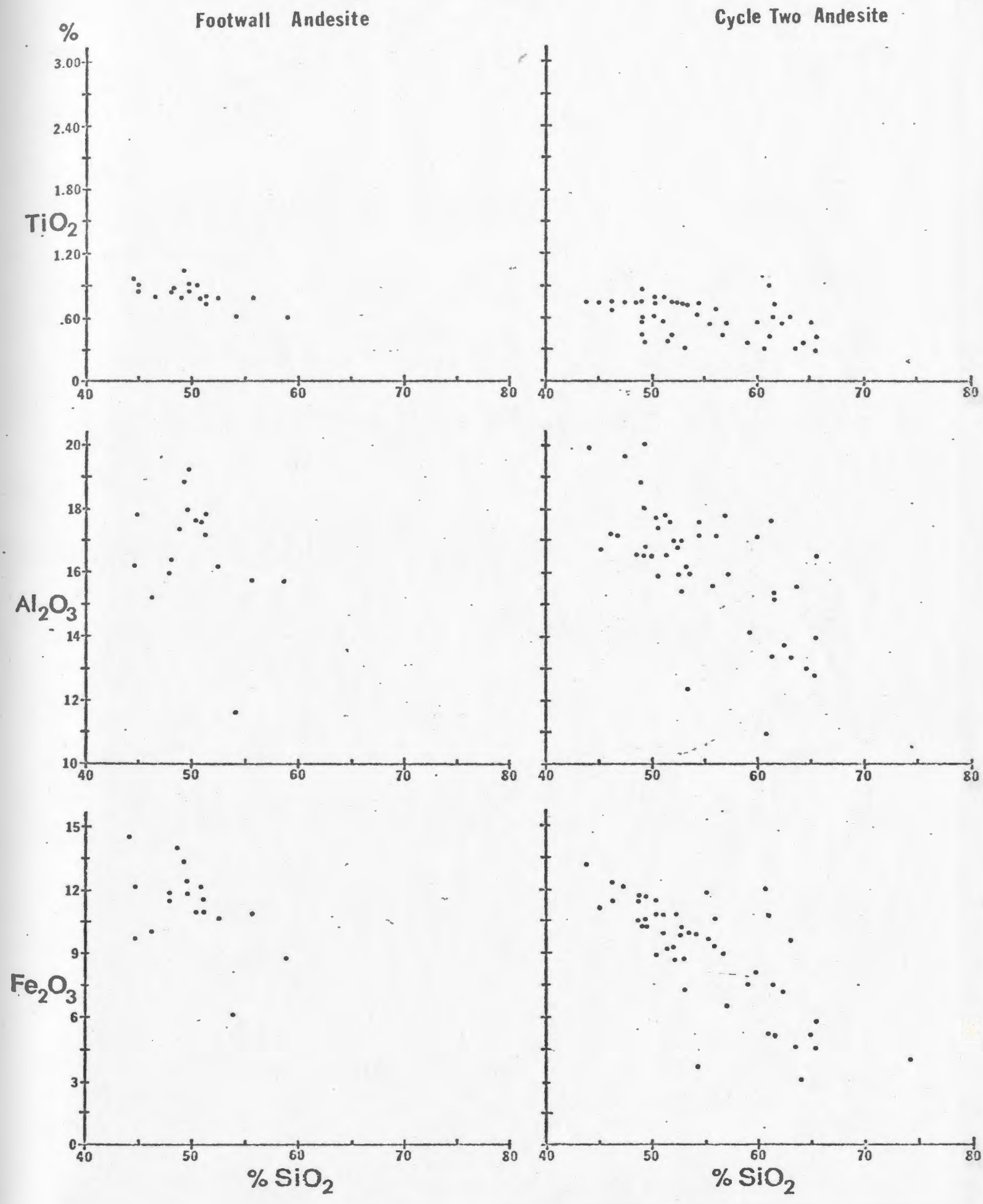

Fig. 16 (Cont'd.)

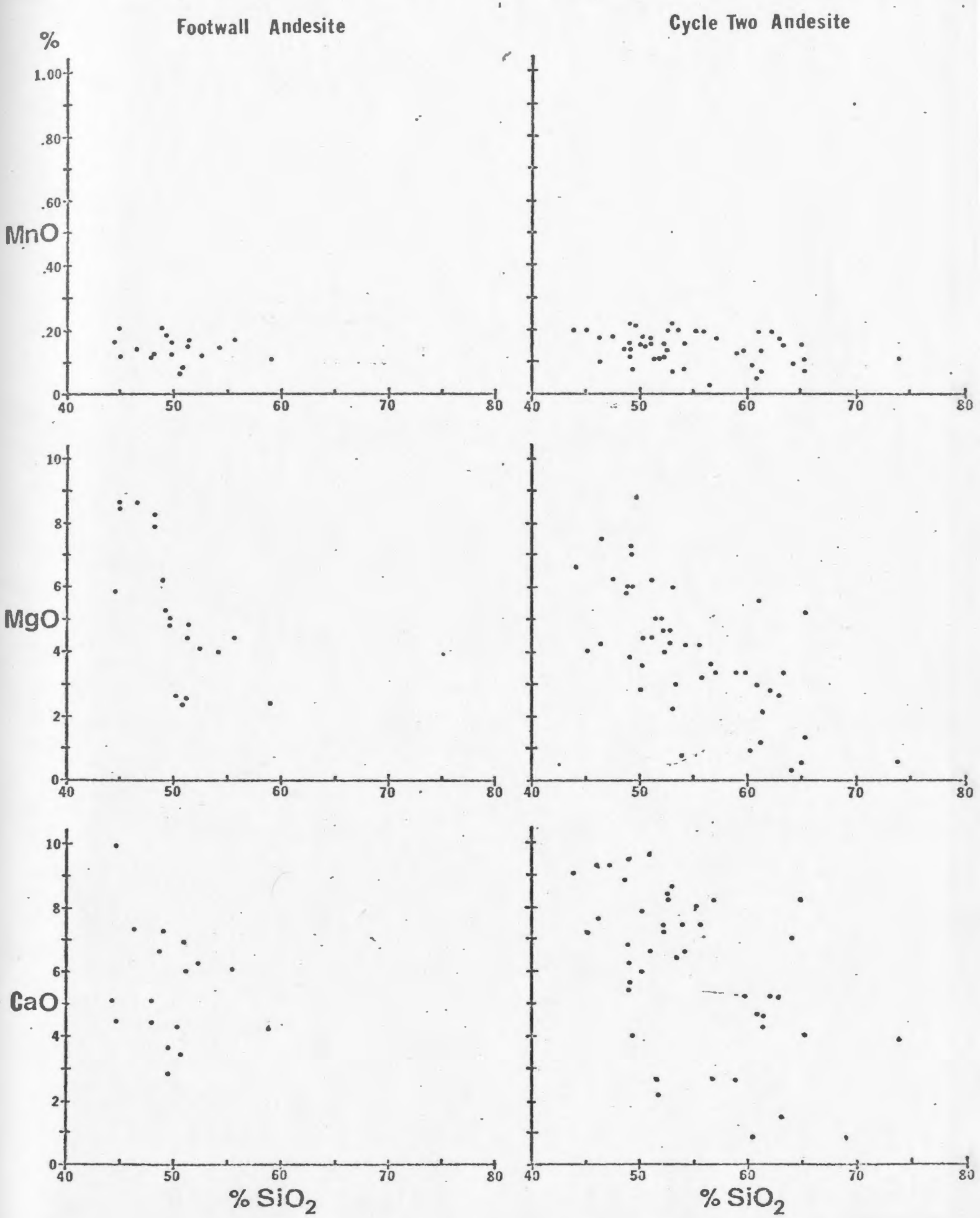
Footwall Andesite
Cycle Two Andesite
%
MnO
1.00
.80
.60
.40
.20
0
MgO
10
8
6
4
2
0
CaO
10
8
6
4
2
0
40
50
60
70
80
% SiO2
% SiO2

Fig. 16 (Cont'd.)

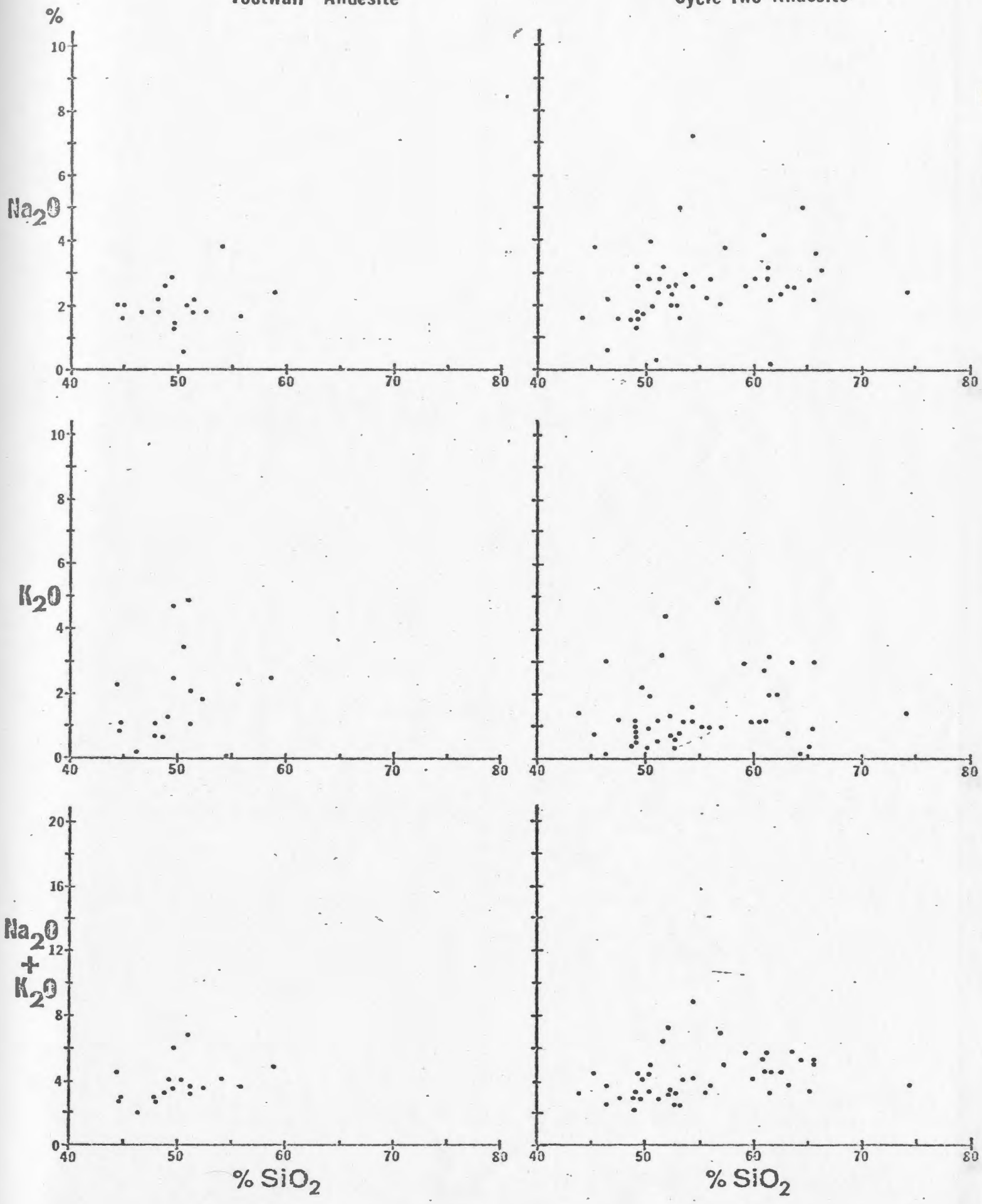
Footwall Andesite
Cycle Two Andesite
%
Na_2O
K_2O
$Na_2O + K_2O$
% SiO_2
% SiO_2

Fig. 16 (Cont'd.)

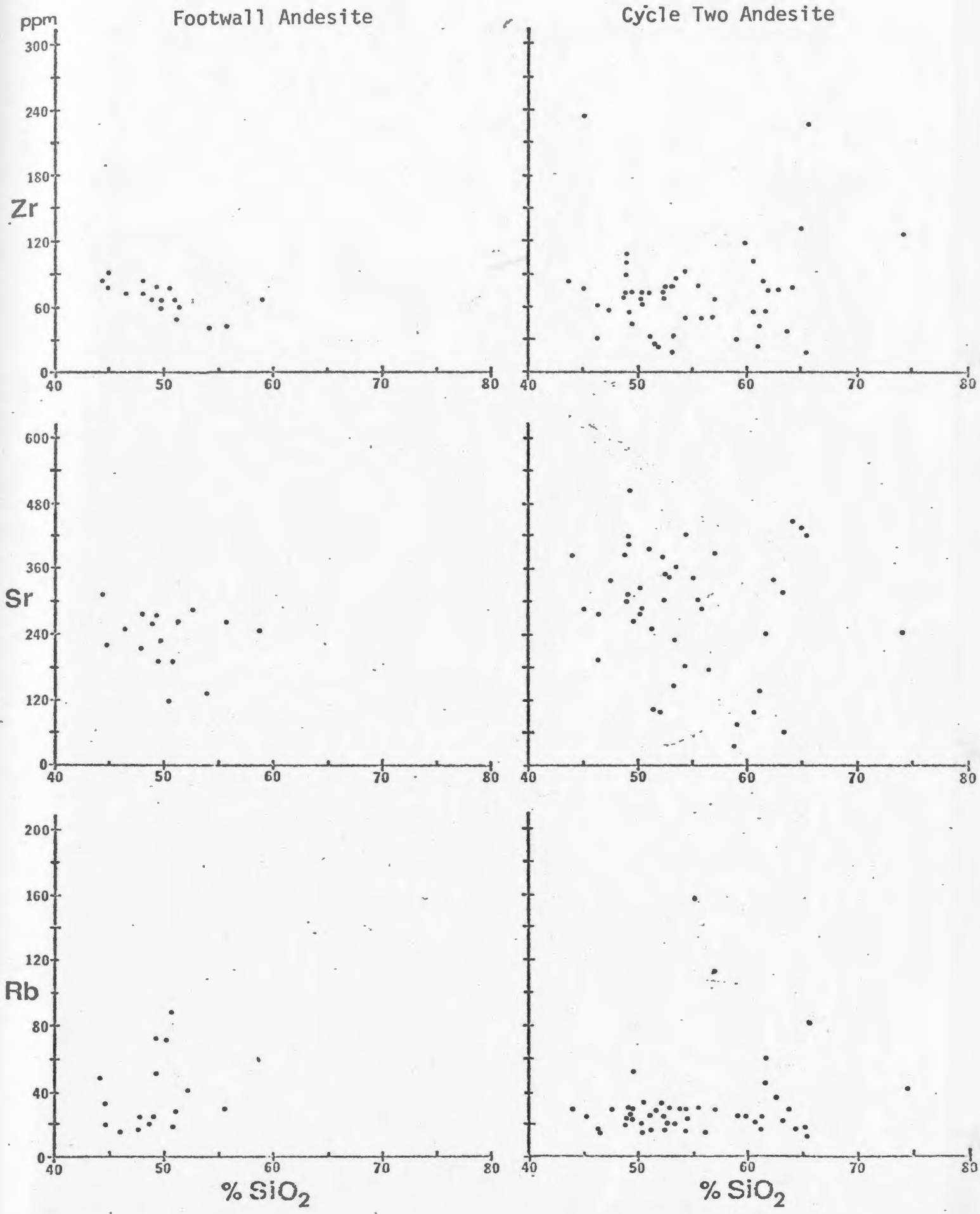

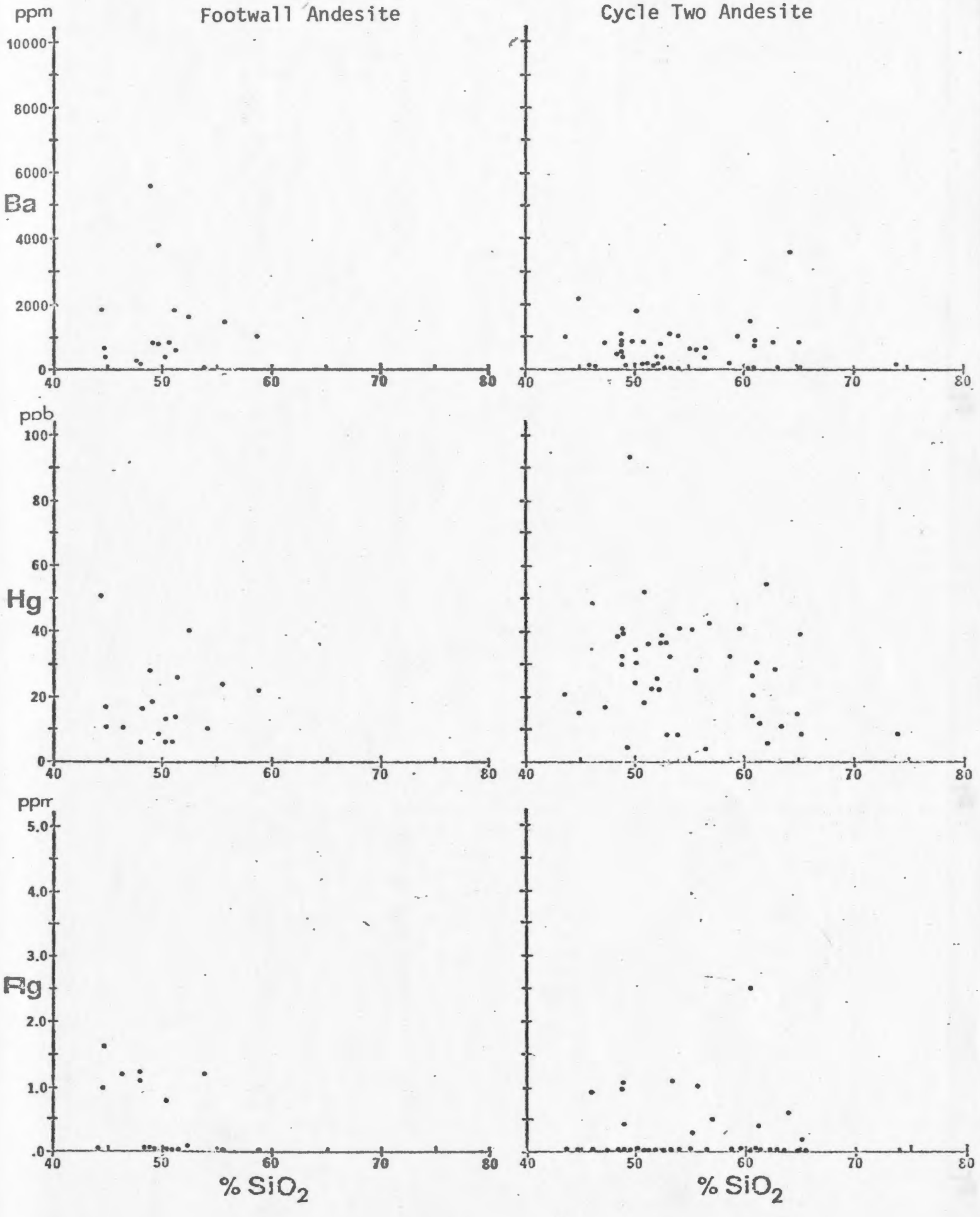
Footwall Andesite
Cycle Two Andesite
ppm
Ba
10000
8000
6000
4000
2000
0
ppb
Hg
100
80
60
40
20
0
ppm
Ag
5.0
4.0
3.0
2.0
1.0
.0
40
50
60
70
80
% SiO2

Fig. 16 (Cont'd.)

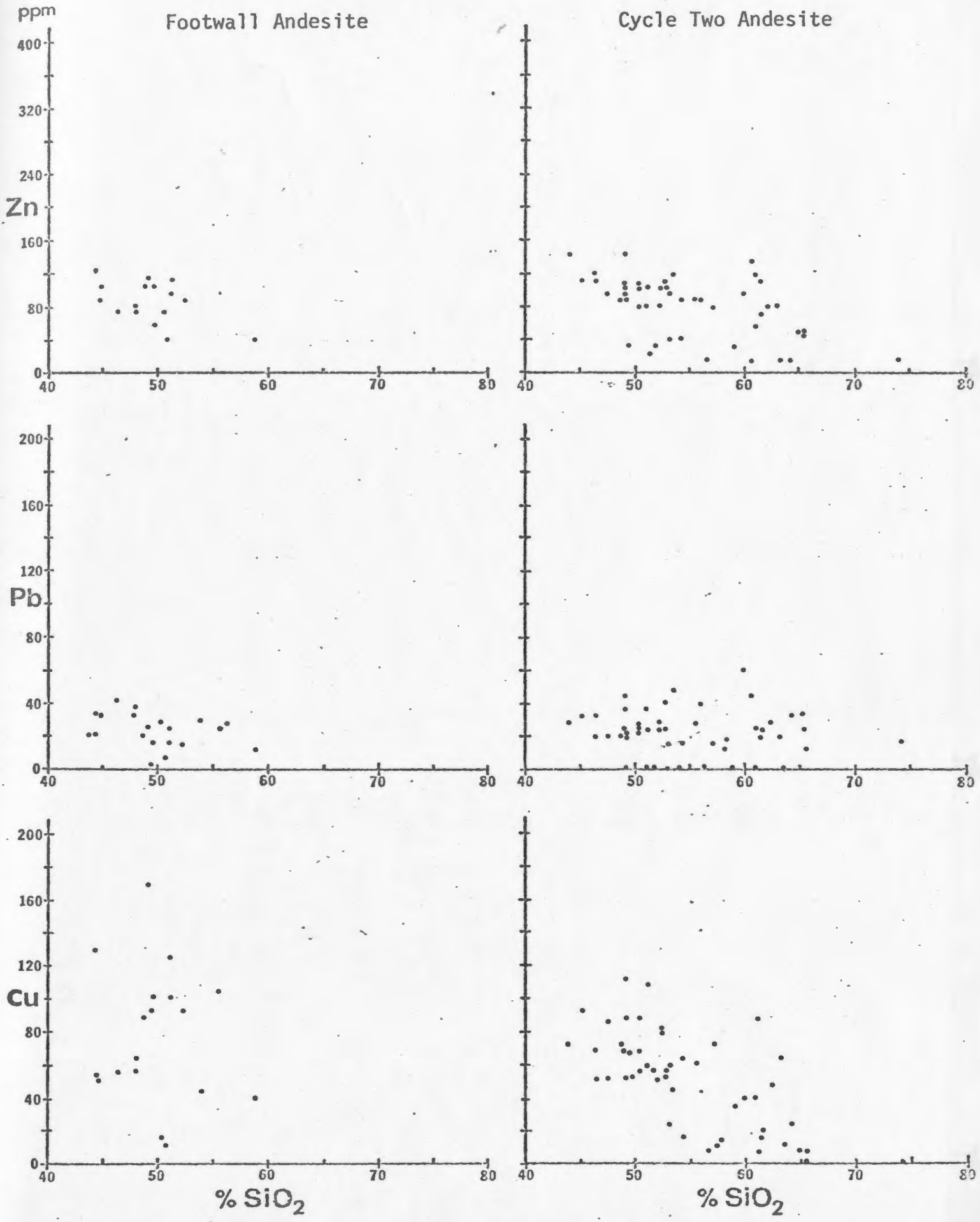
ppm
Footwall Andesite
Cycle Two Andesite
Zn
Pb
Cu
400
320
240
160
80
0
200
120
40
50
60
70
% SiO_2

Fig. 16 (Cont'd.)

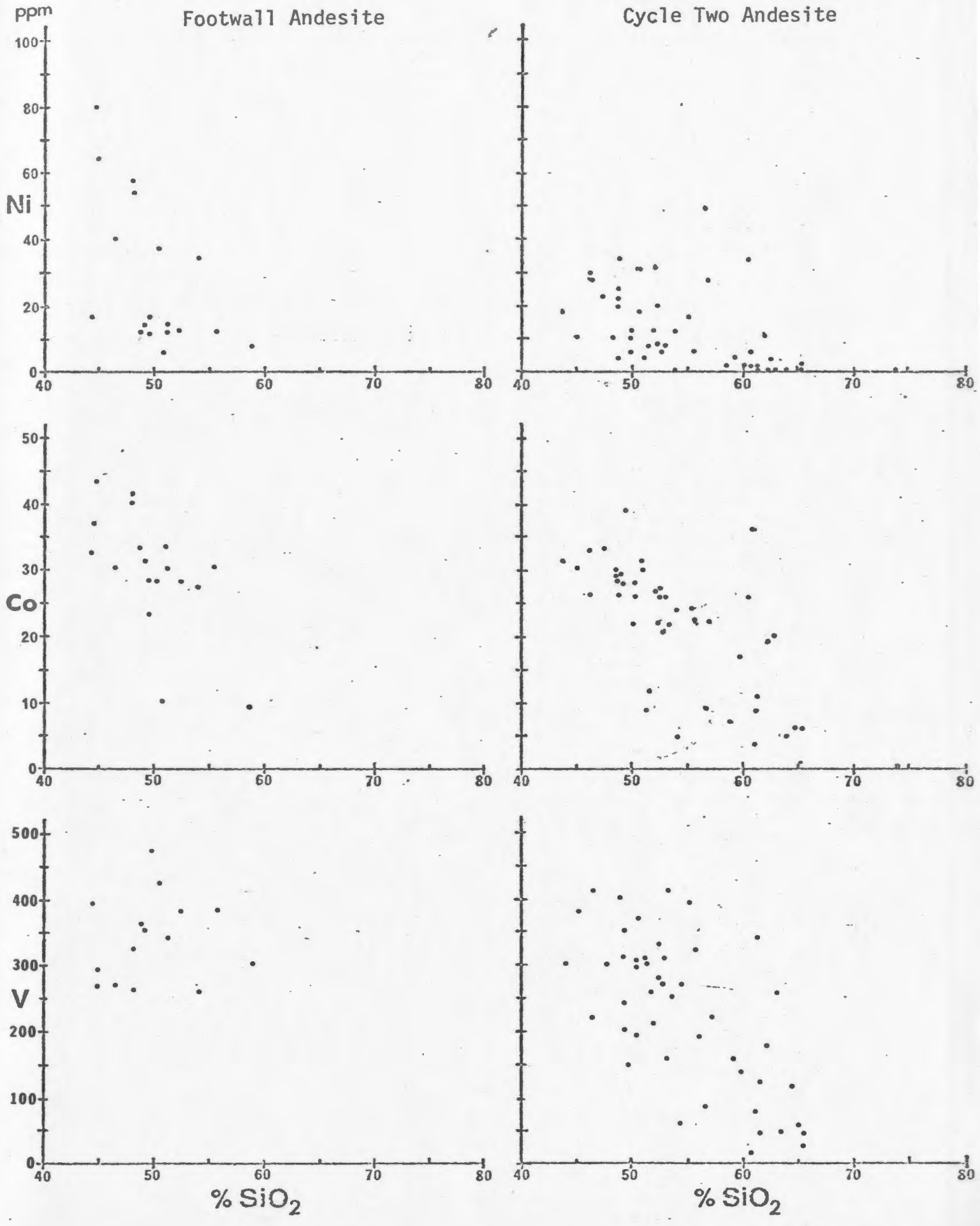
ppm
Footwall Andesite
Cycle Two Andesite
Ni
Co
V
100
80
60
40
20
0
50
30
10
500
400
300
200
100
40
50
60
70
80
% SiO2
% SiO2

Fig. 16 (Cont'd.)

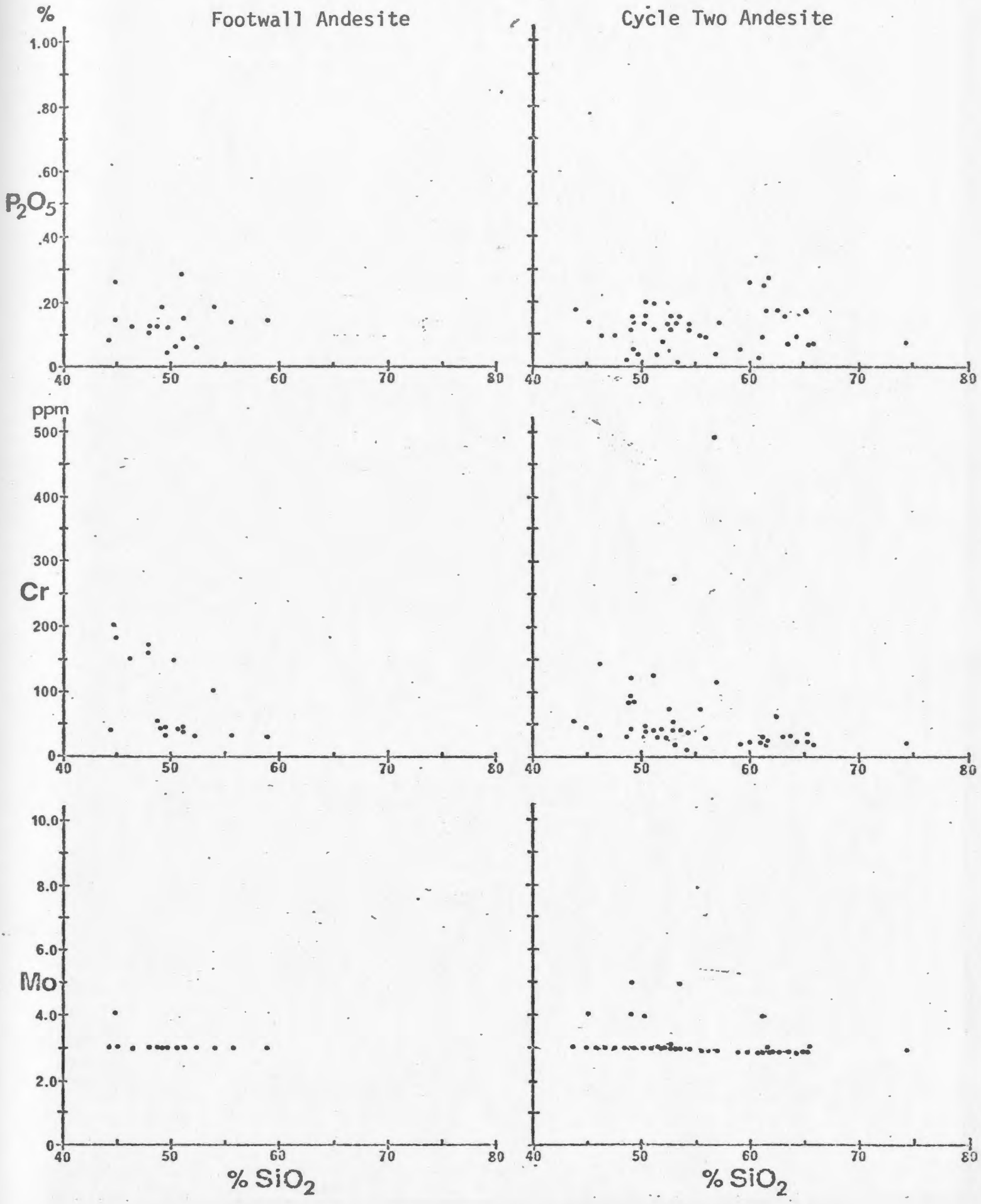
Footwall Andesite
Cycle Two Andesite
%
1.00
.80
.60
P_2O_5
.40
.20
0
ppm
500
400
300
Cr
200
100
0
10.0
8.0
6.0
Mo
4.0
2.0
0
40
50
60
70
80
% SiO_2

Table 13

Correlation Matrix comparing Footwall and Cycle Two Andesites.

Upper Figures: Cycle Two Andesite
Significance = .001 @ .42
= .01 @ .34

Lower Figures: Footwall Andesite
Significance = .001 @ .64
= .01 @ .55

	Fe_2O_3	TiO_2	P_2O_5	SiO_2	CaO	K_2O	MgO	Al_2O_3	Na_2O	L.O.I.	MnO	Zr	Sr	Rb	Zn	Cu	Ni	Ba	Pb	Ni	Co	Cr	V	Mg
TiO_2	56 77																							
P_2O_5	12 -21	59 - 9																						
SiO_2	-77 -34	-51 -54	0 -13																					
CaO	34 -43	50 -22	28 37	-54 -43																				
K_2O	-21 28	-32 20	-31 1	17 31	-64 -64																			
MgO	59 16	11 32	-16 9	-43 -72	19 34	- 7 -62																		
Al_2O_3	48 85	53 71	6 -22	-72 -13	25 -61	13 54	52 -10																	
Na_2O	-33 -34	- 9 -44	4 39	17 19	5 44	-24 -52	-46 0	-15 -46																
L.O.I.	1 -10	-15 18	-22 -15	-27 - 2	- 1 -29	20 -13	2 27	- 7 -10	0 - 9															
MnO	41 16	54 17	38 23	-28 -44	46 67	-40 -45	- 1 48	19 - 4	0 31	-35 -45														
Zr	-14 36	13 57	23 12	27 -65	10 3	-15 -11	-35 48	- 2 36	2 -24	-40 17	17 1													
Sr	26 33	37 17	28 5	-24 -17	59 17	-51 -18	7 36	24 29	7 2	-41 -48	41 56	66 17												
Rb	-19 23	-20 14	-19 - 4	21 27	-36 -67	63 54	-11 -63	9 50	-28 -51	- 5 - 3	-40 -61	30 6	- 6 -31											
Zn	66 32	85 41	56 - 6	-57 -29	53 36	-44 -28	30 29	49 26	-26 19	-16 -26	67 70	15 1	66 51	-30 -48										
Cu	73 50	55 38	19 -26	-66 2	48 - 2	-34 -11	44 2	35 49	-24 17	0 -36	53 52	-11 -11	40 52	-36 -26	61 67									
Mo	22 -19	-15 12	-18 48	5 -24	-31 34	- 5 -14	-21 36	-25 - 7	-13 1	20 0	- 7 32	0 41	-14 41	- 7 -18	- 9 16	1 -15								
Ba	- 9 50	8 11	22 -16	15 10	2 -10	- 2 27	-17 -13	-16 40	1 1	-19 -26	25 36	15 -23	21 24	7 15	10 34	6 33	6 -11							
Pb	32 -16	42 14	41 9	- 8 -42	28 41	-46 -64	-21 75	0 -38	- 7 4	-15 40	48 27	47 27	57 7	-21 -66	57 24	28 -19	35 22	21 -32						
Ni	19 -22	-20 -19	-20 23	-31 -53	16 31	5 -48	55 75	3 -30	-28 - 8	23 45	-27 18	-26 55	4 14	20 -42	-13 4	18 -43	-11 56	- 9 -46	-31 -77					
Co	86 24	57 46	20 -16	-74 -55	53 25	-44 -67	61 79	35 3	-26 - 6	1 25	42 41	17 32	35 37	-31 -66	66 61	81 23	11 20	1 - 6	31 71	44 67				
Cr	14 -23	-23 17	-31 19	-20 -66	0 32	24 -46	44 70	8 -35	-24 -14	7 48	-39 0	-21 56	0 -12	51 -37	-23 - 8	0 -54	- 9 43	- 8 -50	-36 79	86 97	26 60			
V	72 30	68 13	27 15	-73 19	62 -50	-43 74	48 -56	46 45	-13 -27	- 7 - 9	53 -39	-18 -13	28 -23	-40 71	66 -32	75 - 1	-21 -19	2 14	18 -75	4 -54	74 -55	- 5 -51		
Mg	18 41	- 5 13	- 8 -35	6 11	-15 -13	-24 12	-23 -13	-25 41	29 5	6 -35	0 23	0 +11	8 50	-25 4	- 4 53	13 53	77 -15	15 55	41 -27	-22 -44	13 2	-22 -53	- 6 -10	
Ag	17 -43	- 9 - 1	-20 24	1 -54	-13 52	-10 -57	-22 67	-20 -57	11 7	15 45	8 9	- 4 42	- 2 -18	-13 -49	4 - 5	7 -54	78 39	- 2 -53	49 29	-11 90	12 52	-12 94	-20 -59	75 -50

and Hg are moderately correlative but have no affinity for the above-mentioned group. Ba exhibits no affinity for the base metals and has an anomalously low correlation coefficient with K (.20). Ba and K have nearly identical ionic radii and the higher charge of the Ba^{++} ion allows it to be captured in magmas in early formed K minerals, principally K-feldspar (Taylor, 1965). The lack of any Ba:K coherence seems to indicate that the high Ba concentrations found in the Footwall Andesite are independent of any magmatic process and instead are a function of other processes, for example precipitation of interstitial sulphate during deposition, or post-depositional migration from the orebodies. In view of the limited extent of dispersion patterns around the orebodies (see section 5.2.) the former seems much more probable.

Correlations within the Cycle Two Andesite are markedly different in character than those in the Footwall Andesite. Fe exhibits stronger correlations with the other ferromagnesian elements, and Pb and Ag display no coherence with this group. Instead Fe, Co, V, Cu and (Zn) exhibit strong mutual correlations. Hg, Ag, and Mo form an independent association. It is difficult to interpret the significance of these correlations without knowledge of the trace element content of the various mineral phases present. Ba varies independently of K (-.02) in the central and southeastern portions of the N60W section, probably indicating a secondary origin for the high Ba content in these areas. However Ba and K exhibit a strong correlation (.80) in the Cycle Two Andesites of diamond drill hole 2666, indicating original magmatic control over Ba distribution with little

or no secondary enrichment. From this it may be assumed that the Ba content of this portion of the Cycle Two Andesite is probably a reasonable estimate of the original Ba content of the unit as a whole.

5.1.3. Hangingwall and Footwall Dacites

In general, trends on the Harker variation diagrams (Fig. 17) are well defined and compact for both the Footwall and Hangingwall Dacites. The only obvious differences between the two units are more diffuse patterns in the Footwall for MgO and $Na_2O + K_2O$ and the presence of several anomalously high Zn and Pb values. Na increases and K decreases with silica in both units but a strong negative correlation between the two elements is found only in the Hangingwall where altered matrix glass is more abundant.

As in the Footwall Andesite, Fe displays little or no coherence with Ni, Co, Cr, V and Mg in the Hangingwall Dacite (Table 14). Ni, Co and V exhibit near perfect positive correlations (greater than .97) indicating that these elements are entering a single mineral phase in fixed proportions. The only major elements with which this group is correlative are Mg and Al, almost certainly indicating that the mineral is a magnesian chlorite. Cu and, to a lesser extent, Zn correlate strongly with Ni, Co and V, indicating that the concentration of these base metals in the Hangingwall Dacite is probably largely dependent upon chlorite content. Pb, Hg and Ag in the Hangingwall Dacite are independent of chlorite content and show little mutual correlation.

The behaviour of base metals in the Footwall Dacite is considerably different and more complex than in the Hangingwall. Cu, Pb and Cr

Fig. 17. Harker Diagrams comparing Footwall and Hangingwall Dacite.

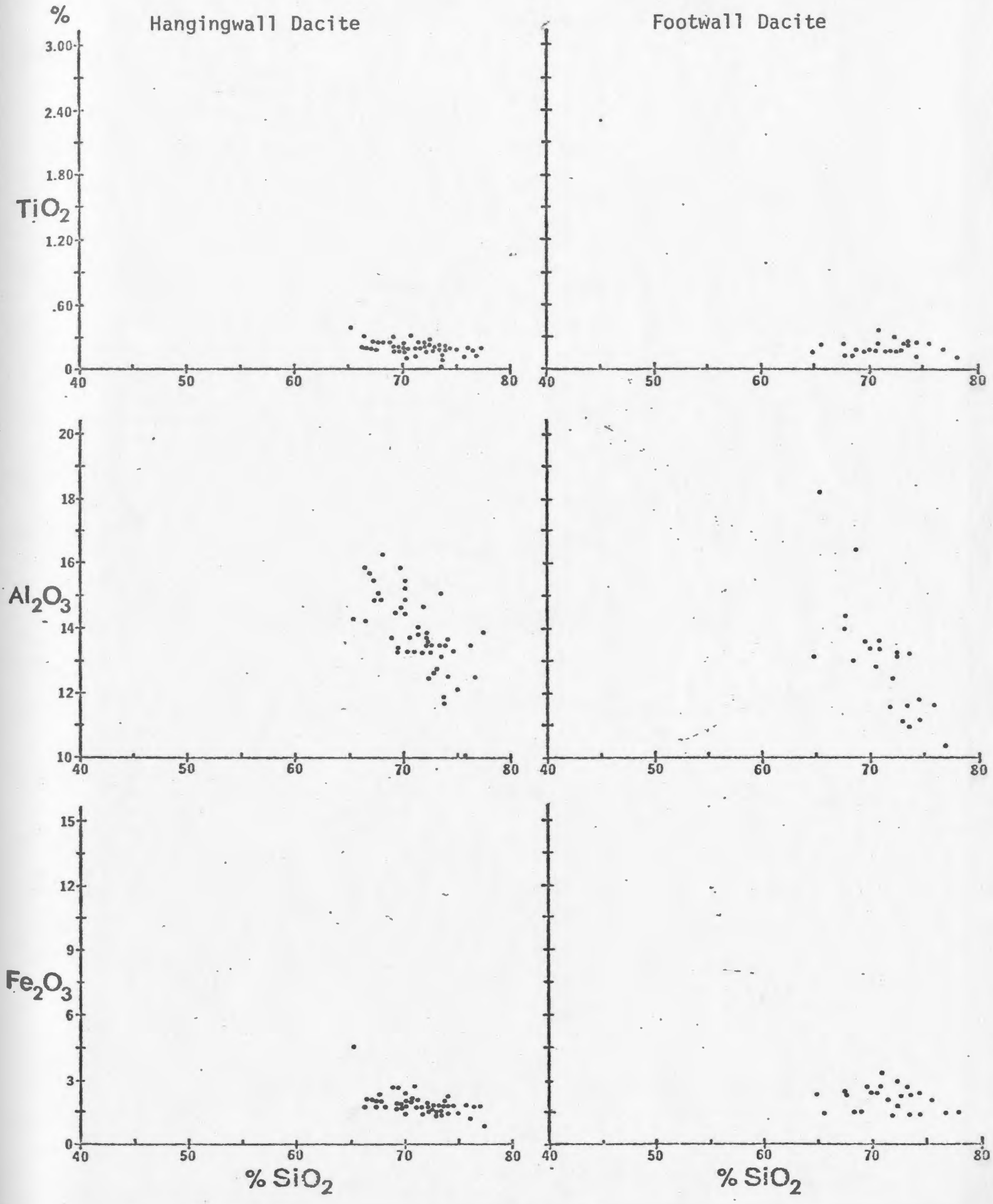

Fig. 17 (Cont'd.)

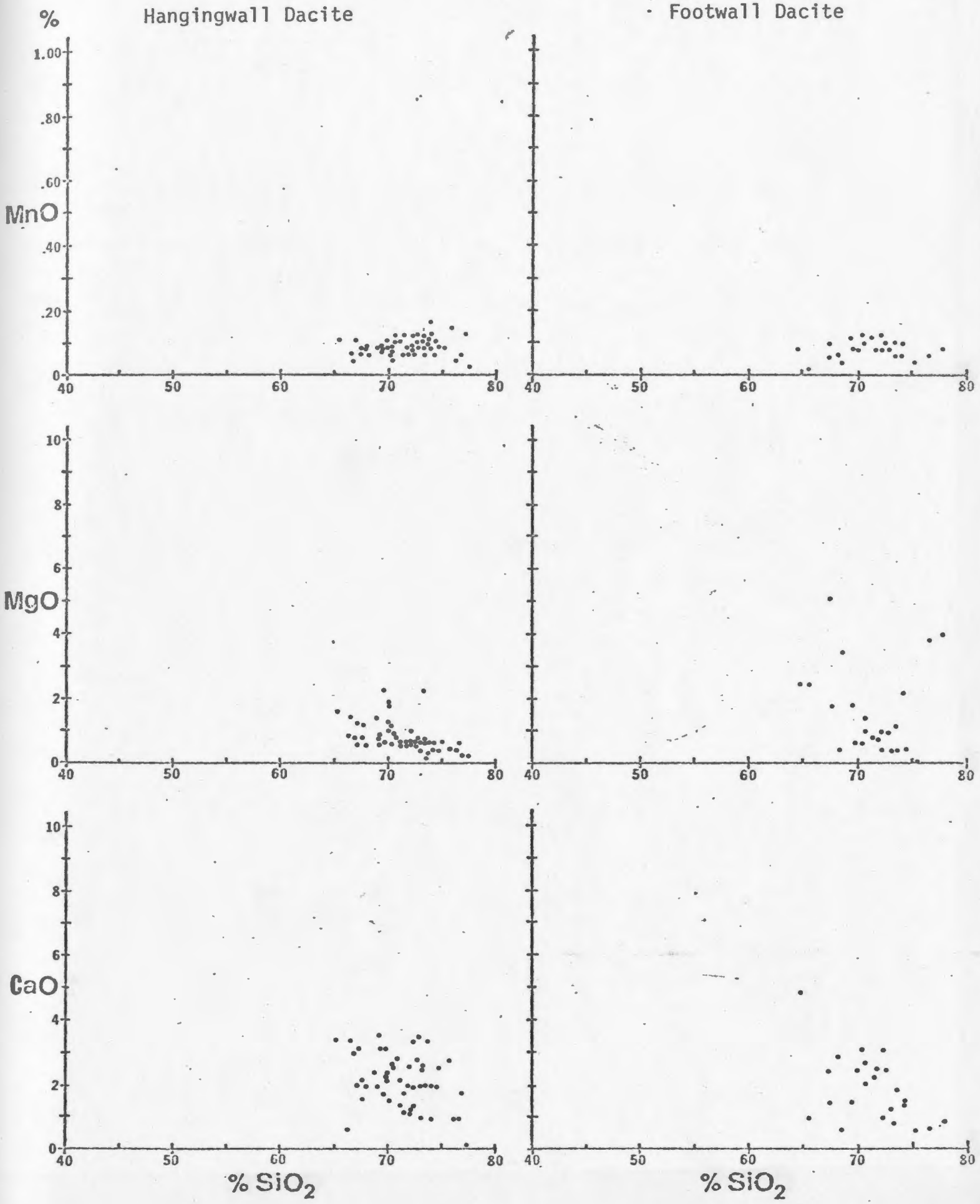

Fig. 17 (Cont'd.)

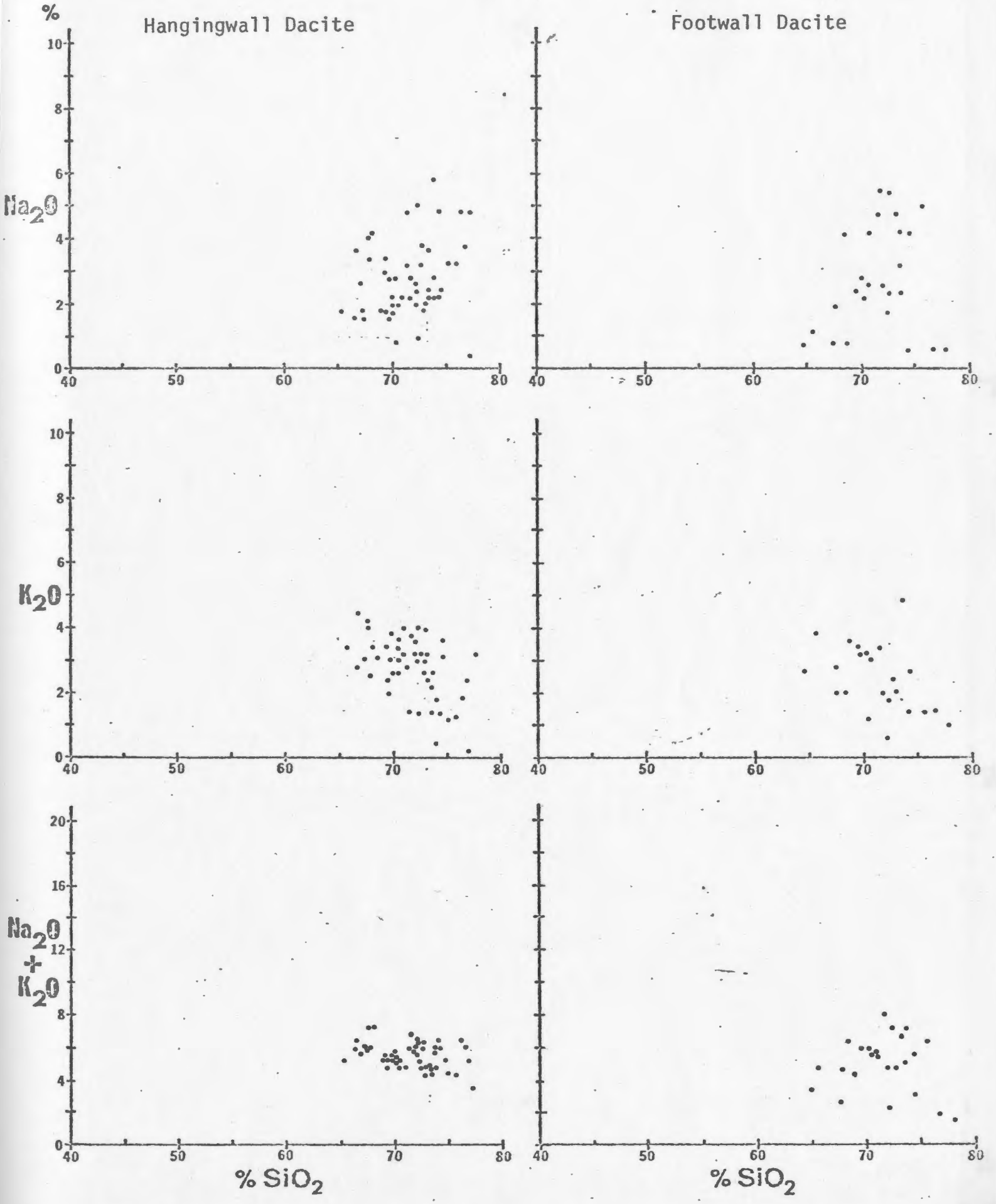
%
Hangingwall Dacite
Footwall Dacite
Na_2O
K_2O
$Na_2O + K_2O$
% SiO_2
% SiO_2

Fig. 17 (Cont'd.)

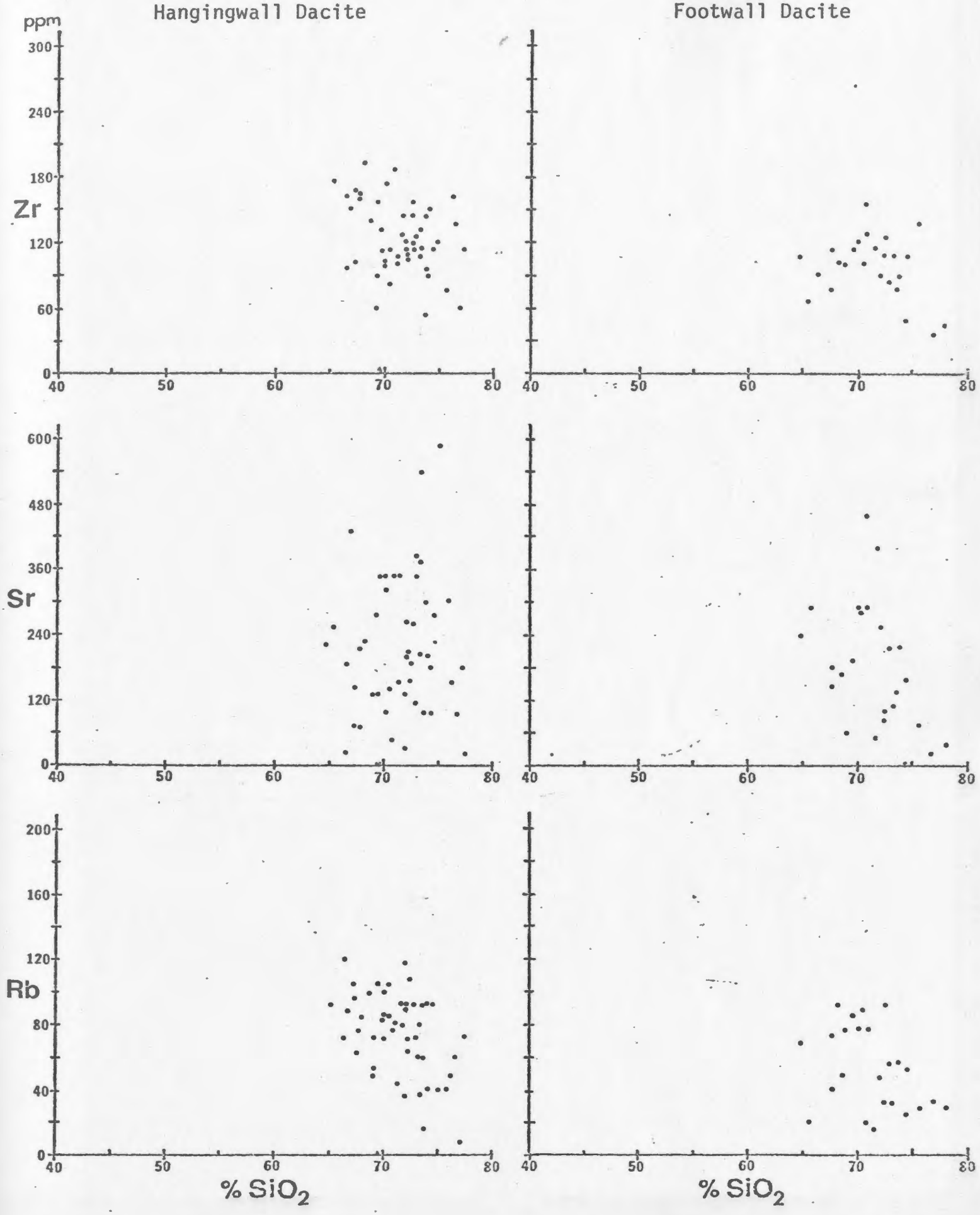

Fig. 17 (Cont'd.)

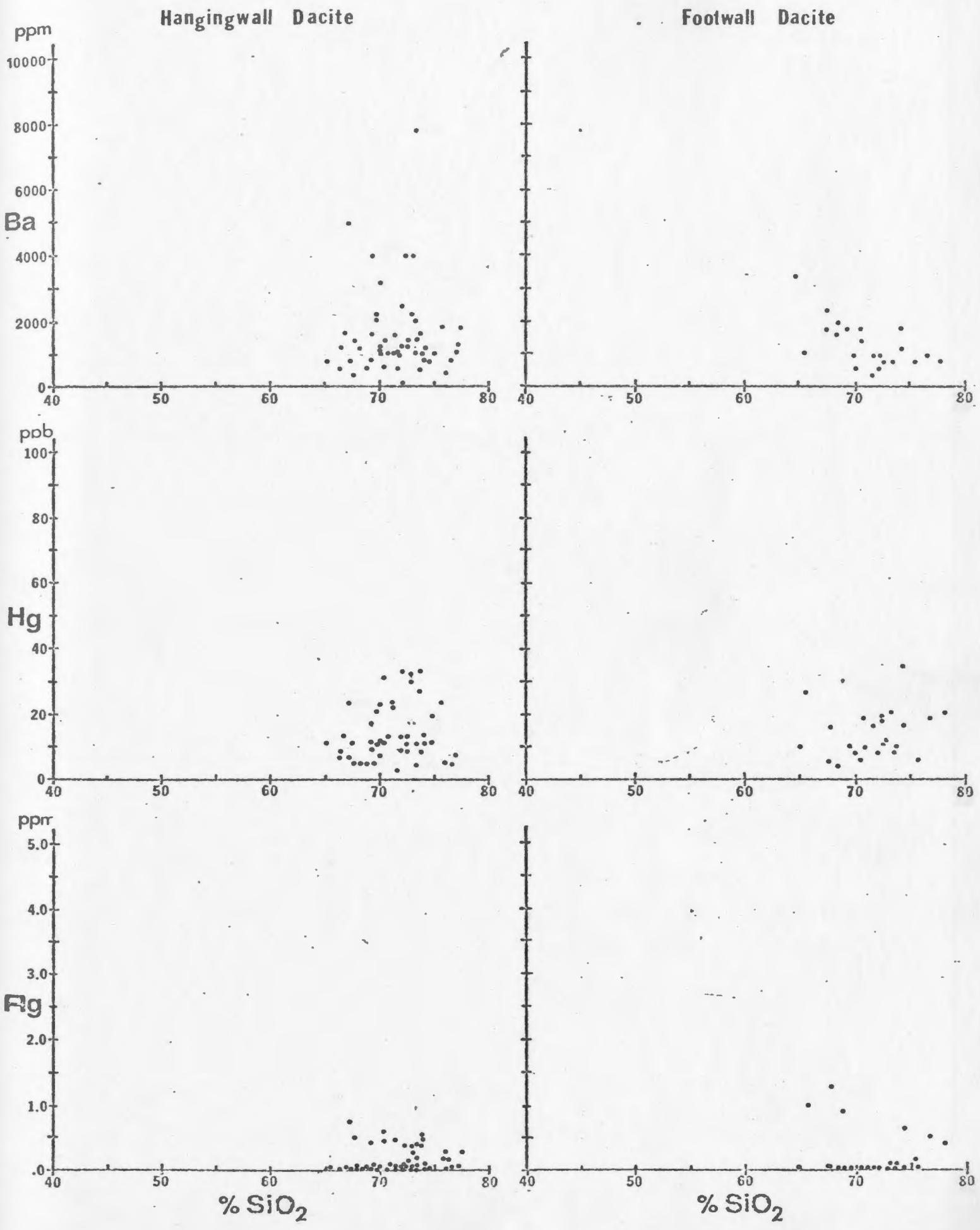
Hangingwall Dacite
Footwall Dacite
ppm
Ba
10000
8000
6000
4000
2000
0
ppb
Hg
100
80
60
40
20
0
ppm
Ag
5.0
4.0
3.0
2.0
1.0
.0
40
50
60
70
80
% SiO2

Fig. 17 (Cont'd.)

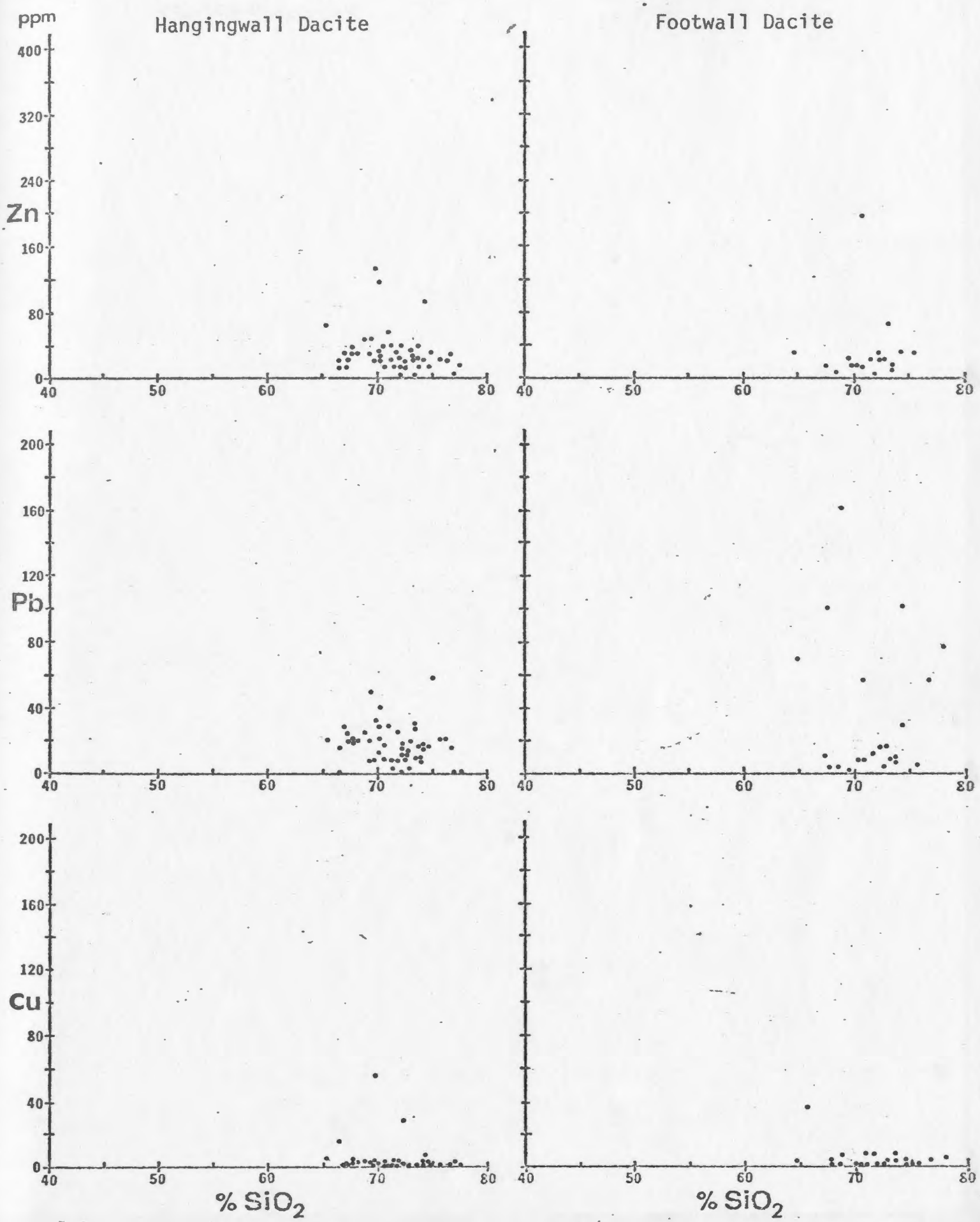
ppm
Hangingwall Dacite
Footwall Dacite
Zn
Pb
Cu
400
320
240
160
80
0
200
120
40
50
60
70
80
% SiO2

Fig. 17 (Cont'd.)

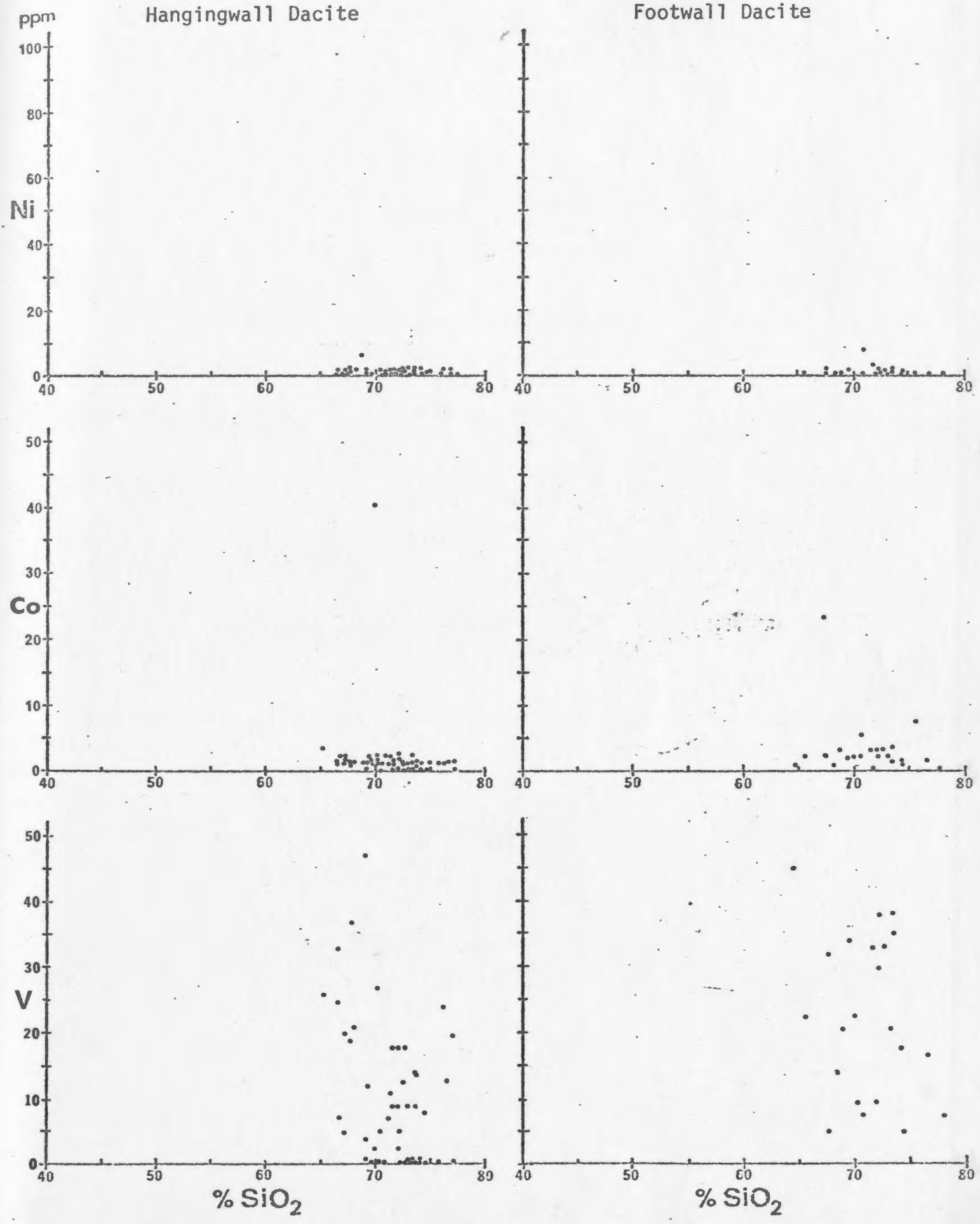

Fig. 17 (Cont'd.)

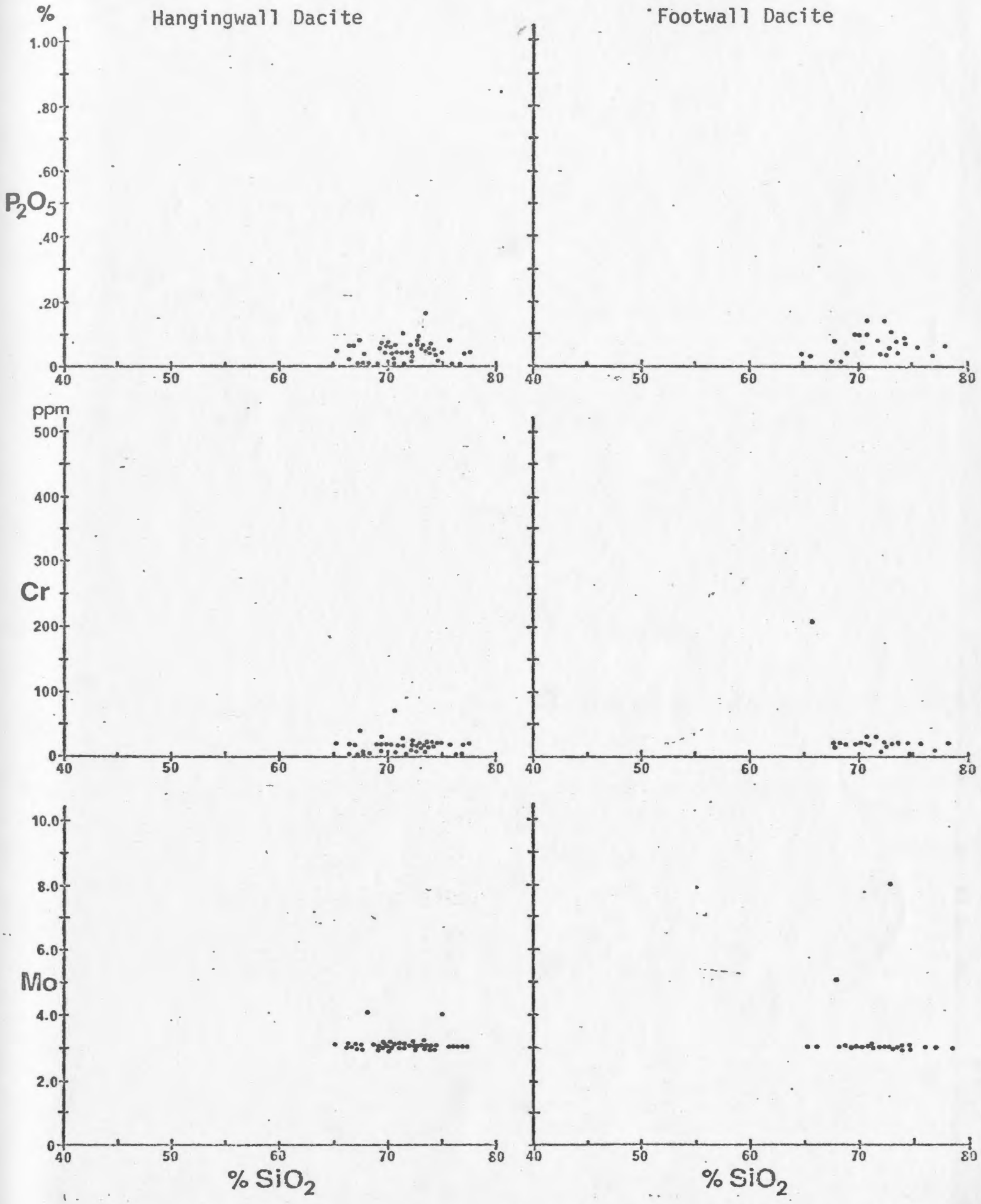
Hangingwall Dacite
Footwall Dacite
%
P_2O_5
1.00
.80
.60
.40
.20
0
ppm
Cr
500
400
300
200
100
0
Mo
10.0
8.0
6.0
4.0
2.0
0
40
50
60
70
80
% SiO_2

Table 14

Correlation Matrix comparing Footwall and Hangingwall Dacite.

Upper Figures: Hangingwall Dacite
Significance = .001 @ .40
= .01 @ .33

Lower Figures: Footwall Dacite
Significance = .001 @ .56
= .01 @ .46

	Fe_2O_3	TiO_2	P_2O_5	SiO_2	CaO	K_2O	MgO	Al_2O_3	Na_2O	L.O.I.	MnO	Zr	Sr	Rb	Zn	Cu	Mo	Ba	Pb	Ni	Co	Cr	V	Mg
TiO_2	59 63																							
P_2O_5	9 77	- 2 71																						
SiO_2	-52 -18	-46 - 9	8 10																					
CaO	34 25	14 - 6	31 - 3	-33 -50																				
K_2O	17 -15	35 - 5	8 - 9	-50 -44	- 2 - 5																			
MgO	34 -20	34 -45	-17 -36	-49 -10	-11 -22	35 - 9																		
Al_2O_3	10 5	36 23	-17 0	-71 -80	-15 7	61 37	58 18																	
Na_2O	9 45	-25 58	- 9 52	22 17	-22 - 4	-75 -18	-34 -77	-29 -19																
L.O.I.	24 -38	14 -55	2 -57	-61 -50	57 29	51 4	33 74	33 39	-61 -79															
MnO	30 71	-29 17	47 55	12 3	45 27	-31 -11	-27 -13	-53 -22	15 33	3 31														
Zr	24 68	48 73	-44 55	-26 -30	-18 32	31 - 3	28 -59	37 22	- 8 68	- 8 -50	-37 34													
Sr	- 2 43	2 34	8 30	9 -46	23 52	-28 26	13 -30	- 5 29	9 30	-27 -14	11 41	27 51												
Rb	15 4	28 -15	-13 -12	-39 -34	- 3 41	88 30	35 - 7	47 23	-69 -38	38 18	-26 3	51 14	- 4 - 5											
Zn	30 -43	15 -31	- 2 -33	-19 3	5 -50	3 1	45 81	16 27	- 6 -62	2 55	11 42	10 -56	19 -40	7 -19										
Cu	0 -26	11 8	- 6 -18	-14 -41	-13 -18	- 1 41	37 27	22 61	9 -27	- 9 37	- 9 37	0 -23	7 26	0 -27	54 44									
Mo	-12 - 3	-10 - 8	7 -25	7 - 4	23 18	4 -39	- 9 13	-10 11	-10 -19	12 24	9 3	1 1	16 -18	10 33	- 1 - 2	- 6 -10								
Ba	- 9 20	6 - 2	5 -10	0 -52	21 28	- 2 20	6 33	- 4 21	-18 -30	14 44	10 - 2	- 1 5	27 - 7	- 6 18	12 12	- 7 4	6 -10							
Pb	12 -36	17 - 7	-16 -25	-18 -38	25 -25	0 25	25 48	12 66	8 -45	6 56	3 -48	39 -37	54 2	12 -26	38 66	5 90	10 - 3	18 8						
Ni	- 1 58	5 55	-11 46	-14 - 8	- 9 31	17 -15	47 -15	27 - 4	-15 36	5 23	- 3 44	11 51	9 59	19 -20	62 -26	85 4	- 3 3	5 5	22 -20					
Co	0 14	3 35	- 1 17	-13 -21	- 3 5	14 6	43 - 6	24 16	-15 6	5 1	4 -20	5 32	14 5	17 13	62 -15	85 -10	- 2 - 1	3 7	21 -11	99 22				
Cr	6 -24	0 12	25 -10	9 -39	12 -18	- 1 28	- 8 11	- 9 64	- 8 -13	9 28	21 -40	-15 -16	- 3 25	6 -31	- 5 29	- 1 91	- 4 - 8	-13 -14	- 8 88	- 2 -10	3 - 2			
V	2 46	7 54	-11 37	-18 -28	- 7 42	19 6	46 -16	27 14	-13 16	6 - 4	- 4 25	10 39	7 48	21 6	61 -26	87 23	- 3 10	2 21	16 - 7	99 80	97 19	- 2 4		
Mg	-29 -25	-14 - 8	21 4	33 8	-15 -41	1 [redacted]	-30 [redacted]	-10 25	-30 -38	- 7 36	- 7 -20	-23 -41	-18 -34	- 5 -23	-12 75	-16 43	10 8	2 7	-26 64	-13 -14	-10 -23	5 34	-15 - 7	
Ag	-17 -36	-38 -38	45 -42	11 -21	21 -40	[redacted]	[redacted]	-15 44	- 8 -63	11 66	31 -34	-34 -57	- 3 -31	- 2 -18	- 5 87	-21 51	9 12	-10 23	-12 25	-15 -33	- 4 -15	11 42	-16 -35	40 67

(coefficients .88 to .91), and Zn, Ag and Mg (coefficients .81 to .87) form semi-independent groups linked by a moderately correlative (coefficients .64 to .75) Zn, Pb, Hg group. The base metals show no coherence with Ni, Co or V in the Footwall. The reason for the markedly different behaviour of the base metals between the Footwall and Hangingwall Dacites is not readily apparent. In view of their similar chemistry (see section 5.4.4.1.) the difference must be related to differing depositional and post-depositional processes.

Ba and K exhibit no coherence in both the Hangingwall and Footwall Dacites (coefficients -.02 and .20 respectively).

5.1.4. Cycle One and Cycles Two and Three Siltstones

Comparison of the Harker variation diagrams for the Cycle One and Cycles Two and Three Siltstones (Fig. 18) shows that the scatter for the Cycle One Siltstone is more compact for most elements than for the siltstones of the upper cycles. This is partly a function of the more limited silica range in the Cycle One Siltstones but also reflects the relative lithologic homogeneity of the unit. In general, the Cycle One Siltstone has a flatter distribution for such elements as Fe, Ti, P, Ca, Mg, Al, Sr, Co and Cr than the Cycles Two and Three Siltstones which have more "igneous-like" trends. The Cycle One Siltstone is unimodal for Cu, bimodal for Pb, and trimodal for Zn reflecting varying degrees of detrital and fumarolic introduction of these elements.

With reference to the correlation matrix for the Cycle One Siltstone (Table 15), it is apparent that Fe (a portion of which represents

Fig. 18: Harker diagrams comparing Cycle One and Cycles Two and Three Siltstones.

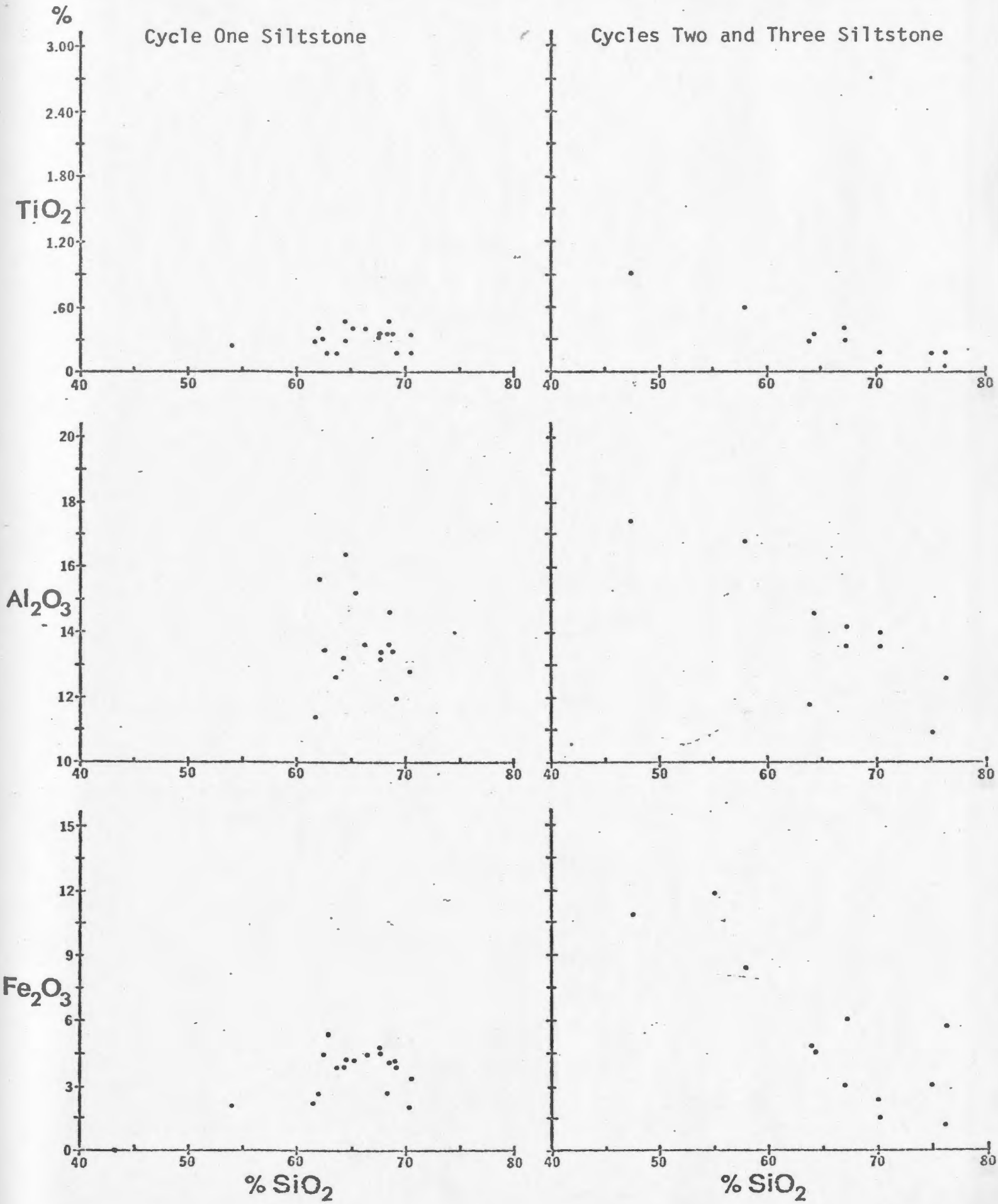

Fig. 18 (Cont'd.)

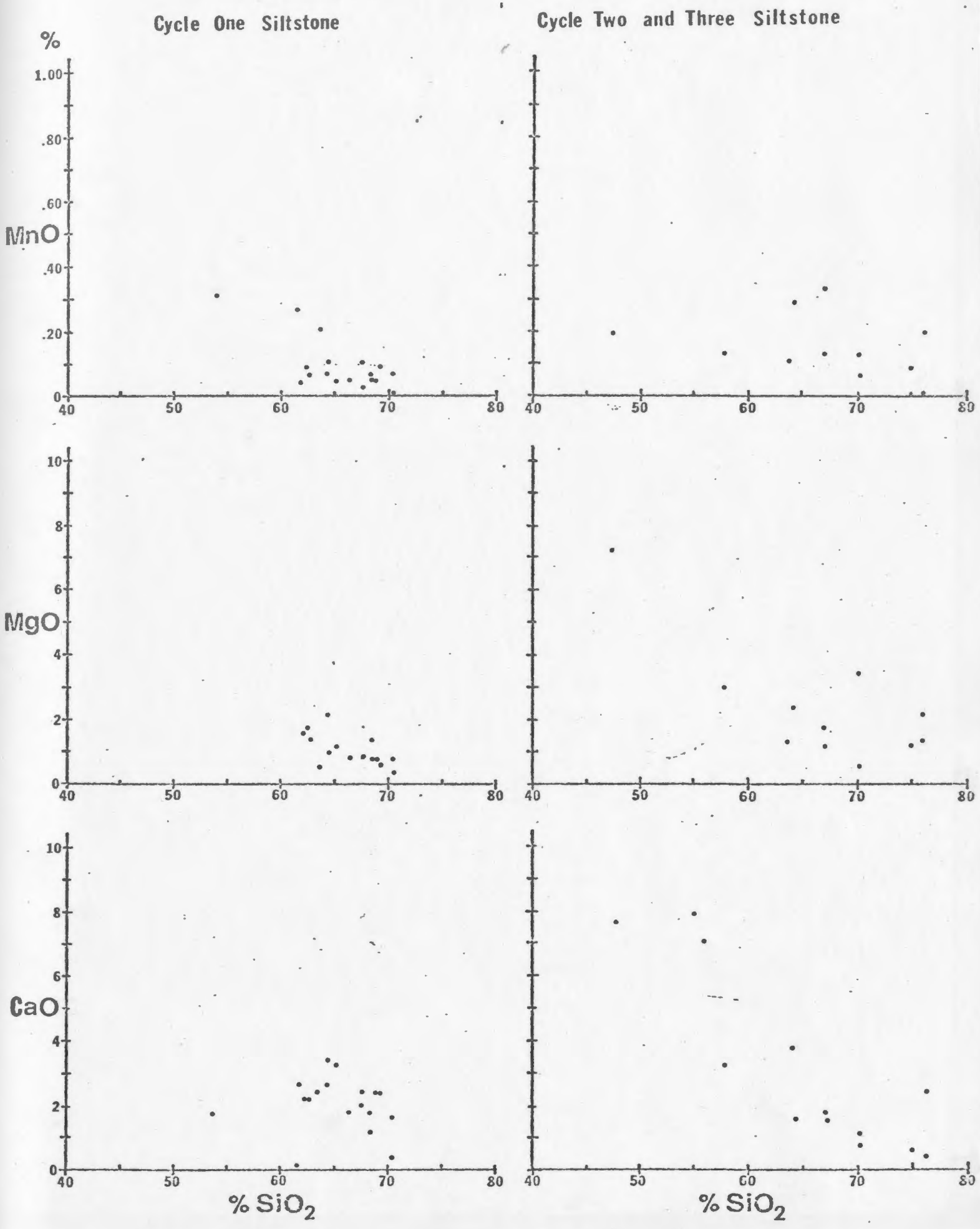
Cycle One Siltstone
Cycle Two and Three Siltstone
%
MnO
MgO
CaO
% SiO2
% SiO2

Fig. 18 (Cont'd.)

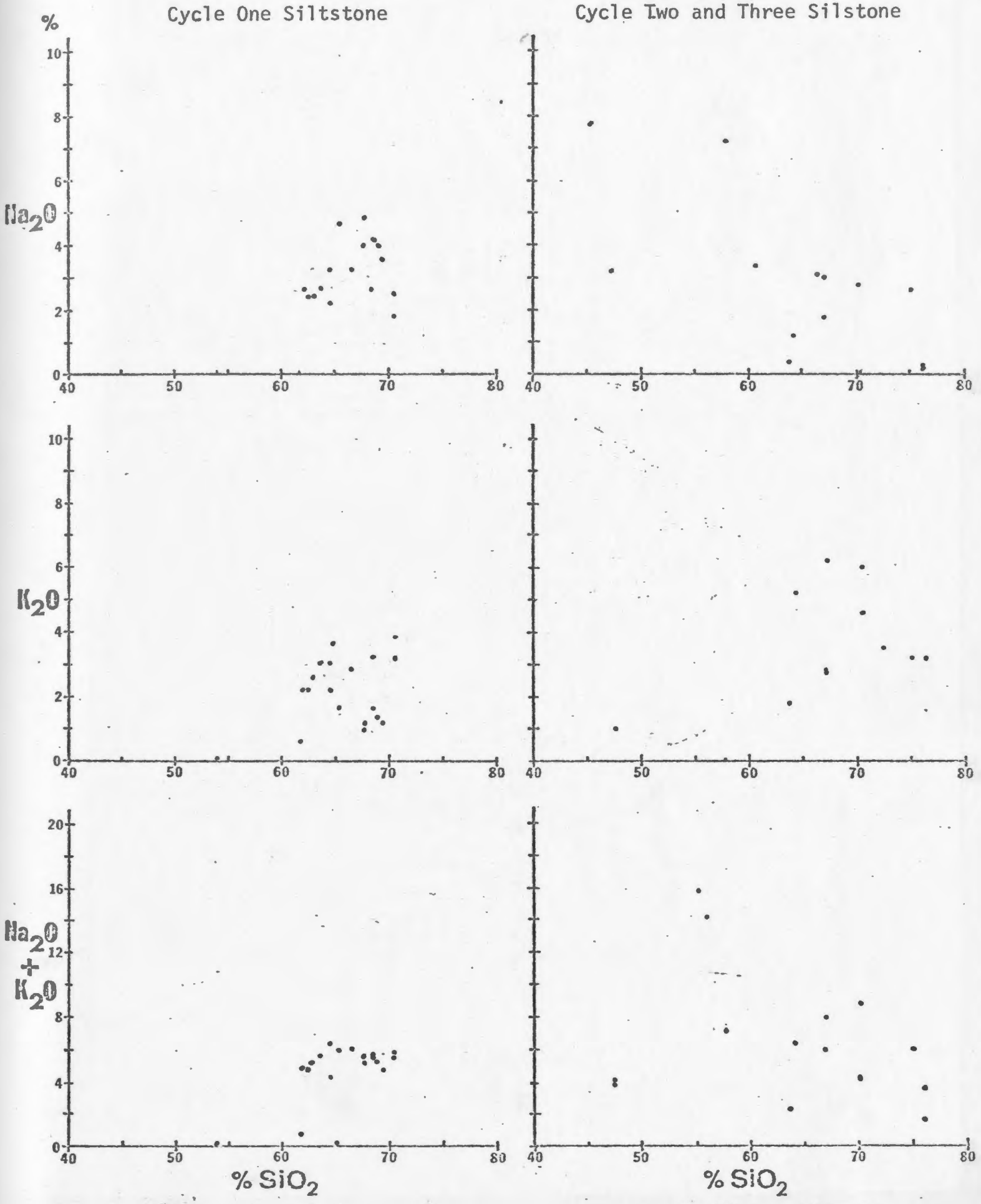
Cycle One Siltstone
Cycle Two and Three Silstone
%
Na_2O
K_2O
$Na_2O + K_2O$
% SiO_2
% SiO_2

Fig. 18 (Cont'd.)

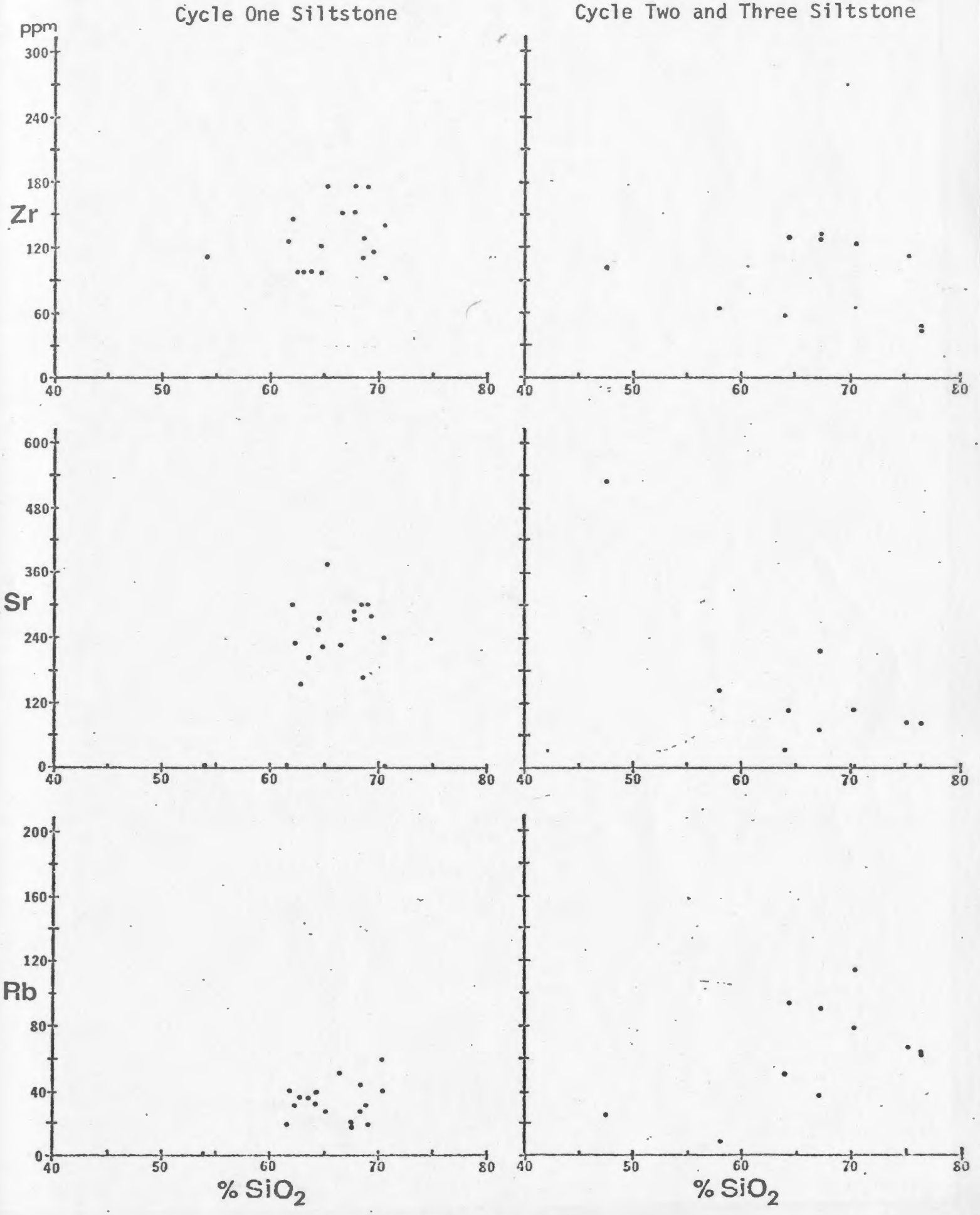
Cycle One Siltstone
Cycle Two and Three Siltstone
ppm
Zr
Sr
Rb
% SiO2
% SiO2

Fig. 18 (Cont'd.)

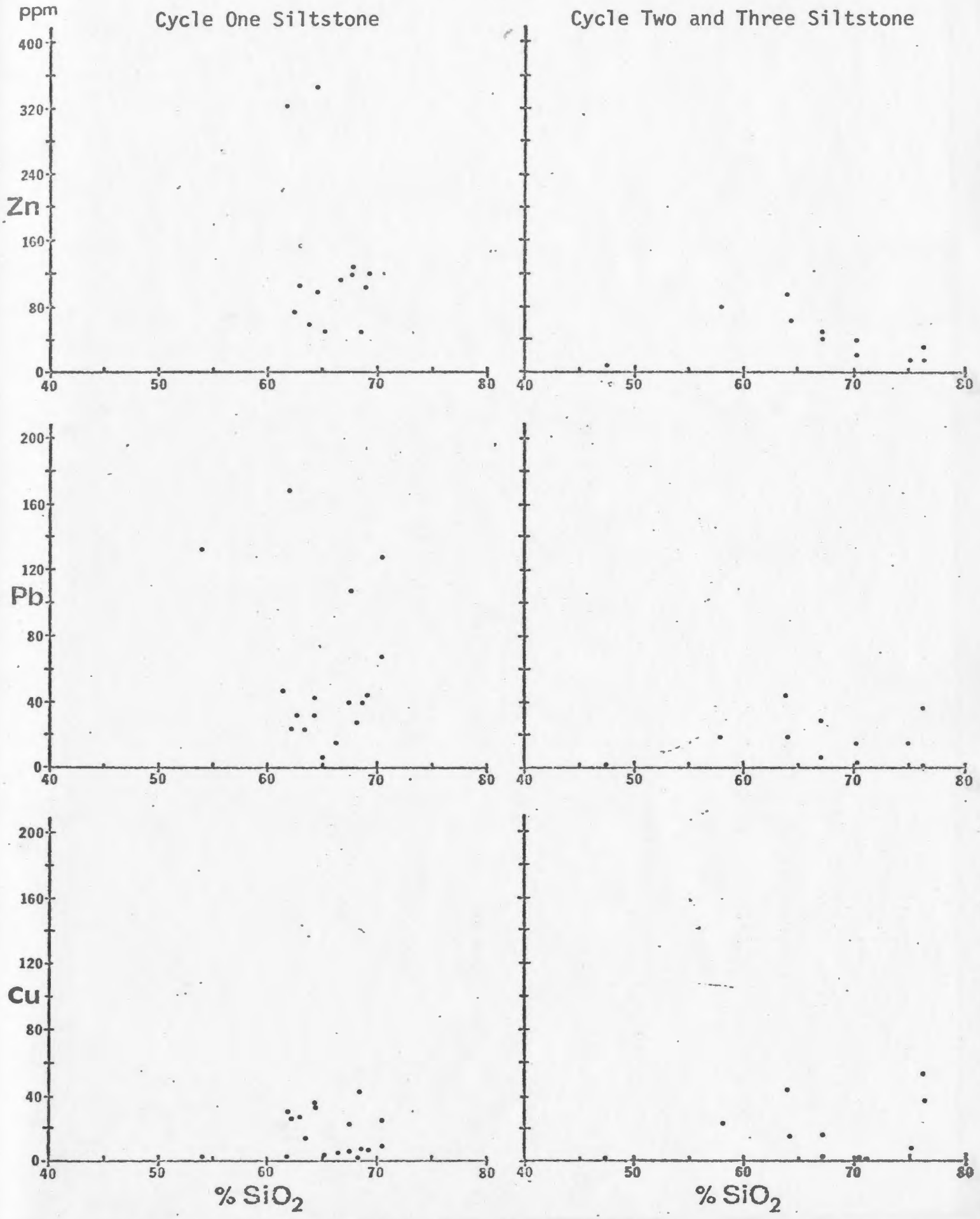

NOTE: Numerous Zn, Pb, and Cu values plot off scale.

Fig. 18 (Cont'd.)

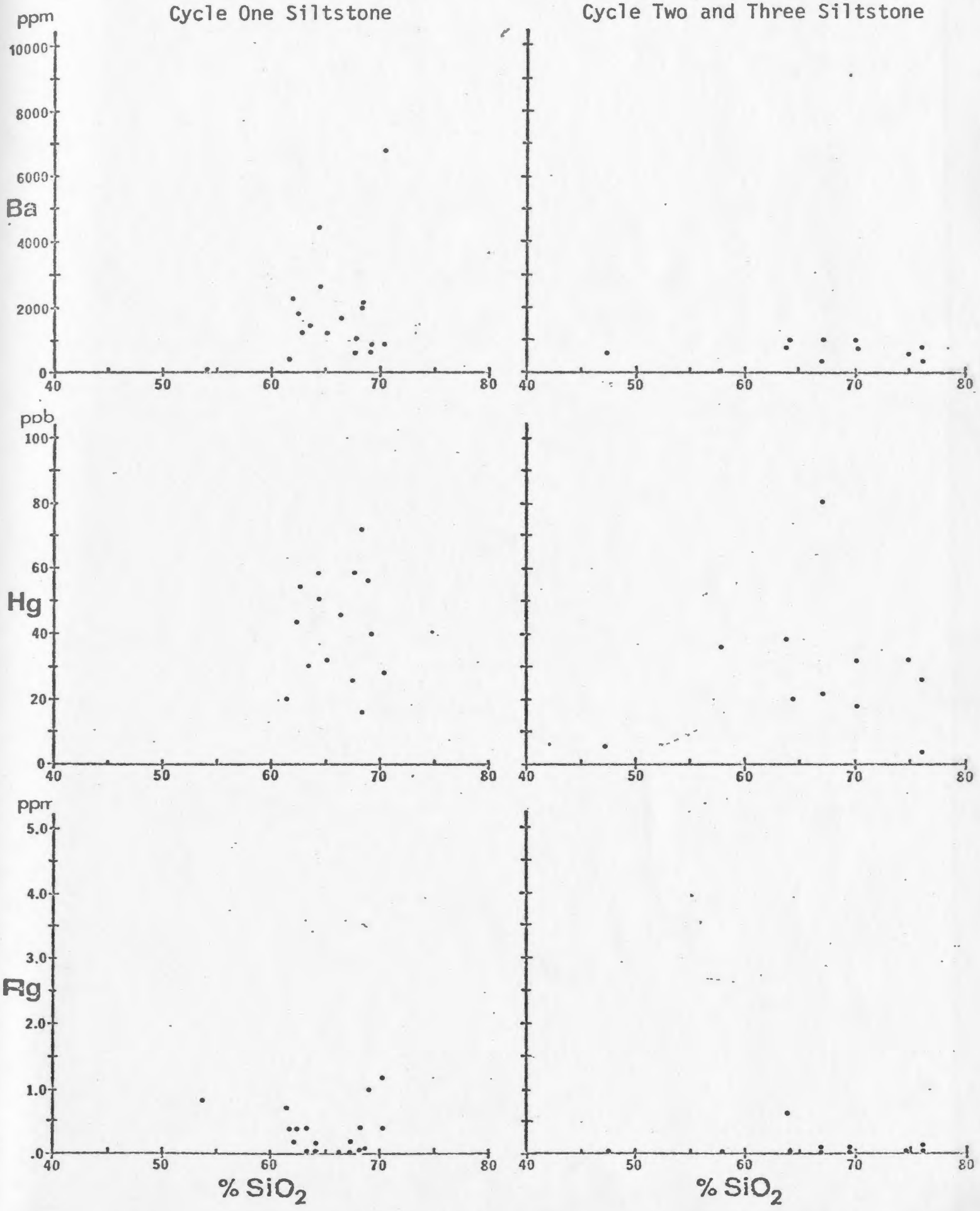
Cycle One Siltstone
Cycle Two and Three Siltstone
ppm
Ba
ppb
Hg
ppm
Ag
% SiO2
% SiO2

Fig. 18 (Cont'd.)

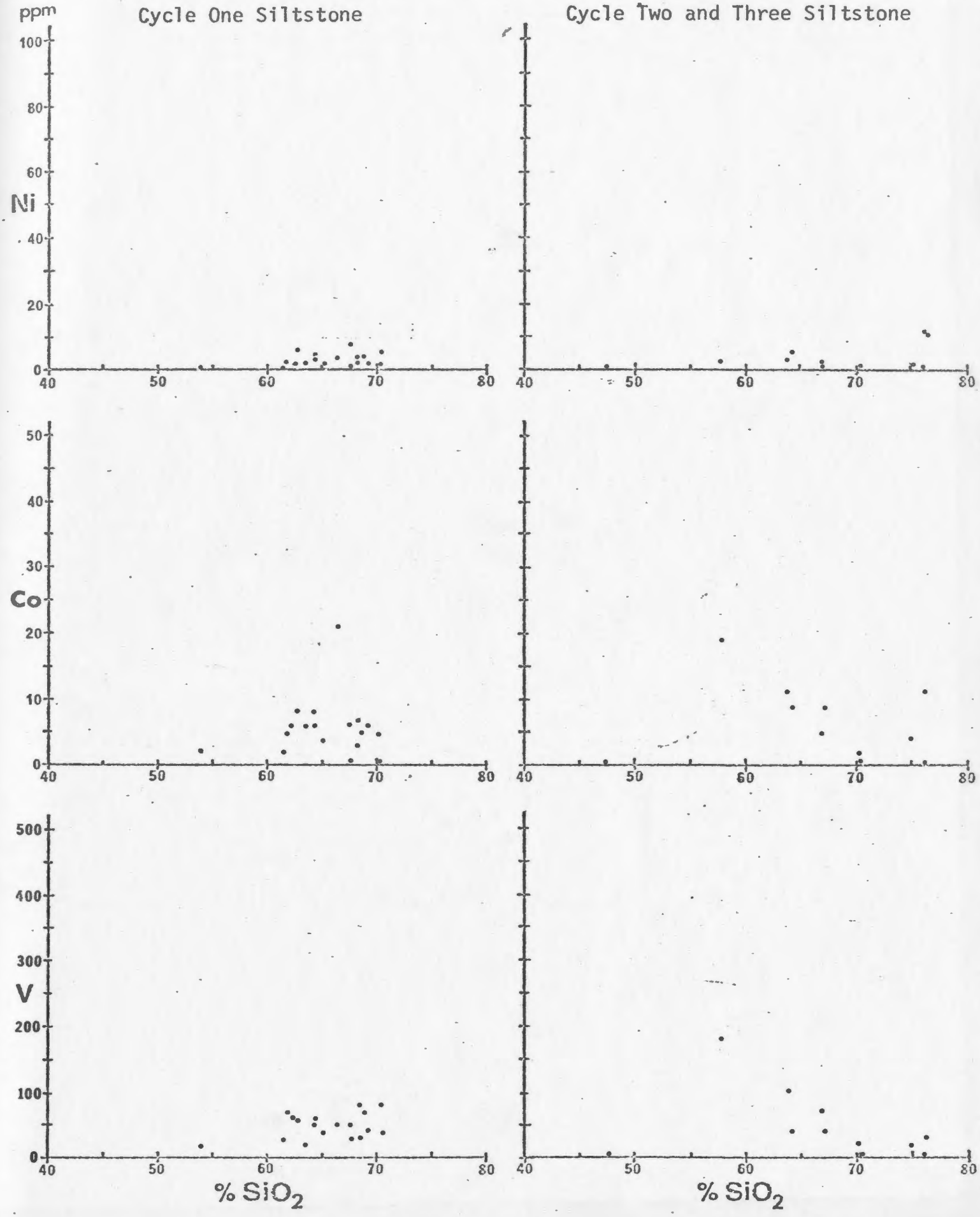
ppm
Cycle One Siltstone
Cycle Two and Three Siltstone
Ni
Co
V
100
80
60
40
20
0
50
30
10
500
400
300
200
100
40
50
60
70
80
% SiO2
% SiO2

Fig. 18 (Cont'd.)

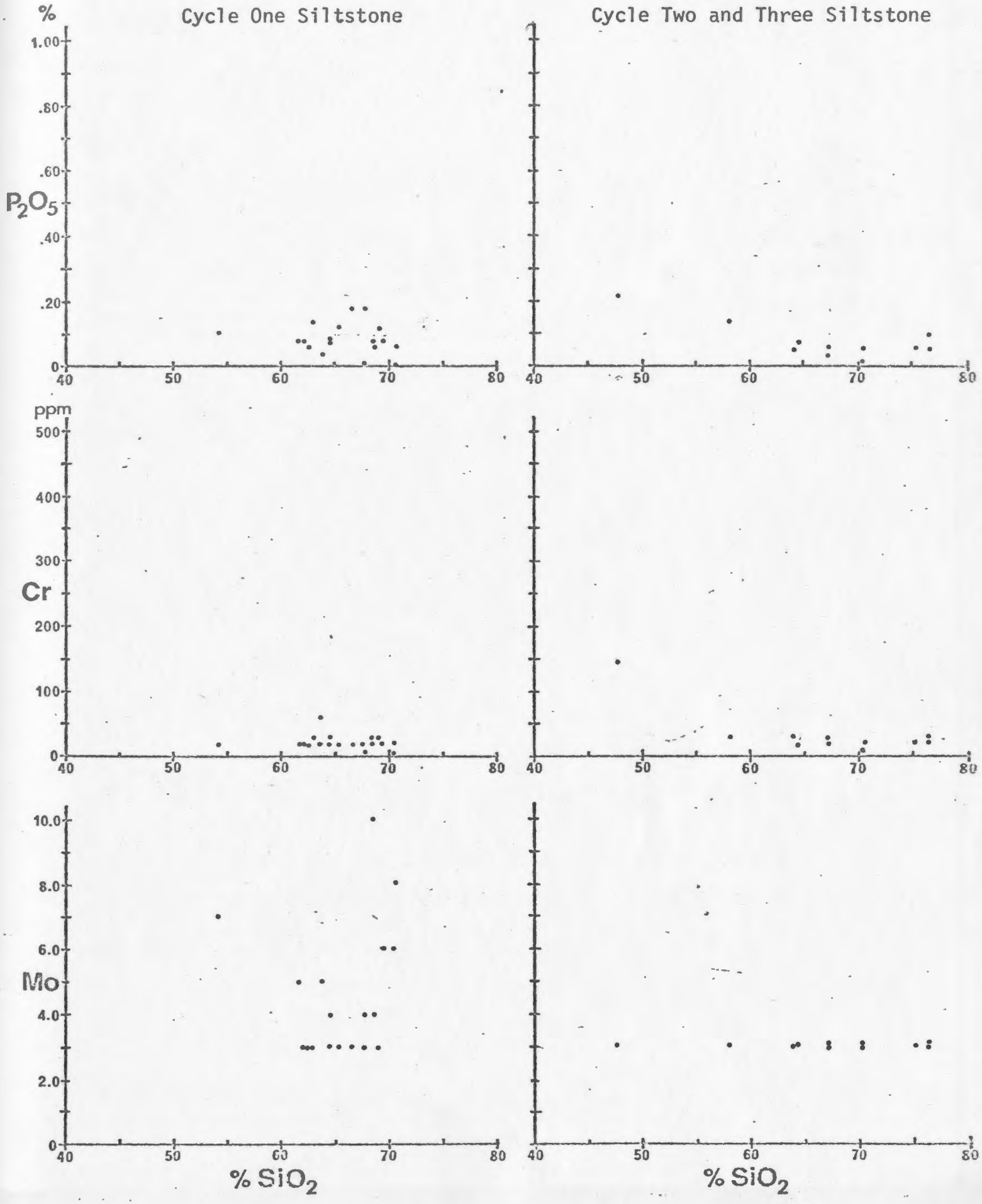
Cycle One Siltstone
Cycle Two and Three Siltstone
%
1.00
.80
.60
P_2O_5
.40
.20
0
ppm
500
400
300
Cr
200
100
0
10.0
8.0
6.0
Mo
4.0
2.0
0
40
50
60
70
80
% SiO_2

Table 15

Correlation matrix comparing Cycle One and Cycles Two and Three Siltstones.

Upper Figures: Cycles Two and Three Siltstone
Significance = .001 @ .78
= .01 @ .68

Lower Figures: Cycle One Siltstone
Significance = .001 @ .65
= .01 @ .54

	Fe_2O_3	TiO_2	P_2O_5	SiO_2	CaO	K_2O	MgO	Al_2O_3	Na_2O	L.O.I.	MnO	Zr	Sr	Rb	Zn	Cu	Mo	Ba	Pb	Ni	Co	Cr	V	Mg
TiO_2	93 11																							
P_2O_5	79 33	84 12																						
SiO_2	-82 19	-94 15	-77 -17																					
CaO	87 40	89 11	80 26	-86 -11																				
K_2O	-72 13	-52 0	-60 -30	40 43	-61 9																			
MgO	67 51	73 -20	79 3	-77 -76	77 -37	-46 -62																		
Al_2O_3	35 9	62 73	52 -15	-75 35	36 25	1 48	57 -58																	
Na_2O	59 55	60 41	52 28	-53 61	31 52	-39 5	22 -77	55 48																
L.O.I.	0 9	5 -6	-3 -20	-24 3	33 -14	-10 13	32 -2	3 1	-57 -24															
MnO	28 -43	33 -42	3 12	-31 -75	22 -24	30 -52	3 85	11 -68	5 -67	-3 3														
Zr	1 25	22 62	-4 15	-18 26	-9 6	59 -23	-12 -14	38 37	23 46	-41 1	52 -37													
Sr	84 37	89 37	83 25	-79 40	83 76	-40 2	78 -68	48 47	44 87	-8 -12	23 -57	29 30												
Rb	-78 13	-68 21	-72 -18	52 51	-63 -16	85 91	-36 -63	-19 57	-66 12	21 19	18 -63	21 5	-58 4											
Zn	17 -10	13 19	-14 -16	-21 2	7 -26	24 23	-24 4	7 8	16 -17	36 -8	16 0	-15 1	-29 -13	-17 16										
Cu	-20 31	-31 16	-7 -40	34 7	-12 12	-29 59	-30 -35	-46 39	-34 -5	32 23	-19 -38	-67 -17	-47 3	-15 45	35 54									
Mo	0 -47	0 -33	0 -42	0 13	0 -54	0 20	0 24	0 -28	0 -40	0 -25	0 23	0 -32	0 -45	0 1	0 63	0 13								
Ba	-53 -28	-23 -18	-32 -11	10 29	-23 20	79 49	-5 -34	16 16	-60 3	41 12	20 -25	41 -46	-20 28	79 34	-19 4	-17 26	0 19							
Pb	3 -12	-11 11	-33 -26	11 9	-5 -30	-5 23	-52 3	50 1	-11 -16	20 -14	38 -3	-10 0	-32 -15	-2 13	61 97	39 52	0 73	-9 9						
Ni	18 61	-10 10	-22 -33	22 37	-2 14	-24 43	-33 -50	-64 31	-12 30	2 14	41 -63	-24 27	-22 14	-6 38	44 -6	37 54	0 -17	-34 -4	70 3					
Co	41 41	23 16	0 58	-14 8	10 19	-48 36	-25 -32	-12 6	45 21	-8 -9	23 -21	-17 1	-12 24	-45 43	80 4	30 7	0 -22	-63 16	61 -5	70 8				
Cr	77 29	82 10	85 58	-78 -6	91 43	-48 -11	87 -21	41 1	26 32	18 -4	11 -5	2 -19	93 40	-53 -10	-31 -9	-29 -7	0 -45	-11 5	-28 -20	-26 -20	-24 28			
V	41 15	32 62	11 -21	-29 39	14 16	-50 32	-16 -52	17 60	64 32	-11 17	5 -74	-14 16	-6 29	-58 48	80 -21	24 30	0 -45	-63 14	45 -22	34 42	91 -7	-17 25		
Mg	-17 -40	-13 -36	-48 -10	6 29	-18 -5	32 33	-38 -18	-2 -5	6 -5	6 -5	50 -16	24 -28	-33 12	27 21	33 9	-4 2	0 38	20 82	52 17	16 -7	27 3	-34 -20	29 -6	-
Ag	-3 -54	-8 -78	-16 -34	7 -11	9 -35	-25 -5	-32 37	-33 -60	-32 -58	54 1	-9 38	-31 -47	-31 -46	-17 -20	69 14	67 -12	0 65	-3 23	66 22	35 -24	62 -30	-20 -36	39 -40	16 53

detrital pyrite) displays no affinity for the ore metals including Zn which is largely present in the form of detrital sphalerite. Zn and Pb show a strong correlation but by eliminating excessively enriched samples this correlation is considerably weakened. Ba and Hg are strongly correlative and act independently of the other base metals. Ba displays only a weak affinity for K.

Correlations within the Cycles Two and Three Siltstones are quite unlike those found in Cycle One. Mg, Ti, P, Fe, Ca, Sr and Cr exhibit strong mutual correlations and are strongly negatively correlated with silica. Among the trace elements, three mutually interdependent groups may be distinguished, i.e., Zn-Co-V, Zn-Pb-Ag, and Co-Pb-Ni. An important feature of the Cycles Two and Three Siltstones which sets them apart from the Cycle One Siltstone and the Cycles One and Two volcanics is the strong positive correlation between Ba and K. This, combined with the relatively low Ba abundances suggests that Ba distribution was magmatically controlled in the rocks from which the Siltstone was derived and that no secondary enrichment occurred at deposition.

5.1.5. Cycle Three Dacite

Although only eight samples of Cycle Three Dacite were analyzed, significant differences are detectable between this group and the Cycle One Dacite. Strong mutual correlations exist within Cycle Three between Fe, Ti, Ni, Co, Cr and V (Table 16), a feature that was curiously absent in the Cycle One Dacite. Ba, K and Rb also exhibit moderately strong correlations, unlike that found in all of Cycle One and a large portion of Cycle Two.

Table 16

Correlation matrix for Cycle Three Dacite

Significance = .001 @ .89
= .01 @ .79

	Fe_2O_3	TiO_2	P_2O_5	SiO_2	CaO	K_2O	MgO	Al_2O_3	Na_2O	L.O.I.	MnO	Zr	Sr	Rb	Zn	Cu	Mo	Ba	Pb	Ni	Co	Cr	V	Hg
TiO_2	86																							
P_2O_5	80	68																						
SiO_2	-70	-70	-78																					
CaO	2	40	28	-24																				
K_2O	21	-24	16	- 4	-84																			
MgO	27	3	-18	- 3	-73	64																		
Al_2O_3	41	49	58	-75	40	- 3	0																	
Na_2O	55	75	61	-73	64	-47	-34	72																
L.O.I.	-52	-15	-18	- 2	54	-51	-53	8	0															
MnO	79	45	67	-53	-30	62	53	33	9	57														
Zr	47	47	74	-57	35	17	- 7	65	30	22	56													
Sr	-65	-65	-23	-52	13	-12	-67	-27	-21	24	-61	-25												
Rb	27	-11	14	0	-83	83	47	-12	-26	-62	36	-12	3											
Zn	39	33	44	0	0	7	-35	-21	16	-22	5	10	27	44										
Cu	74	47	86	-70	- 1	43	14	44	28	-28	89	70	-41	18	12									
Mo	- 9	27	15	-13	61	-39	-42	38	27	72	-31	57	11	-39	16	-14								
Ba	-10	-38	-11	-17	-66	66	53	25	-16	-31	19	-17	1	61	-36	8	-43							
Pb	27	58	50	-29	86	-60	-65	29	52	48	- 5	59	1	-58	36	20	73	-81						
Ni	97	86	68	-58	- 6	21	36	36	51	-60	70	35	-65	35	43	57	- 9	- 8	20					
Co	93	86	80	-62	23	- 5	- 5	35	70	-49	56	32	-40	15	54	60	- 8	-26	40	89				
Cr	92	87	72	-55	18	- 7	0	20	60	-47	56	26	-49	12	54	56	-12	-36	40	90	98			
V	96	89	91	-74	24	6	- 1	48	67	-33	68	59	-48	14	49	74	10	-25	50	89	95	92		
Hg	-14	-38	38	0	- 3	36	-46	- 3	-20	12	12	34	63	22	30	40	1	11	9	-29	- 9	-18	1	
Ag	10	27	15	-13	61	-39	-42	38	27	72	-31	57	11	-39	16	-14	100	-43	73	- 9	- 9	-11	10	1

5.2. Vertical Elemental Variations (Concentration:Depth Plots)

5.2.1. Introduction

One of the major problems to be investigated in this study was the question of the existence of geochemical aureoles in the vicinity of the orebodies and, if present, their application to exploration. It was decided that the most effective method of investigating the problem and presenting the data was through the use of simple concentration:depth plots for each element directly on the N60W section.

The geochemical data and coordinates of each sample point were transferred from computer cards to magnetic tape and a program was devised to plot these data using a Calcomp plotter. The line of the drill hole was used as the abscissa for each plot and the concentration of the oxide or element in question was plotted horizontally to the right of each sample point according to the scale indicated on the section. Diabase and rhyolite dikes cutting the section are represented by horizontal lines extending from the sample point to the respective concentration. The plotter is capable of plotting accurately to within 1/100 inch but slight variations in the size of individual copies of the section have caused the introduction of a small plotting error. The resultant plots for each element are depicted in Figs. 19a through 19z (in back pocket).

It was originally planned to discuss each section for each element individually but the nature of the data and the difficulty in summarizing all the plots in a coherent fashion dictate against this method of description. Instead, the pertinent vertical variations will be discussed for each

lithologic unit and a summary section is presented in Fig. 20 (in back pocket).

A casual inspection of figures 19a to 19z reveals that vertical variations for most elements are very erratic and show no consistent trend. Indeed the best trends are somewhat vague and their existence and significance may be questionable.

5.2.2. Footwall Andesite

Although the Footwall Andesite is penetrated at the bottom of several drill holes, only diamond drill hole (ddh) 542 offers a section of reasonable thickness. Rocks in the lower half of the hole are characterized by pervasive calcite alteration and display very high Ca and loss on ignition and lower Mg and Cu than the upper less altered portion. The lack of base metal anomalies in this area suggests that this carbonate alteration is unrelated to ore. Mn shows a gently increasing trend upward in the upper less altered portion and silica gradually increases upward throughout the entire section. The upper portion of the Footwall Andesite in this hole is cut by swarms of diabase dikes which may have followed original fractures. Although such fractures might have served as mineralizing conduits to the overlying mineralized Intermediate Footwall, neither the dikes nor the surrounding Andesite display any unusual response to any of the 25 elements determined and thus, on geochemical grounds, it would appear that mineralizing solutions have not passed through this area.

5.2.3. Intermediate Footwall

The Intermediate Footwall is cut by portions of ddh 1214 and ddh 792, but the best sections are represented in ddh 202 and ddh 542. Ca and Sr in the latter two holes are extremely low and constant while Mn and, to a lesser extent, Ag are very high and erratic. Ca, Sr, Mn and Ag anomalies are considerably less pronounced to the west in ddh 1214 and ddh 792.

The mineralized Intermediate Footwall is distinct from the unmineralized portion of the unit by the near total removal of Na and K, but not Rb. High concentrations and erratic trends for Mg, Fe, Mn, Zn, Pb, Cu, Ba, Hg, Ag and Mo are also characteristic of the unit, reflecting varying degrees of mineralization and alteration. Ca, which was removed from the lower unmineralized portion of the unit is higher, but very erratic in the mineralized Intermediate Footwall.

5.2.4. Cycle One Siltstone and Dacite

The sequence of Cycle One Siltstones below Rothermere Orebody displays some of the most distinctive geochemical trends on the entire section. Ag, Zn and Pb increase up section (towards the ore) while Cu, Mg, Fe, Ti, V, and loss on ignition show decreasing trends. The negative correlation of trends between Cu and the other base metals suggests that this distribution is not entirely a function of weathering of the mineralized Intermediate Footwall, and implies that another mechanism, e.g. fumarolic acitivity and base metal precipitation, was also influencing the distribution of these elements.

Footwall Dacite at a distance from ore (greater than 100 feet) is intersected only beneath MacLean Orebody on the N60W section. Ca rises sharply with depth from 150 feet to 380 feet below the ore and then gradually decreases to a minimum about 900 feet below the ore. Pb and loss on ignition strongly decrease and Ba and Mn increase with depth over the same interval. Zn shows a slight tendency to decrease with depth through the entire section below the orebody. Total alkalis exhibit a strong decreasing trend with depth from 100 to 660 feet below the ore and then assume a higher more constant distribution. Rb behaves quite differently by increasing with depth and then assuming a lower more erratic distribution.

It is difficult to determine the cause of these variations but it seems probable that they are unrelated to ore. The upward Pb increase is not continuous within 150 feet of ore and the Zn increase is poorly defined. Ba decreases with proximity to ore. The other elements which show variations (Ca, Mn and alkalis) are all mobile and may have been influenced by depositional or post-depositional remobilization.

However, dacite samples within 100 feet of ore in the footwall (ddh's 1917, 792 and 202) display anomalous abundances and trends which are probably related to their proximity to ore. Zn, Pb and Cu are consistently higher in the immediate footwall (within 100 feet of ore) than in barren hangingwall dacites, and Ba, Ag, Ti and V, while not systematically higher, are generally present in above normal concentrations. Trends are distinctly erratic in the immediate footwall and only Fe (ddh 792) and Mg (ddh 202) show strong increasing trends towards ore beginning about 50 feet below the ore. The immediate Footwall Dacites are barren of sulphides (except sparsely

disseminated pyrite) and were obviously not the site of hypogene stockwork mineralization. Thus the above noted anomalies may be attributed to (1) magmatic changes in dacite near the ore, (2) changes in metal bearing content of (sea?)water due to fumarolic activity prior to ore deposition, (3) downward percolation of metal-bearing waters through unconsolidated and semi-consolidated tuffs during and after ore formation, or (4) migration of heavy metals during metamorphism. Intuitively it seems probable that one or more of the latter three possibilities is the cause of these anomalies.

Dacite samples immediately above MacLean and Rothermere Orebodies are anomalous in ddh's 1493, 869 and 792. Zn, Pb, Cu and Ba are anomalously high 20 feet above the ore in ddh 1493 while Fe and Mg become anomalous within 10 feet of ore. Cu, Ag, Mn, Fe, Mg and Ca are anomalous up to 30 feet above ore in ddh 869. Approximately 40 feet of sparsely mineralized (geochemically anomalous) breccias overlie Rothermere Orebody in ddh 792. Cu, Zn, Ba, Sr and Mg begin to show erratic trends about 80 feet above the top of the breccia and Zn, Pb, Cu, Ag, Mg and Fe begin a consistent rise toward ore about 50 feet above the ore. The cause of these anomalies is probably similar in nature to that which produced anomalies in the immediate Footwall Dacite.

Hangingwall Dacites at a distance from ore (i.e., greater than 75 feet) display some geochemical trends, although they are probably not related to ore. Na and K reach a peak about 250 feet above Maclean Orebody in ddh's 1493 and 869 and decline in both directions from the peak. A similar peak for total alkalis exists in the upper portions of the Hangingwall Dacite approximately 450 feet above Rothermere Orebody (ddh 792) but only a

weak corresponding peak is found between these two peaks in ddh 1214. Zn increases at a rate of about 2 ppm per 100 feet through 400 feet of the Hangingwall Dacite toward MacLean Orebody but such a rise cannot be considered significant as the magnitude of the anomaly is within the limits of sampling and analytical error. Sr begins a steady rise towards ore about 200 feet above MacLean Orebody in ddh 1493 but a corresponding increase is not present in ddh 869.

5.2.5. Cycle Two Andesite

The Cycle Two Andesite immediately overlying the Cycle One Dacite above MacLean Orebody has been altered by pervasive vein and matrix calcite and displays high concentrations and erratic trends for Ca and loss on ignition. This alteration is not accompanied by any anomalous base metal abundances and indeed it seems unlikely, in view of the previous evidence, that any anomalies above the top of the Cycle One Dacite are caused by dispersion or alteration related to the cycle one orebodies.

The major portion of the Cycle Two Andesite represented on the N60W section is broadly divisible into two portions, i.e., the northwestern portion intersected by ddh 2666 and the central portion intersected by ddh's 869, 868, 1214 and 792. The central portion contains consistently higher Ti, Mn, Ca, Zn, Cu, Ba, Pb, Co, V, Zr and Sr than the northwestern portion which contains consistently higher K. Thus, no stratigraphic correlation can be made between these two portions of the Cycle Two Andesite on the basis of geochemical data.

The northwestern portion (ddh 2666) may be divided into three geochemically distinct units (Fig. 20), i.e., an upper mafic unit (SiO_2 average 53.5%), a lower intermediate unit (SiO_2 average 62.1%) and a basal mafic unit (SiO_2 average 51.7%). The upper unit is characterized by high concentrations and erratic Ca, Sr, Ni and Cr trends whereas the lower and basal units display distinctly lower concentrations and more regular trends. Ca and Sr increase regularly with depth through the lower unit. A zone of pyritic mineralization in the middle part of the lower unit gives rise to strong positive anomalies for Fe, Zn, Pb, Mo, Ag, Hg and loss on ignition, and a negative Si anomaly.

The central portion of the Cycle Two Andesite is divisible into upper and lower high K_2O units (averaging 1.53% and 1.36% respectively) separated by a low K_2O unit (averaging .61%). No other element yields a distinct separation of these units. All three units are correlative between ddh's 869, 868 and 1214 (Fig. 20). There appears to be no lithologic control on the K variation as each unit consists of mixed proportions of lapilli tuffs, agglomerate, flow breccia and flows.

Ca increases regularly with depth from the tops of ddh's 869, 868 and 1214 and reaches a maximum in the central portion of the low K_2O unit from which point the trend generally becomes erratic. This trend is paralleled by a similar increase in Mg which is well developed in ddh's 868 and 1214 and an increase in Ni which reaches a peak at about 525 feet below surface in all three drill holes. The disposition of the high and low K_2O units and the Ca, Mg and Ni trends strongly suggest a stratigraphic control over these variations (Fig. 20). The exact cause of the variations cannot be determined without further petrographic and geochemical study.

5.2.6. Conclusions

It is apparent from inspection of the concentration:depth plots and from the previous discussion that vertical geochemical trends are generally erratic and that little meaningful information can be gained from the plots. Consistent vertical geochemical trends occur only in certain portions of certain units and the majority of these trends are probably unrelated to ore. Anomalies related to the presence of ore occur only within approximately 100 feet above or below the ore and are probably caused by migration of metal-bearing fluids through the host rocks during and after ore formation. The anomalies are relatively weak and are generally erratic and spatially inconsistent, rendering them of little use to exploration even on a local scale.

5.3. Lateral Elemental Variations

Lateral elemental variations along lithologic units will be discussed in this section in an attempt to identify trends which were not readily apparent in the concentration:depth plots. The average concentration of all elements in each lithologic unit in each drill hole were computed and the results are shown to the left of the drill holes on the concentration: depth plots (Fig. 19). Where a unit has been previously subdivided into sub-units (e.g., Cycle Two Andesites), average abundances are shown for the sub-units. A summary of the lateral variations is presented in Fig. 21.

The Footwall Andesite is penetrated at the bottom of ddh's 2666, 2704, 868, 1214, 202 and 542 although only one sample was obtained from

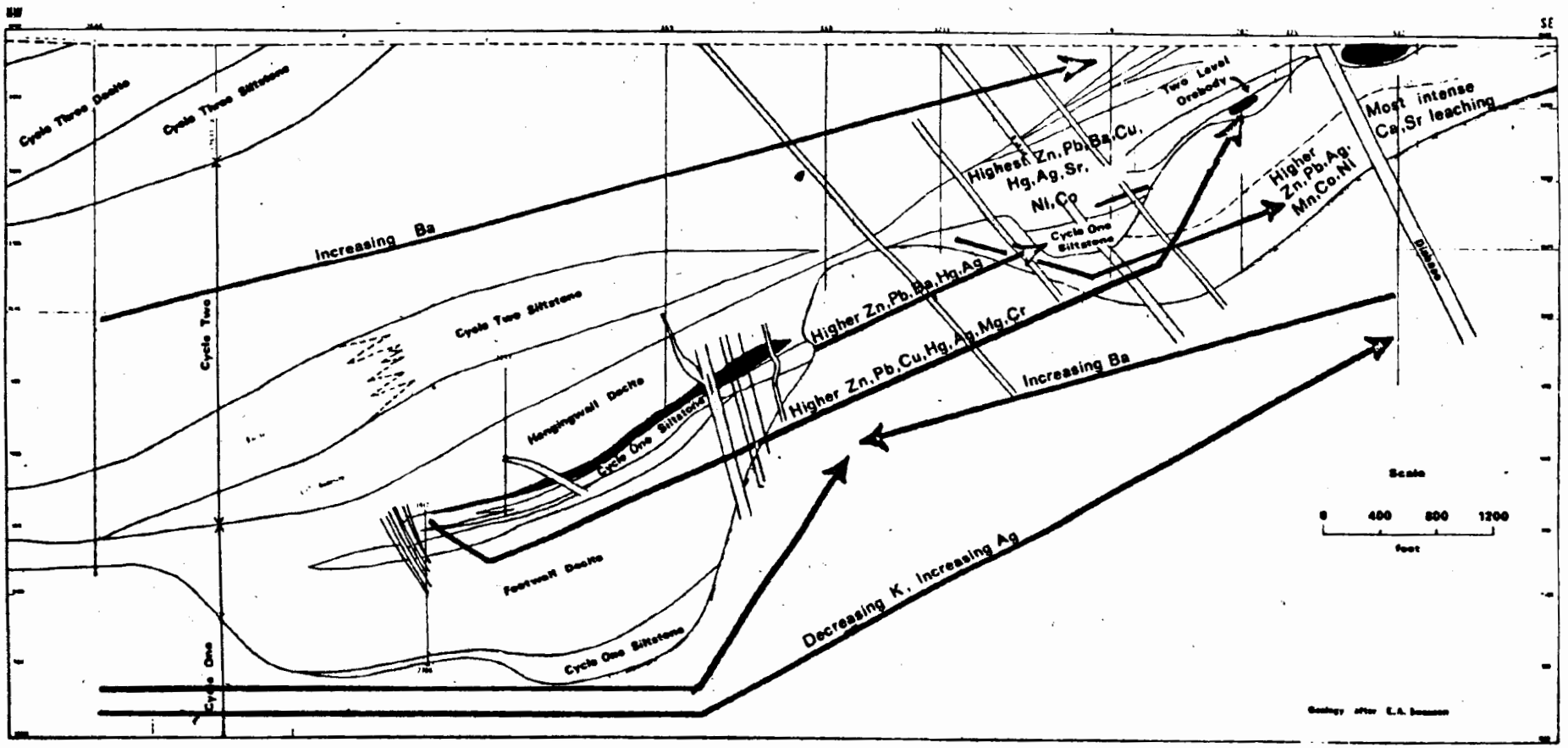

FIG. 21 - Summary of lateral elemental variations within specific units.

ddh's 2704 and 202 (the latter being extensively altered). Omitting these single sample locations, it appears that K decreases regularly southeastward to a minimum in ddh 542. Rb displays a similar but more poorly defined decrease. Ba varies independently of K and reaches a maximum (2778 ppm average) at the bottom of ddh 868 and decreases both northwesterly and southeasterly from this point. Ag increases regularly from below detection in ddh 2666 to a maximum of 1.3 ppm in ddh 542. The Footwall Andesites of ddh 542 are somewhat enriched in Ca, Mg, Cr and Ni over the areas to the northwest although no consistent increasing trend is seen for these elements.

The Intermediate Footwall is intersected by ddh's 1214, 792, 202 and 542 from northwest to southeast respectively. Zn, Pb, Ag, Mn, Co and Ni are enriched in ddh's 542 and 202 relative to ddh's 1214 and 792. Fe and Mo are also slightly higher in the southeastern portion of the unit. The characteristic leaching of Ca and Sr from the Intermediate Footwall is strongest in ddh's 542 and 202 and the intensity of this alteration decreases north west.

Significant variations in base metal content exist between the Cycle One Siltstones below Rothermere and MacLean Orebodies. The Rothermere Siltstones are considerably higher in Zn, Ba and Hg and slightly higher in Pb and Ag than the MacLean Siltstones. Otherwise, no significant differences exist for any major or trace element. Similarly no significant compositional differences exist between the upper and lower MacLean Siltstones. The higher concentrations of base metals in the Rothermere Siltstones appears to be a reflection of their proximity to the mineralized Intermediate Footwall from which they were in part derived.

The thickest sections of the immediate Footwall Dacite are found in ddh's 1917 and 202 below MacLean and Two Level Orebodies respectively. The dacites below Two Level Orebody are considerably enriched in Zn, Pb, Cu, Hg, Ag, Cr and Mg and depleted in Na, V, Zr and Sr relative to their MacLean equivalents.

The Hangingwall Dacites display no significant variation of major elements along the section. Similarly, no regular trace element variations are apparent but ddh 792 is enriched over all other drill holes in Zn, Cu, Ba, Pb, Ni, Co and Sr and ddh 1214 is enriched in Hg and Ag.

In summarizing the lateral variations throughout cycle one lithologies, it is apparent that Pb, Zn, Ag, Ba and Hg either increase towards the southeast in most lithologies or are present in higher concentrations in the southeast relative to the northwest. This southeastward concentration of those elements strongly enriched in the ore is not paralleled by any other consistent major or trace element variation common to all lithologies. As such, this southeastward enrichment appears to be overprinted on the original chemistry and may indicate that the ore metals have their derivation from a direction with a southeasterly component.

It is interesting to note that Ba displays a similar variation in the Cycle Two Andesite. Ba is low (176 ppm average) in ddh 2666, intermediate in ddh's 869, 868 and 1214 (850 ppm average) and high in ddh 792 (2050 ppm average) defining a broad northwest to southeast increase. This increase occurs independently of K which is highest in ddh 2666 (2.67% average) and much lower (1.14% average) in the southeasterly drill holes. The lack of any Ba:K correlation in the Cycle Two Andesite makes it necessary

to invoke a controlling process other than magmatic changes to explain this variation. It seems unlikely that such a variation is related to proximity to cycle one ore in view of the limited vertical dispersion of ore metals from the major orebodies. However, it is possible that this variation is related to increasing lateral proximity to cycle two ore which lies approximately one mile off section to the east. The lateral Ba variation is probably not related directly to dispersion from the orebodies per se but more likely represents precipitation of $BaSO_4$ from (sea?)water saturated in Ba by volatiles associated with volcanism, with a break in volcanism allowing accumulation of the volatiles in chemically favourable sites near active fumaroles, causing ore formation.

With respect to the positions of fumarolic centers, future studies might include the application of Mn/Fe ratios as described by Whitehead (1973). Mn is more soluble than Fe under acid reducing conditions (Krauskopf, 1967) found in the vicinity of submarine fumaroles (Bonatti, 1972; Butuzova, 1966). Thus the Mn/Fe ratio would be expected to decrease in chemical sediments with proximity to the fumarole. Unfortunately, the dominantly clean, clastic nature of the sediments sampled in this study renders them unsuitable for interpretation of Mn/Fe ratios.

K/Rb ratios in argillaceous sediments may provide another method of determining the direction to fumarolic centers. Assuming that the fumarolic emanations are enriched in the alkali metals, the preferential adsorption of Rb on clay minerals should produce a decrease in K/Rb ratios with proximity to fumarolic centers. Again, however, no suitable samples were obtained in this study.

5.4. Elemental Abundances and Exploration Significance

5.4.1. Introduction

The previous sections have dealt with vertical and lateral elemental variations within lithologic units. The significance of large discrepancies in elemental abundances which exist between units associated with mineralization and those unrelated to mineralization are the subject of this section.

5.4.2. Cycle One vs. Cycles Two and Three Siltstones

The Cycle One Siltstones sampled during this study are intimately associated with the MacLean and Rothermere Orebodies as outlined in section 2.2.2. whereas the Cycle Two Siltstone within the Cycle Two Andesite and Cycle Three Siltstone are spatially unrelated to ore. Consequently one might expect and indeed finds, distinct geochemical differences between these two groups. Ba, Hg and Ag are enriched by factors of two, Pb by four and Zn by seven times in the Cycle One Siltstones over the Cycles Two and Three Siltstones (Table 17). A test of the statistical significance of these readily apparent discrepancies (using the Mann-Whitney U test) reveals that the two populations are distinct with respect to Zn at the 99.99% confidence level, Pb at 99.9%, Ba and Hg at 98% and Ag at the 95% confidence level.

The presence of this siltstone bearing detrital sulphides is important to exploration in that it indicates, (1) a depression suitable for deposition, (2) the presence of reducing conditions favourable for ore formation, and (3) a direct link to known mineralization in the mineralized Intermediate Footwall which must have been exposed for erosion. The lateral

TABLE 17

COMPARISON OF ABUNDANCES OF ORE METALS IN CYCLE ONE AND CYCLES TWO AND THREE SILTSTONES

Element	Cycle One Siltstone	Cycles Two and Three Siltstones	Confidence Level (%)
Ba	1850 ppm	760 ppm	98
Zn	364	48	99.99
Pb	88	19	99.9
Ag	.43	.16	95
Hg	67 ppb	30 ppb	98
N=	18	11	

TABLE 18

COMPARISON OF ABUNDANCES OF ORE METALS IN FOOTWALL AND CYCLE TWO ANDESITES

Element	Footwall Andesite	Central Cycle Two Andesite	Northwestern Cycle Two Andesite
Ba	1261 ppm	921 ppm	176 ppm
Zn	91	102	37
Pb	25	29	6.8
Cu	78	64	33
Ag	.55	.29	.26
Hg	21 ppb	36 ppb	35
N=	20	32	11

extent of the geochemical anomalies in the Cycle One Siltstone, and thus the extent of the zone favourable for ore deposition, is not revealed by this study. A sample of Cycle One Siltstone obtained from over 1000 feet below MacLean Orebody is anomalous, thus defining the minimum vertical extent of the anomalous Siltstone. The samples of Cycle Two Siltstone analyzed in this study were obtained approximately 1000 feet above MacLean Orebody emphasizing that position in the stratigraphic succession, as opposed to proximity to ore, is the dominant influence on the chemistry.

5.4.3. Mafic Volcanics

The Intermediate Footwall, although not visibly mineralized in its lower portion, has been altered by a process related to mineralization of the upper portion of the unit. As a result, the unit contains anomalously high Ba, Pb, Zn, and Ag. There is a tendency for these metals to be enriched in the southeastern portion of the unit (as noted in the previous section) but the lateral extent of this enrichment beyond the N60W section is not known. Further study of the extent of alteration and geochemical anomalies, especially to the east, is warranted.

Both the Footwall and Cycle Two Andesites are geochemically comparable to andesite throughout the world, except for their abnormally high Ba content (Table 18). Such high Ba abundances intuitively imply that all the Ba is not substituting for K in feldspar and mica lattices, a suggestion which is supported by the lack of a Ba:K correlation in these units. These data suggest a secondary enrichment of Ba, probably at

deposition as outlined above, and imply a relationship between the high Ba content of the mafic volcanics and the ore associated with these units. This relationship is given further support in the Cycle Two Andesites by comparing abundances from areas spatially closer to mineralization (ddh's 869, 868, 1214, and 792) to those more removed from ore (ddh 2666). Ba is, on the average, enriched in the former by a factor of five times over the abundances of ddh 2666, and Pb is enriched by a factor of four. It should be emphasized at this point that these enrichments are not merely a consequence of trace elements sympathetically increasing with the large cationic major elements. Indeed, K_2O is more than twice as abundant in ddh 2666, a fact that makes the strong Ba enrichment in other parts of the unit even more remarkable. Ca is depleted by a factor of one half in ddh 2666, offering a possible explanation for the depletion in Pb, but negative correlation (-.35) between these two elements suggests that the low Pb abundances are unrelated to Ca.

Another feature of interest with regard to the Cycle Two Andesites of ddh 2666 is the presence of a strong Ba:K correlation (.80). This seems to indicate a primary magmatic control over Ba distribution and suggests that the average Ba abundance (176 ppm) closely represents that originally present in the magma. An abundance of this magnitude compares favourably with normal abundances found in modern calc-alkaline volcanic rocks.

A final, but significant point of comparison between these two portions of the Cycle Two Andesite is that both Zn and Cu are enriched by factors of two in the central portion of the Cycle Two Andesite.

The Mann-Whitney U test was employed to quantify the significance of the above noted differences between the two portions of the Cycle Two Andesite. The results show that the two portions are distinct with respect to Ba, Pb and Zn at the 99.99% confidence level and with respect to Cu at the 99% confidence level. Comparison of the population for these elements from the Footwall Andesite and the Cycle Two Andesite of ddh 2666 reveals even greater discrepancies.

In light of the above evidence it seems logical to ascribe the anomalies to some geochemical relationship between the ore and its host rocks. Fortunately, the differences between lithologies associated with ore and those unrelated to ore are large and readily identifiable, rendering them useful for exploration purposes. Future exploration lithogeochemical programs in the Buchans area would thus benefit from study of the Ba distribution in the mafic volcanic rocks. The distribution and abundances of Pb, Zn and Cu, while not as anomalous as Ba, also justify careful scrutiny.

5.4.4. Dacites

5.4.4.1. Footwall vs. Hangingwall Dacite - One might intuitively expect to find distinct geochemical differences between the Footwall and Hangingwall Dacite, especially with respect to the ore metals. Such differences would be a valuable aid to exploration especially at distances from ore where reliable correlation is impossible. Compositional differences might arise from primary differences in composition or from dispersion from

the orebodies after deposition. In view of the findings of the previous sections with respect to dispersion, it is likely that this has had little effect especially at a distance from ore. However, primary differences in composition might be expected. The similarity of the major element analyses (Table 19) strongly suggests that the Footwall and Hangingwall Dacites are related, and probably derived from the same magma. Making this assumption and also assuming that the ore is derived from incompatible volatiles which escaped from the magma chamber, one might expect the Hangingwall Dacite to be strongly depleted in the ore metals as a result of ore deposition. However the ore metals have not been depleted but are all present in amounts slightly greater than the Footwall (Table 19). The Mann-Whitney U test reveals that no significant differences exist between Hangingwall and Footwall with respect to the ore metals, except for Ag which is higher in the Hangingwall at the 99% confidence level. It is concluded that the magma was not depleted in the ore metals as a result of ore formation. This conclusion may form the basis for future speculations on the size of the magma chamber, its original base metal content and on the timing of separation of volatiles, and hence allow a better understanding of the general processes of massive sulphide ore deposition.

The U test does reveal significantly higher Fe, Ni and Co in the Footwall Dacite at the 99.9% confidence level, and higher V at the 99% confidence level. These distinctions are apparently more a function of the small variances of these elements than widely divergent abundances (Table 19). The author suggests that designation of samples as Footwall or Hangingwall

TABLE 19

COMPARISON OF AVERAGE ABUNDANCES IN FOOTWALL AND HANGINGWALL DACITE

Element	Hangingwall Dacite	Footwall Dacite (greater than 100 ft. from ore)
SiO_2	73.43%	73.20%
TiO_2	.23	.24
Al_2O_3	14.15	13.29
Fe_2O_3	2.14	2.56
MnO	.09	.10
MgO	.93	1.34
CaO	2.33	2.45
Na_2O	2.93	2.96
K_2O	2.99	2.55
P_2O_5	.05	.08
Rb	74 ppm	61 ppm
Ba	1684	1421
Sr	226	217
Zr	125	114
Mo	3	3
Ni	2.6	3.1
Co	2.8	5.9
V	17	28
Cr	25	24
Cu	5.0	4.8
Zn	37	28
Pb	19	18
Ag	.20	.01
Hg	17 ppb	12 ppb
N=	50	9

on the basis of Ni, Co and V abundances would be dubious at the low concentrations of these elements in the Dacite. Fe would prove more analytically reliable in this respect, but the relatively small difference in abundance and the myriad of possibilities of secondary redistributions of Fe suggest some uncertainty in using this element as an indicator. The use of discriminant functions or other multivariate statistical techniques may allow a more satisfactory separation of these two groups.

5.4.4.2. Cycle One vs. Cycle Three Dacite - The Cycle One and Cycle Three Dacites represented on the N60W section are lithologically similar ignimbrite units with local crystal, lithic and vitric tuff. The major economic difference between the two units is the association of the major orebodies with the Cycle One Dacite and a complete lack of mineralization associated with Cycle Three. Thus the distinction between these two units is of great importance to exploration.

The major element chemistry of the two units is remarkably similar except for slightly higher K and much higher Mn in Cycle One (Table 20). However, the trace elements reveal some profound differences of similar character to those noted between the Cycle Two Andesites associated with mineralization and those which were not. Ba and Pb are enriched in the Cycle One Dacites by factors greater than two and three times respectively, and Zn is enriched by a factor slightly less than two (Table 20). Statistically, it is probable at the 99.99% confidence level that the Ba and Pb analyses were not drawn from the same population and the same

TABLE 20

COMPARISON OF AVERAGE ABUNDANCES IN CYCLE ONE AND CYCLE THREE DACITE

Element	Cycle One Dacite	Cycle Three Dacite
SiO_2	73.51%	73.58%
TiO_2	.23	.27
Al_2O_3	13.88	14.32
Fe_2O_3	2.22	2.39
MnO	.09	.04
MgO	1.18	1.50
CaO	2.22	2.33
Na_2O	2.88	2.89
K_2O	2.85	1.98
P_2O_5	.06	.04
Rb	67 ppm	55 ppm
Ba	1612	674
Sr	214	364
Zr	118	134
Mo	3	3
Ni	2.6	2.3
Co	3.2	2.3
V	19	19
Cr	27	23
Cu	5.5	6.9
Zn	35	19
Pb	18	4.6
Ag	.21	.01
Hg*	17 ppb	14 ppb

applies to Zn and Mn at the 99.9% confidence level. Comparing the Ba abundances to normal calc-alkaline rhyolites (e.g. see Table 7) the Cycle Three Dacite is normal whereas the Cycle One Dacite is distinctly anomalous.

It is possible that a part of the higher Ba content of Cycle One is petrologically related to generally higher K, but the degree of enrichment is considerably greater than that of K. Furthermore Ba and K show little correlation in Cycle One (-.02 in the Hangingwall and .20 in the Footwall) suggesting that the high Ba abundances are essentially unrelated to K. However, as in the Cycle Two Andesites of ddh 2666, the Cycle Three Dacite exhibits a moderately strong Ba:K correlation (.67) probably indicating magmatic control over Ba distribution with little or no secondary enrichment. The high Ba abundances in the Cycle One Dacite and the lack of any Ba:K correlation suggest a secondary enrichment of Ba. The dominantly terrestrial nature of the Dacite precludes precipitation of Ba as sulphate from sea water as a cause of enrichment as was proposed for the mafic volcanics. In this case, the enrichment is probably due to a high Ba content in the vapour phase which drove the explosive ignimbrite eruption and was swept along with the rapidly moving fluidized ash flow. After the eruption and during autocompaction of the unit, Ba was probably deposited during escape of the vapour phase. This active vapour phase probably also caused the characteristic and pronounced Na:K redistributions in the volcanic glass (cf. Scott, 1966). In essence, it may be seen that this explanation of the high Ba content differs only superficially from that proposed for the mafic volcanics. The fundamental similarity lies in the

enrichment of incompatible Ba in late stage fluids and only the mechanism of eruption and the mechanism and environment of deposition differ.

On the basis of distinct discrepancies of Ba, Pb and Zn between the Cycle One and the Cycle Three Dacites a geochemical distinction between the two units is possible and a relationship to cycle one mineralization is strongly implied. As such, the geochemistry may be used as a powerful exploration tool in separating mineralized from unmineralized ash flow sequences. Future geochemical exploration programs should thus include study of Ba, Pb and Zn variations within the Dacites in conjunction with similar studies of the mafic volcanics as outlined above. These studies should not be restricted to the mineralized cycles but should also include the vast (and to date unproductive) upper cycles with a view to outlining areas of potential mineralization.

CHAPTER 6

SUMMARY AND EXPLORATION APPLICATION

6.1. Summary

The following is a brief summary of the findings of this study.

(1) The Buchans orebodies are associated with calc-alkaline volcanism lithologically and chemically similar to that of modern day island arcs.

(2) The orebodies display many features in common with the Kuroko deposits of Japan.

(3) The ore is intimately associated with volcaniclastic siltstones and laharic breccias within a rhyolitic ignimbrite sequence.

(4) The ore formed in chemically favourable depressions by precipitation of base metals from (sea?)water enriched in these components by submarine fumarolic activity during quiescent phases in volcanism.

(5) Breccias associated with the ore are laharic debris flows which preferentially accumulated within the depressions.

(6) The topographically controlled ignimbrites and laharic breccias may not have originated from the vicinity of the Sandy Lake "volcanic center". An area more to the northeast or east may be an alternative source area.

(7) The mineralized Intermediate Footwall is distinct in both time and space from the major orebodies.

(8) Geochemical evidence indicates that fracture zones now occupied by diabase dikes were not the conduits through which mineralizing solutions passed.

(9) Studies of elemental distributions in the vicinity of the orebodies indicate that secondary dispersion of base metals is generally restricted to within 100 feet of the orebodies. The immediate Footwall Dacites (i.e., within 100 feet of ore) are in general only slightly enriched in base metals over the Hangingwall Dacite. Only a vague geochemical distinction can be made between Footwall Dacite and Hangingwall Dacite at a distance from ore.

(10) Study of lateral elemental variations indicates a broad general increase in base metals in most lithologic units on the N60W section from northwest to southeast possibly suggesting a direction to the fumarolic center with a southeasterly component.

(11) Profound differences in elemental abundances exist between lithologic units associated with ore and those unrelated to ore. The most abundant metallic constituent of the ore, Ba, is consistently and significantly higher in units associated with mineralization (Cycle One Siltstone, Cycle One Dacite, Footwall Andesite, Intermediate Footwall and the southeastern portion of the Cycle Two Andesite) than in units unrelated to ore (Cycles Two and Three Siltstone, Cycle Three Dacite and the northwestern

portion of the Cycle Two Andesite). Where Ba abundances are low (i.e. normal), Ba and K exhibit a strong ppsitive correlation indicative of primary magmatic control over Ba distribution. Where Ba abundances are high, no Ba:K correlation exists suggesting a secondary enrichment of Ba. The Ba enrichment is attributed to a Ba-rich volatile phase which accompanied volcanism in lithologic units related to mineralization.

Zn and Pb, the next most abundant metallic ore constituents exhibit the same relative differences between units associated with mineralization and those unrelated to mineralization, although their relative abundances are not as anomalous as Ba. Cu, Ag and Hg are, in some instances, higher in units associated with mineralization.

6.2. Exploration Application

On the basis of the findings of this study, further geochemical-geological studies appear justified as an aid to outlining areas of potential mineralization. The area of future study should be expanded to include representative portions of all volcanic cycles and greater attention should be focused on the upper volcanic cycles which underlie the major portion of the Buchans area, in an attempt to identify lithogeochemically anomalous units. Within these cycles the location of lithologically and chemically favourable environments of ore deposition is of paramount importance. The possibility that the upper cycles of volcanism are entirely terrestrial would preclude the probability of ore formation of a similar character to that found in

the initial cycles, assuming that an aqueous phase was necessary for ore deposition.

The location of the volcanic centre is of great interest to exploration and is at present not known with a high level of confidence. Future geochemical and geological studies may provide new data which might either confirm or destroy present speculations as to the location of this important feature.

REFERENCES

Abbey, S., 1968. Analysis of rocks and minerals by atomic absorption spectroscopy; Part 2; Determination of total iron, magnesium, calcium sodium and potassium. Geol. Surv. Can. Paper 68-20, 21 p.

Alcock, J.B., 1961. Oriental No. Two Orebody. Unpub. B.Sc. Thesis, Royal School of Mines, London.

Bonatti, E., Kraemer, T., and Rydell, R., 1972. Classification and genesis of submarine iron-manganese deposits in Ferromanganèse Deposits on the Ocean Floor, D.R. Horn. (ed.), pp. 149-166.

Boyle, R.W., 1961. The geology, geochemistry, and origin of the gold deposits of the Yellowknife District. Geol. Surv. Can. Memoir 310, 193 p.

_____, 1965. Geology, geochemistry and origin of the lead-zinc-silver deposits of the Keno Hill-Galena Hill area, Yukon Territory. Geol. Surv. Can. Bull. 111, 302 p.

Boyle, R.W., Dass, A.S., Church, D., Mihailou, G., Durham, C., Lynch, J. and Dyck, W., 1969. Research in geochemical prospecting methods for native silver deposits, Cobalt area, Ontario. Geol. Surv. Can. Paper 67-35.

Boyle, R.W. and Garrett, R.G., 1970. Geochemical Prospecting - a review of its status and future. Earth Science Review, v. 6, pp. 51-75.

Bradshaw, P.M.D., Clews, D.R. and Walker, J.L., 1970. Exploration Geochemistry - Part 4: Primary dispersion. Mining in Canada, 1970.

Bradshaw, P.M.D., and Koksoy, M., 1968. Primary dispersion of mercury, from cinnibar and stibnite deposits, W. Turkey. Int. Geol. Cong. Report, v. 7, pp. 342-355.

Butuzova, D.Yu., 1966. Iron ore sediments of fumarole field of Santorin volcano; their composition and origin. Dokl. Akad. Navk. S.S.R., v. 168, pp. 215-217.

Cann, J.R., 1970. Rb, Sr, Y, Zr and Nb in some ocean floor basaltic rocks. Earth and Planet. Sci. Let., v. 10, pp. 7-11.

Catherall, D.J., 1960. Engine House Orebody. Unpub. B.Sc. Thesis, Royal School of Mines, London.

Davenport, P.H. and Nichol, I., 1972. Bedrock geochemistry as a guide to areas of base metal potential in volcano-sedimentary belts of the Canadian Shield. in Geochemical Exploration 1972, Proc. of the fourth International Geochemical Exploration Symposium, London, M.J. Jones (ed.), pp. 45-57.

Descarreaux, J., 1972. A lithogeochemical cross section of the Abitibi Volcanic belt. Paper presented to Can. Inst. Min. Metall. meeting, Ottawa, April, 1972.

Engel, A.E., Engel, C.G. and Havens, R.G., 1965. Chemical characteristics of oceanic basalts and the upper mantle. Bull. Geol. Soc. Amer., v. 76, pp. 719-734.

Ewart, A. and Bryan, W.B., 1972. Petrography and geochemistry of the igneous rocks from Eua, Tongan Islands. Bull. Geol. Soc. Amer., v. 83, pp. 3281-3298.

Ewart, A., Taylor, S.R. and Capp, A.C., 1968. Trace and minor element geochemistry of the rhyolitic volcanic rocks, Central North Island, New Zealand. Total rock and residual liquid data. Contrib. Min. Petrol., v. 18, pp. 76-104.

Fisher, R.V., 1960a. Criteria for the recognition of laharic breccias, Southern Cascade Mountains, Washington. Bull. Geol. Soc. Amer., v. 71, pp. 127-132.

_____, 1960b. Classification of volcanic breccias. Bull. Geol. Soc. Amer., v. 71, pp. 973-982.

Gale, G.H., 1969. The primary dispersion of Cu, Zn, Ni, Co, Mn and Na adjacent to sulphide deposits, Springdale Peninsula, Newfoundland. Unpub. M.Sc. Thesis, Memorial University of Nfld., St. John's, 143 p.

George, P.W., 1937. Geology of lead-zinc-copper deposits at Buchans, Newfoundland. Amer. Inst. Min. Metall. Eng., T.P. 816; (Class I, Mining Geology, No. 70).

Gorshkov, G.S., 1970. Volcanism and the upper mantle. Investigations in the Kurile Island Arc. Plenum Press, N.Y., 385 p.

Govett, G.J.S. and Pantazis, Th. M., 1971. Distribution of Cu, Zn, Ni and Co in the Troodos Pillow Lava Series, Cyprus. Trans. Inst. Min. Metall., v. 80, pp. B27-B46.

Graf, D.K. and Kerr, P.F., 1950. Trace element studies, Santa Rita, New Mexico, Bull. Geol. Soc. Amer., v. 61, pp. 1023-1052.

Hart, R., 1970. Chemical exchange between sea water and deep ocean basalts. Earth and Planet. Sci. Let., v. 9, pp. 269-279.

Hawkes, H.E., and Webb, J.S., 1962. Geochemistry in mineral exploration. Harper and Row, N.Y., 415 p.

Heier, K.S. and Adams, J.A.S., 1964. Geochemistry of the alkali metals. Phys. and Chem. of the Earth, v. 5, pp. 253-381.

Horikoshi, E., 1969. Volcanic activity related to the formation of the kuroko type deposits in the Kosaka District of Japan. Mineral. Deposita, v. 4, pp. 321-345.

Irvine, T.N., and Baragar, W.R.A., 1971. A guide to the chemical classification of the common volcanic rocks. Can. Jour. Earth Sci., v. 8, pp. 523-548.

Isacks, B., Oliver, J. and Sykes, L.B., 1968. Seismology and the new global tectonics. Jour. Geophys. Res., v. 73, pp. 5855-5899.

Jakeš, P. and White, A.J.R., 1969. Structure of the Melanesian arcs and correlation with distribution of magma types. Tectonophysics, v. 8, pp. 223-236.

_____, 1970. K/Rb ratios of rocks from island arcs. Geochim. Cosmochim. Acta, v. 34, pp. 849-856.

Jakeš, P. and White, A.J.R., 1971. Composition of island arcs and continental growth. Earth and Planet. Sci. Let., v. 12, pp. 224-230.

_____, 1972. Major and trace element abundances in volcanic rocks of orogenic areas. Bull. Geol. Soc. Amer., v. 83, pp. 29-40.

Jolly, W.T. and Smith, R.E., 1972. Degradation and metamorphic differentiation of the Keweenawan tholeiitic lavas of Northern Michigan, U.S.A. Jour. Petrol., v. 13, no. 2, 273 p.

Kean, B.F., 1973. Geology, stratigraphy and geochemistry of the volcanic rocks of Long Island, Notre Dame Bay, Newfoundland. Unpub. M.Sc. Thesis, Memorial Univ. Nfld., St. John's, 154 p.

Konstantynowicz, E., 1972. Mineral distribution in the Permian formations of western Poland. Int. Geol. Cong., 24th Session, Sec. 4, pp. 373-380.

Krauskopf, K.B., 1967. Introduction to Geochemistry. McGraw-Hill, New York, 721 p.

Kuno, H., 1966. Lateral variation of basalt magma type across continental margins and island arcs. Bull. Volcan., v. 29, pp. 195-222.

_____, 1968. Differentiation of basalt magmas. in Basalts, v. 2, H.H. Hess and A. Poldervaart (eds.), Intersci. Publ., N.Y., pp. 623-688.

Langmhyr, F.J. and Paus, P.E., 1968. The analysis of inorganic siliceous materials by atomic absorption spectrophotometry and the hydrofluoric acid decomposition technique. Part I: The analysis of silicate rocks. Anal. Chim. Acta, v. 43, pp. 397-408.

MacDonald, G.A., 1972. Volcanoes. Prentice-Hall, New Jersey, 510 p.

MacDonald, G.A. and Katsura, T., 1964. Chemical composition of Hawaiian Lavas. J. Petrol., v. 5, pp. 82-133.

MacKenzie, D.E. and Chappell, B.W., 1972. Shoshonitic and calc-alkaline lavas from the highlands of Papua, New Guinea. Contrib. Min. Petrol., v. 35, pp. 50-62.

Morris, H.T. and Lovering, T.S., 1952. Supergene and hydrothermal dispersion of heavy metals in wall rocks near orebodies, Tintic District, Utah. Econ. Geol., v. 47, pp. 685-716.

Newhouse, W.H., 1931. Geology and ore deposits of Buchans, Newfoundland. Econ. Geol., v. 26, pp. 399-414.

Peacock, M.A., 1931. Classification of igneous rock series. Jour. Geol., v. 39, pp. 54-67.

Relley, B.H., 1960. The Geology of the Buchans Mines. Unpub. Ph.D. Thesis, McGill Univ., Montreal, 281 p.

Roscoe, S.M., 1965. Geochemical and isotopic studies, Noranda and Matagami areas. Can. Inst. Min. Metall. Bull., pp. 965-971.

Sakrison, H.C., 1967. Chemical studies of the host rocks of the Lake Dufault mine, Quebec. Unpub. Ph.D. Thesis, McGill Univ., Montreal.

_____, 1971. Rock geochemistry - its current usefulness on the Canadian Shield. Can. Inst. Min. Metall. Bull., Nov., pp. 28-31.

Sangster, D.F., 1972. Precambrian volcanogenic massive sulphide deposits in Canada: A review. Geol. Surv. Can. Paper 72-22, 44 p.

Scott, R., 1966. Origin of chemical variations within ignimbrite cooling units. Amer. Jour. Sci., v. 264, pp. 273-288.

Shapiro, L., and Brannock, W.W., 1962. Rapid analysis of silicate carbonate and phosphate rocks. U.S.G.S. Bull. 1144A, p. A31.

Siegel, S., 1965. Nonparametric statistics for the behavioural sciences. McGraw-Hill, New York, 312 p.

Strong, D.F., 1973a. Lushs Bight and Roberts Arm Groups of Central Newfoundland: Possible juxtaposed oceanic and island-arc volcanic suites. Bull. Geol. Soc. Amer., in press.

_____, 1973b. Plate tectonic setting of Appalachian-Caledonian mineral deposits as indicated by Newfoundland examples. Society of Mining Engineers of A.I.M.E., Preprint number 73-I-320, 31 p.

Sugimura, A., 1968. Spatial relations of basaltic magmas in island arcs. in Hess, H.H. and Poldervaart, A. (eds.), Basalts. New York, Interscience, pp. 573-577.

Swanson, E.A. and Brown, R.L., 1962. Geology of the Buchans Orebodies. Can. Inst. Min. Bull., v. 55, pp. 618-626.

Sykes, L.R., 1966. The seismicity and deep structure of island arcs. Jour. Geophys. Res., v. 71, pp. 2981-3006.

Tatsumi, T., 1970. Volcanism and ore genesis. Univ. of Tokyo Press, 448 p.

Taylor, S.R., 1965. The application of trace element data to problems in petrology. Phys. and Chem. of the Earth, v. 6, pp. 133-213.

_____, 1968. Geochemistry of Andesites, in Origin and Distribution of the elements, L.H. Ahrens (ed.). Pergamon Press, Oxford, 1968, pp. 559-583.

Thompson, R.N., Esson, J. and Dunham, A.C. Major element chemical variation in the Eocene lavas of the Isle of Skye, Scotland. Jour. Petrol., v. 13, pp. 219-253.

Whitehead, R.E., 1973. Environment of stratiform sulphide deposition; Variation in Mn:Fe ratio in host rocks at Heath Steele Mine, New Brunswick, Canada; Mineral. Deposita, v. 8, in press.

Williams, H., 1964. The Appalachians in northeastern Newfoundland: A two-sided symmetrical system, Amer. Jour. Sci., v. 262, pp. 1137-1158.

Williams, H., 1967. Silurian rocks of Newfoundland. Geol. Assoc. Can. Spec. Paper, No. 4, pp. 93-137.

_____, 1970. Red Indian Lake (east half), Newfoundland. Geol. Surv. Can. Map No. 1196A.

Williams, H., Kennedy, M.J. and Neale, E.R.W., 1972. The Appalachian Structural Province, in Price, R.A. and Douglas, J.W. (eds.), Variations in Tectonic Styles in Canada. Geol. Assoc. Can. Spec. Paper, No. 11, pp. 182-261.

Woakes, M., 1954. A microscopic study of the ore sulphides from Buchans mine, Buchans, Newfoundland. Unpub. B.Sc. Thesis, Royal School of Mines, London.